



HAL
open science

Plant lipids: Key players of plasma membrane organization and function

Adiilah Mamode Cassim, Paul Gouguet, Julien Gronnier, Nelson Laurent, Véronique Germain, Magali Grison, Yohann Boutté, Patricia Gerbeau-Pissot, Françoise Simon-Plas, Sebastien Mongrand, et al.

► **To cite this version:**

Adiilah Mamode Cassim, Paul Gouguet, Julien Gronnier, Nelson Laurent, Véronique Germain, et al.. Plant lipids: Key players of plasma membrane organization and function. Progress in Lipid Research, 2018. hal-02997549

HAL Id: hal-02997549

<https://hal.science/hal-02997549>

Submitted on 10 Nov 2020

HAL is a multi-disciplinary open access archive for the deposit and dissemination of scientific research documents, whether they are published or not. The documents may come from teaching and research institutions in France or abroad, or from public or private research centers.

L'archive ouverte pluridisciplinaire **HAL**, est destinée au dépôt et à la diffusion de documents scientifiques de niveau recherche, publiés ou non, émanant des établissements d'enseignement et de recherche français ou étrangers, des laboratoires publics ou privés.

1
2
3 **1 Plant lipids: key players of plasma membrane organization and function**
4
5
6
7
8
9
10
11
12
13
14
15
16
17
18
19
20
21
22
23
24
25
26
27
28
29
30
31
32
33
34

6 Adiilah Mamode Cassim^{1#}, Paul Gouguet^{1#}, Julien Gronnier^{1§}, Nelson Laurent², Véronique Germain¹,
7 Magali Grison¹, Yohann Boutté¹, Patricia Gerbeau-Pissot², Françoise Simon-Plas^{2*}, Sébastien
8 Mongrand^{1*}

11 ¹. Laboratoire de Biogenèse Membranaire (LBM), CNRS, University of Bordeaux, UMR 5200, F-33882
12 Villenave d'Ornon, FRANCE

13 ². Agroécologie, AgroSup Dijon, INRA, University of Bourgogne Franche-Comté, F-21000 Dijon, ERL
14 6003 CNRS, Dijon, FRANCE

22 #, AMC and PG must be considered as co-first authors

23 *, FSP and SM must be considered as co-corresponding and last authors

24 §, Present address: Cyril Zipfel's laboratory. Institute of Plant Biology, University of Zurich,
25 Zollikerstrasse 107. 8008 Zurich Switzerland

31 For correspondence: Sébastien Mongrand. Laboratoire de Biogenèse Membranaire (LBM), Unité
32 Mixte de Recherche UMR 5200, CNRS, University of Bordeaux, F-33882 Villenave d'Ornon. FRANCE;
33 sebastien.mongrand@u-bordeaux.fr
34

61
62
63
64
65
66
67
68
69
70
71
72
73
74
75
76
77
78
79
80
81
82
83
84
85
86
87
88
89
90
91
92
93
94
95
96
97
98
99
100
101
102
103
104
105
106
107
108
109
110
111
112
113
114
115
116
117
118
119
120

1 **Abstract**

2 The plasma membrane (PM) is the biological membrane that separates the interior of all cells from
3 the outside. The PM is constituted of a huge diversity of proteins and lipids. In this review, we will
4 update the diversity of molecular species of lipids found in plant PM. We will further discuss how
5 lipids govern global properties of the plant PM, explaining that plant lipids are unevenly distributed
6 and are able to organize PM in domains. From that observation, it emerges a complex picture
7 showing a spatial and multiscale segregation of PM components. Finally, we will discuss how lipids
8 are key players in the function of PM in plants, with a particular focus on plant-microbe interaction,
9 transport and hormone signaling, abiotic stress responses, plasmodesmata function. The last chapter
10 is dedicated to the methods that the plant membrane biology community needs to develop to get a
11 comprehensive membrane organization in plants.

12
13
14
15
16
17
18
19
20 **Keywords**

21 Plant, plasma membrane, sphingolipids, sterols, phospholipids, signaling, domain, raft,
22 plasmodesmata, liposome, model membrane, detergent, biophysics, registration, interdigitation,
23 pinning
24

121
122
123
124
125
126
127
128
129
130
131
132
133
134
135
136
137
138
139
140
141
142
143
144
145
146
147
148
149
150
151
152
153
154
155
156
157
158
159
160
161
162
163
164
165
166
167
168
169
170
171
172
173
174
175
176
177
178
179
180

1 **Abbreviations:**

2 ASG, acylated steryl glycosides ; CER, ceramides ; DRM, detergent-resistant membrane fraction ;
3 DRP1A, DYNAMIN-RELATED PROTEIN1A ; EVs, Extracellular vesicles ; GIPC, Glycosyl Inositol
4 Phosphoryl Ceramides ; GIPCs, Glycosyl Inositol Phosphoryl Ceramides ; gluCER, glucosylceramide ;
5 gluCER, glucosylceramide ; GUV, giant unilamellar vesicles ; hVLCFA ,2-hydroxylated Very Long Chain
6 Fatty Acid ; ISO, Inside Out vesicles ; Ld, liquid-disordered ; Lo, liquid-ordered ; MCS, Membrane
7 contact site ; MSC, Membrane Surface charge ; PAMPs, Pathogen-associated Molecular Patterns ;
8 PDCB1, Plasmodesmata Callose Binding 1 ; PDs, plasmodesmata ; PIN, PINFORMED ; Plasmodesmata,
9 PdBG2, beta-1,3-glucase ; REM, Remorin ; RSO, Right Side Out vesicles ; SG, Steryl glycosides ; So,
10 solid-ordered ; VLCFA, Very Long Chain Fatty Acid.

11

181
182
183
184
185
186
187
188
189
190
191
192
193
194
195
196
197
198
199
200
201
202
203
204
205
206
207
208
209
210
211
212
213
214
215
216
217
218
219
220
221
222
223
224
225
226
227
228
229
230
231
232
233
234
235
236
237
238
239
240

1	Table of content
2	1 Update on the lipid content of plant PM: how to visualize them?
3	1.1 Glycerolipids: galactolipids, phospholipids and phosphoinositides
4	1.2 Sphingolipids
5	1.3 Free and esterified phytosterols
6	
7	2 Lipids govern global properties of the plant PM
8	2.1 Fluidity of PM
9	2.2 Phytosterols are crucial regulators of membrane order
10	2.3. Involvement of sphingolipids in PM membrane order
11	2.4. Electrostatic charge and pH domains of the PM
12	3 Plant lipids are unevenly distributed within the PM and able to organize into domains
13	3.1 Asymmetric composition of inner and outer leaflets
14	3.2 Membrane phases in model and biological membranes
15	3.2.1 <i>Membrane phases, dyes and modeling approaches</i>
16	3.2.2 <i>Solubilization by detergents: evidences from model membranes</i>
17	3.2.3 <i>Isolation of Detergent Resistant Membranes from PM, biochemical fractions with a</i>
18	<i>specific lipid composition.</i>
19	3.2.3.1. <i>Glycerolipids in plant DRMs</i>
20	3.2.3.2 <i>Sterols in plant DRMs</i>
21	3.2.3.3 <i>Sphingolipids in plant DRMs</i>
22	3.2.4 The use of DRMs to study the segregation of lipids in plant PM; some limits but
23	significant contributions.
24	
25	4. Spatial and multiscale segregation of lipids and proteins: a complex picture emerging from
26	the combined use of various imaging techniques
27	4.1. Micro- and nano-domains coexist in the plant PM
28	4.2 PM lipids are critical regulators of plant PM organization at a nanometer scale
29	4.3. PM heterogeneity might originate from a tight control along the secretory pathway
30	4.3. First models of plant PM organization, interdigitation, pinning and registration
31	4.3.1. <i>A model for plant PM organization: mechanisms at work</i>
32	4.3.2. <i>PM asymmetry, interdigitation, pinning and registration</i>
33	
34	5. Lipids are key players in plant PM function
35	5.1 Plant-microbe interactions
36	5.1.1 Membrane lipids in plant microbe interaction
37	5.1.2 Sphingolipids as receptors of necrotrophic toxins and plant-pathogen elicitors
38	5.1.3. Lipid domain-associated proteins in plant microbe interaction
39	5.1.4 GPI-anchored proteins & outer-leaflet PM domains
40	5.1.5 Extracellular vesicles & host-induced gene silencing
41	5.2 Hormone signalling and transport
42	5.3 Abiotic stress
43	5.4 Plasmodesmata function
44	
45	6. Conclusions and perspectives: How to get a comprehensive membrane organization in
46	plants?
47	

241
242
243
244
245
246
247
248
249
250
251
252
253
254
255
256
257
258
259
260
261
262
263
264
265
266
267
268
269
270
271
272
273
274
275
276
277
278
279
280
281
282
283
284
285
286
287
288
289
290
291
292
293
294
295
296
297
298
299
300

1 Introduction

2 The Plasma Membrane (PM) is a key structure protecting the cell, regulating nutrient exchanges
3 and acting as a control tower allowing the cell to perceive signals. Plasma comes from the greek
4 πλάσμα meaning “which molds”, meaning that the PM takes the shape of the cell by delimitating it.
5 The PM harbors the appropriate signaling cascades allowing adaptive responses ensuring proper cell
6 functions in a continuously fluctuating environment, crucial for cell survival. To address this
7 challenge, the PM needs to be both stable and robust yet incredibly fluid and adaptable. This
8 amazing combination of long-term stability and short-term dynamics in order to adapt to signals
9 relies on its fascinating molecular organization. PMs are extremely complex systems, harboring many
10 different molecular species of lipids in which heterogeneity is more likely to occur than homogeneity.
11 In plants as in animals, the recent development of proteomics, lipidomics and methods to visualize
12 lipids and proteins *in vivo* has greatly increased our knowledge of the PM.

13 The combination of biophysical, biochemical, and cell biology approaches, recently including super-
14 resolution imaging both of the PM's physical state and of the nanometric distribution of its
15 constituents has significantly broadened our vision of PM organization. In this update review, we will
16 present the current state of knowledge of the plant-PM lipid composition, then we will examine how
17 lipids govern the nano- and micro-scopic properties and organization of the plant PM. We will
18 illustrate how the available data show that lipids are not distributed homogeneously within and
19 between each leaflet of the PM. The role of interdigitation and registration between these two
20 leaflets will be also discussed. Finally, we will show how lipids contribute to the organization of the
21 PM, and how this organization plays a decisive role in a certain number of essential processes of
22 plant cell physiology including immunity, abiotic stress and cell-to-cell communication through
23 plasmodesmata. Note that the involvement of lipids as signaling second messenger molecules are
24 not reviewed in details here, except for plant microbe interactions, and we prompted the readers to
25 refer to reviews [1].
26

301
302
303 1 **1. Update on the lipid content of plant PM: How to visualize them?**
304
305

306 2 The PM is an asymmetric proteo-lipidic matrix. The lipid-to-protein ratio (mass/mass) was
307 3 experimentally determined to be close to 1.3 in tobacco PM [2]. Therefore, one can estimate a molar
308 4 ratio of 1 protein for 50-100 molecules of lipids. Proteomic data on purified plant PM identified ca.
309 5 500-1000 proteins in the PM, and the lipidome is theoretically made up of thousands molecular
310 6 species of glycerophospholipids, sphingolipids and sterol-based structures [3]. A conserved feature of
311 7 cellular organelles is the distinct lipid composition of their membranes, essential to specify their
312 8 identity and function.

313 9 Highly purified RSO (right side out) PM vesicles are easily obtained using a two-phase aqueous
314 10 polymer partition system from various plant material [4]. Enzymatic reactions or western blotting are
315 11 generally used to address the purity of the PM fractions and the absence of contaminants. In parallel,
316 12 development of high-throughput lipidomic methods by LC-MS allow the complete characterization of
317 13 the main class of lipids present in the plant PM [5, 6]: phospholipids [7], phosphoinositides [8],
318 14 sphingolipids [9, 10] and sterols [11, 12]. Such procedures allow the characterization of the molecular
319 15 species of each lipid class at a level of detail including the fatty acid position for glycerolipids, the
320 16 nature of long-chain bases for sphingolipids and the many classes of phytosterols [13]. Besides these
321 17 biochemical tools, strategies have been developed to visualize lipids *in vivo* using biosensors showing
322 18 affinity for lipids. Imaging lipidomics have also been developed, particularly in seeds [14, 15] but the
323 19 resolution is not yet high enough to allow the characterization of lipids inside a given membrane.
324 20 Recently, "Imaging lipidomics: automated MS imaging of tissue with lipid structure identification" by
325 21 Ellis *et al.* (Nature Methods) reported a method that enables the acquisition of lipid tandem mass
326 22 spectrometry data in parallel with a high-resolution mass spectrometry imaging experiment. Authors
327 23 developed a lipidome-per-pixel approach able to identify in rat cerebellar tissue hundreds of lipid
328 24 molecule species and their spatial locations [16, 17]. Nano-SIMS (Secondary-ion mass spectrometry)
329 25 has also been developed with labeled lipids allowing the deciphering of lipid segregation in the plane
330 26 of the PM in animal cell culture with a lateral resolution of 90nm [18]. This high-resolution method is
331 27 yet to be introduced in plants as the cell wall could strongly impair access to the PM.
332
333
334
335
336

337 28
338 29 **1.1 Glycerolipids: galactolipids, phospholipids and phosphoinositides**

339 30 Phospholipids represent ca. 30% of tobacco PM lipids [2]. As can be expected,
340 31 Phosphatidylcholine (PC) and Phosphatidylethanolamine (PE) are the major phospholipids of plant
341 32 PM with palmitic and linoleic acids as main acyl chains [7, 19-24]. Phosphatidylglycerol (PG),
342 33 phosphatidylinositol (PI), phosphatidylserine (PS) are minor phospholipids. Among these
343 34 phospholipids, only PS is associated with a high proportion of very long chain fatty acids e.g., behenic
344 35 C22 and lignoceric C24 acid.

345 36 Polyphosphoinositides or phosphatidylinositol-phosphates (PIPs) represent a minor fraction of
346 37 total phospholipids; they are composed of a PI backbone with up to 3 phosphorylations on the
347 38 inositol moiety. PIPs are involved in many regulatory processes, such as cell signaling and
348 39 intracellular trafficking. Membrane compartments are enriched or depleted in specific PIPs, providing
349 40 a unique signature for these compartments. The precise subcellular localizations and dynamics of
350 41 PIPs were revealed in plants thanks to the design of genetically encoded biosensors with distinct
351 42 relative affinities [25, 26]. Recently, a full set of phospholipid biosensors was generated in
352 43 *Arabidopsis thaliana* called "PIP-lines" [27]. This library extended the range of available PIP
353 44 biosensors and allowed rapid progress in the understanding of PIP dynamics in plants as well as its
354 45 monitoring *in vivo*, see below. Hence, not only phosphatidylinositol-4-phosphate (PI4P),
355
356
357
358
359
360

361
362
363 1 phosphatidylinositol-3-phosphate (PI3P), phosphatidylinositol-4,5-bisphosphate (PI4,5P₂),
364 2 phosphatidylinositol-3,5-bisphosphate (PI3,5P₂), phosphatidylinositol-3,4,5-bisphosphate (PI3,4,5P₃),
365 3 but also phosphatidylserine (PS) and phosphatidic acid (PA) can be visualized *via* these biosensors
366 4 [27-30]. Quantitative imaging analysis revealed that there is a gradient of PI4P throughout the cell,
367 5 with the highest concentration at the PM, intermediate concentration in post-Golgi/endosomal
368 6 compartments, and the lowest concentration in the Golgi apparatus. A similar gradient of PI3P was
369 7 observed from high concentrations in late endosomes to low concentrations in the tonoplast. Inside
370 8 the PM, polyphosphoinositides (PI4P and PI4,5P₂) were enriched in DRMs compared with the whole
371 9 PM, suggesting that PIPs could be present inside domains at the PM [31]. This hypothesis was further
372 10 supported by the visualization of nanodomain-like clustering by immunogold labeling [31].
373 11 Importantly, PIPs and PS influence membrane biophysical properties, which emerge as important
374 12 features in specifying cellular territories; this is discussed in the chapter 2.

375 13 Note that Digalactosyldiacylglycerol (DGDG), present in plastids, is also found in the plant PM
376 14 particularly in response to phosphate deprivation [32, 33]. Neutral lipids like diacylglycerol (DAG)
377 15 were also visualized *in vivo* [34] and showed to be present at the PM of root epidermal cells in the
378 16 transition zone, at the trans-Golgi network, the cell plate during cytokinesis, and the apex of growing
379 17 root hairs.

380 18

381 19 **1.2 Sphingolipids**

382 20 Sphingolipids are ubiquitous in eukaryotes with a sphingoid backbone called the long-chain
383 21 amino-alcohol base (LCB). They are abundant and essential components of biological membranes
384 22 and they can represent up to 10 % of total lipids in plants [35]. Detected for the first time in 1870 in
385 23 brain samples, their name comes from the greek Σφίγξ “to squeeze, to strangle” related to the strong
386 24 amide bond that composes the link between their two lipophilic moieties and with an allusion to the
387 25 Sphinx for the cryptic nature of these lipids at the time of their discovery. In animal PMs, the main
388 26 sphingolipid class is sphingomyelin, which is not present in plants. Minor sphingolipids called
389 27 gangliosides are a class of acidic glycolipids that play an important role in immunity and modulate
390 28 cellular signal transduction events [36]

391 29 Plant sphingolipids are of four major classes: ceramides (CER), glucosylceramide (gluCER), Glycosyl
392 30 Inositol Phosphoryl Ceramides (GIPCs) and free Long Chain Bases (LCBs), representing ca., 2%, 34%,
393 31 64% and 0.5 % of total sphingolipids, respectively in *Arabidopsis thaliana* [10]. In addition to the PM,
394 32 sphingolipids are enriched in endosomes and tonoplasts, representing around 10 to 20% of total
395 33 membrane lipids [37]. The complex structural diversity of plant sphingolipids arises from the possible
396 34 occurrence of three very diverse building blocks: the polar head, the fatty acyl chain linked by an
397 35 amide bond (forming a ceramide) to the LCB [38].

398 36 In this review, we will mostly focus on GIPCs because recent discoveries on the role of these lipids
399 37 in the organization of the PM [39] and as toxin receptors [40] swung them into the spotlight. GIPCs
400 38 are representatives of a class of acidic glycolipids from plants, possibly analogous to the acidic
401 39 gangliosides found in animal cell membranes. They have been discovered during the late 1950's by
402 40 Edward Carter [41] and have been forgotten until the beginning of the 2000's. GIPCs are composed
403 41 of a ceramide and a glycan polar head group. The diversity of GIPCs resides in: 1/ the length, the
404 42 number and position of hydroxylations and unsaturations in the FA chain; 2/ the hydroxylation
405 43 degree, saturation and position of double bond(s) in the LCB; 3/ the nature and the number of
406 44 glycans, and the type of glycosidic links between the glycans that compose the polar head group [38]
407 45 [42]. In general, the ceramide moiety of plant GIPCs consists mainly of a t18:0 (trihydroxylated LCB of

1 18 carbon atoms) or a t18:1 (trihydroxylated LCB of 18 carbon atoms and an unsaturation) as LCB,
2 amidified to a Very Long Chain Fatty Acid (VLCFA) or 2-hydroxylated VLCFA (hVLCFA). Hence, 95
3 mol% of PM VLCFA and hVLCFA are amidified in GIPCs [39]. The polar head of GIPCs is made up of a
4 phosphate linked to an inositol to which glycan moieties are bound. The degree of glycosylation of
5 the GIPC polar head groups defines the different GIPC series.

6 The basic structure of the GIPC polar head is an inositol phosphoryl ceramide (IPC) backbone
7 linked to a glucuronic acid (GlcA). A sugar unit bound to GlcA-IPC forms the series A GIPCs. Only a few
8 structures have been fully resolved with the exact sugars and the nature of the sugar bond: tobacco
9 series A GIPCs has the most basic known structure: GlcNAc(α 1- \rightarrow 4)GlcA(α 1- \rightarrow 2)inositol-1-O
10 phosphorylceramide [43]. Additional sugar moieties such as glucosamine (GlcN), N-acetyl-
11 glucosamine (GlcNAc), arabinose (Ara), galactose (Gal) and mannose (Man) may lead to glycan
12 patterns of three to seven sugars, so-called series B to F GIPCs, see Figure 1. GIPCs found in corn
13 seeds display branched polar heads, see for review [44]. These series are species- and tissue-specific
14 [10, 45-48]. In Arabidopsis, series A Man-GlcA-IPC is predominant in leaves [45, 49], and GlcN(Ac)-
15 GlcA-IPC is mainly in seeds and pollen [50], as well as in vegetative tissues of rice [51] and tobacco
16 [45]. The core structure of series B, predominant in monocots is yet to be deciphered. A broad study
17 of the GIPC polar head of 23 plant species from algae to monocots [46] further showed that polar
18 head structures are largely unknown and versatile for the different biological taxa and may contain
19 up to 19 sugars [52].

20 The polar head also accounts for the high polarity of the GIPCs and its subsequent insolubility in
21 traditional lipid extraction solvents, such as chloroform/methanol (2/1, v/v). Hence, even 50 years
22 after their discovery, the structure and character of GIPC remain elusive. GIPCs are not commercially
23 available but different purification procedures have been published [45, 49, 52-54]. With the
24 emergence of more comprehensive extraction techniques and technological advances in the field of
25 sphingolipidomics over that past decade, more accurate quantification of sphingolipids and the
26 discovery of novel structures are underway.

27 While the synthesis pathway of gangliosides, their animal homologue, are well studied, that of
28 plant GIPCs remain uncharacterized. The biosynthesis of sphingolipids starts with the condensation
29 of serine and palmitoyl-CoA in the Endoplasmic Reticulum (ER), catalyzed by serine palmitoyl
30 transferase (SPT) forming the 3-ketosphinganine [38]. The second step is the reduction of 3-
31 ketosphinganine by the enzyme 3-ketosphinganine reductase (KSR) generating sphinganine (d18:0),
32 the most basic LCB. The next steps are the modifications of LCBs by the LCB C-4 hydroxylase, Δ 4
33 desaturase, and Δ 8 desaturase arising up to nine different LCB structures [9]. The condensation of an
34 LCB with a fatty acyl chain (in the case of GIPC a VLCFA) by ceramide synthases also known as Lag 1
35 Homolog or LOH 1,2 and 3 produce a ceramide. The specificity of these enzymes relies on the length
36 of the acyl chain and the hydroxylation degree (di- or tri-hydroxylation) of the LCB [55]. Ceramides
37 can also be phosphorylated in the ER by ceramide kinases CERK or ACD5 [56]. There can also be a
38 hydroxylation of the alpha-carbon of the fatty acyl chain [35] [45] yielding hydroxyl-ceramide. The
39 hydroxylation of sphingolipids likely plays a role in the interaction of the hydroxyl group between
40 GIPCs and with sterols in the PM [57] [39]. The enzymes responsible for the hydroxylation have been
41 identified in Arabidopsis, named FAH 1 and FAH2. As biosynthetic intermediates, ceramides are used
42 in the synthesis of the two major PM sphingolipids: GluCer and GIPC accounting for 5-10% and 40
43 mol% of PM lipids, respectively [58]. By contrast, the synthesis of GluCer is located in the ER and is
44 catalyzed by plant a glucosylceramide synthase (GCS) with sterol glucoside (SG) acting as a glucosyl
45 donor [59]. The ceramides are converted to GIPCs by several glycosylation steps in the Golgi

481
482
483 1 apparatus. The first enzyme involved in the synthesis of GIPCs is the inositol phosphorylceramide
484 2 synthase (IPCS) converting ceramide into inositol phosphorylceramide (IPC). This enzyme first
485 3 identified as ERH1 (enhance RPW8-mediated Hypersensitive response-like cell death) in plant holds a
486 4 key role in modulating plant programmed cell death associated with defense [60]. The pool of
487 5 ceramide for GluCer or GIPC synthesis is determined by the hydroxylation state of the LCB and acyl
488 6 chain length. In Arabidopsis seedlings, trihydroxy-LCBs (mostly t18:1) are predominant in both GIPCs
489 7 and GlcCers. GIPC are characterized by the presence of t18:0 largely associated with VLCFAs while
490 8 GlcCer are composed of dihydroxy-LCBs (d18:1 Δ 8) in association with LCFAs (C16) [9]. In both cases,
491 9 the KO mutation of GCS or IPCS leads to dramatic functional and developmental impairments.

494 10 The second enzyme of the GIPC synthesis pathway is the inositol phosphoceramide
495 11 glucosyltransferase (IPUT1). IPUT1 encodes an IPC glucuronosyltransferase activity, transferring an
496 12 alpha-glucuronic acid (GlcA) residue onto the IPC backbone. It is the first GIPC glycosylation enzyme
497 13 to be characterized. The silencing of IPUT1 triggers the accumulation of IPC in *Nicotiana*
498 14 *benthamiana*, as well as ceramides and GluCer. Its overexpression increases GIPC content. In
499 15 Arabidopsis, IPUT1 is essential for pollen tube viability. The major defect of the *iput1* mutant pollen is
500 16 a disfunction in tube guidance and ovule fertilization [61]. Further glycosylation patterns of GIPCs
501 17 and glycosyltransferases involved are still not well documented. So far only three more biosynthetic
502 18 enzymes involved in the glycosylation process have been characterized. Understanding the diversity
503 19 of sugar moieties of the polar head and all the biosynthetic pathways involved remain a challenge.
504 20 Golgi-localized nucleotide sugar transporter (GONST1) was shown to be indirectly involved in GIPC
505 21 synthesis by specifically supplying GDP-mannose to the Golgi lumen for GIPC glycosylation.
506 22 Interestingly, in *gonst1* mutants, only mannosylation of GIPC is defective, while that of the cell wall
507 23 polysaccharides remain unchanged [47]. The mutants also have a dwarfed phenotype and display
508 24 spontaneous Hypersensitive Response highlighting the importance of GIPC sugar head groups in
509 25 different plant functions such as defense signaling. Alongside GONST1, Glucosyl-mannosyl
510 26 transferase (GMT1) of the CAZy GT family, located in the Golgi and specifically targeting GIPCs has
511 27 recently been reported to transfer a mannose (Man) onto the GIPC head group by Mortimer team
512 28 [49]. The phenotype of *gmt1* mutant is fairly similar to that of *gonst1* affecting GIPC mannosylation
513 29 level, displaying a constitutive plant immune response and reducing cellulose content. In plants,
514 30 GIPCs are highly glycosylated with the most common pattern being a GlcA-IPC to which additional
515 31 glycan moieties such as Man but also glucosamine (GlcN), N-acetyl glucosamine (GlcNac) and
516 32 arabinose (Ara) can be attached [42, 45]. The most recent GT identified is glucosamine
517 33 inositolphosphorylceramide transferase1 (GINT1). It is involved in GIPC glycosylation in seeds and
518 34 pollen yielding GIPC containing GlcNac and/or GlcN. The study also showed the importance of
519 35 GlcN(Ac) GIPC in Arabidopsis seedling survival but not in its vegetative growth suggesting once again
520 36 the importance of GIPC glycan patterns in essential and specific plant functions [62].

521 37
522 38 Beside biochemical methods (*i.e.* purification of PM coupled with lipidomic analyses), plant
523 39 sphingolipids are hardly located *in vivo* because of lack of appropriate biosensors and fluorescently-
524 40 labeled lipid-probes. Only one publication reported lipid staining protocols and the use of several
525 41 fluorescent lipid analogues in Arabidopsis leaf tissue and protoplasts [63]. As stated earlier, tobacco
526 42 PM contains GIPCs representing up to 40 mol% of total tobacco lipids, enriched in the outer-leaflet
527 43 and interacting with sterols in the formation of microdomains of *ca.* 35 nm. GIPCs are further
528 44 enriched in the DRMs. GIPCs in DRMs are in their polyglycosylated forms [39]. PM biophysical
529 45 modeling approaches propose that acyl terminal ends (six to seven carbon atoms) of the apoplastic

541
542
543 1 leaflet (h)VLCFA of GIPCs penetrate within the inner-leaflet and interdigitate with carbon chains of
544 2 the inner-leaflet phospholipids [39]. This remains to be fully determined *in vivo*. Interdigitation is an
545 3 interesting phenomenon which could explain the limited diffusion of proteins in the PM and thermal
546 4 adaptation [64]. All these aspects of GIPC function will be further discussed in this review.
547
548 5

549 6 **1.3. Free and esterified phytosterols**

550 7 The amount of sterols is relatively stable among plant species i.e. 2–3 mg of total sterols per dry
551 8 gram plant. Synthesized in the ER, sterols accumulate in the PM and reach up to 30mol% of PM lipids
552 9 [58]. Higher-plant cells contain a vast array of sterols: e.g. 61 sterols and pentacyclic triterpenes have
553 10 been identified in maize seedlings [65]. Phytosterols are C₂₇-sterol consisting of the steroid nucleus
554 11 made up of four carbon rings (three with six-carbon and one with five-carbon) and an eight-carbon
555 12 side chain. In most cases, the second ring has a double bond between carbon C5 and C6. Phytosterols
556 13 mainly differ from mammalian cholesterol on the side chain by an extra alkyl group in the C24
557 14 position (Figure 2). For example, campesterol is the phytosterol whose chemical structure is the most
558 15 similar to that of cholesterol, with only an additional methyl group. In contrast, the Δ^5 -sterols, with
559 16 an ethyl group, are represented by β -sitosterol and stigmasterol. Stigmasterol contains an additional
560 17 double bond in the C22 position and is by far the most abundant of plant sterols. Proportions of
561 18 other pathway end-products such as fucosterol are genetically defined in higher plants [66]. In
562 19 comparison with cholesterol, the interesting fucosterol that is the major sterol in algae exhibits
563 20 modifications at the hydrocarbon tail with a branched chain and a double bond at position C24.
564 21 Biosynthesis of phytosterols is described in recent reviews [67].

565 22 Steryl glycosides (SGs) and acylated steryl glycosides (ASGs) are derivatives of a typical
566 23 membrane-bound sterol molecule. The composition of sterols in SG reflects usually the free sterol
567 24 composition of the plant. The sugar moiety, the number of sugar and the configuration of its linkage
568 25 to the sterol may vary. The sugar moiety, most common being the pyranose form of D-glucose, is
569 26 attached to the 3-hydroxy group at the C3-atom of a sterol characterized by a planar sterol backbone
570 27 made up of four condensed aliphatic rings and a hydrocarbon side chain at C17. SGs generally carry
571 28 one or more sugar residues, the steryl D-monoglucopyranoside being the most abundant SG in
572 29 plants. Finally, an acylation of the sugar moiety could increase SG diversity producing ASG forms.
573 30 Indeed, SGs may be acylated, usually at the C60-atom of the sugar moiety with palmitic, oleic and
574 31 less frequently with stearic, linoleic, and linolenic acid. Interestingly, the proportions of SG and ASG
575 32 in PM differ extremely depending on the plant species and the growth conditions [22, 68]. The
576 33 biological role of conjugated sterols has been discussed recently in [67, 69].

577 34 Elucidation of sterol function relies on development of tools for *in situ* visualization. Several
578 35 methods to visualize sterols has been developed, for review [70]. Filipin has been extensively used
579 36 as a specific probe for detection of fluorescent filipin-sterol complexes, including on fixed samples. It
580 37 is the only established tool for sterol visualization in plants [71-74]. Although powerful to visualize
581 38 domains enriched or deprived in sterol, filipin has also been used to measure the asymmetrical
582 39 distribution of sterol using purified Right Side Out (RSO) vs. Inside Out (ISO) PM oat vesicles [75].
583 40 Recently, imaging method using tunable orthogonal cholesterol sensors allowed simultaneous *in situ*
584 41 quantification of cholesterol in two leaflets of various mammalian cell PM [76]. This study revealed a
585 42 marked transbilayer asymmetry of PM cholesterol, with the concentration in the inner leaflet being
586 43 12-fold lower than that in the outer leaflet. The asymmetry was maintained by active transport of
587 44 cholesterol and its chemical retention in the outer leaflet [76]. Development of such sensors for
588
589
590
591
592
593
594
595
596
597
598
599
600

601
602
603
604
605
606
607
608
609
610
611
612
613
614
615
616
617
618
619
620
621
622
623
624
625
626
627
628
629
630
631
632
633
634
635
636
637
638
639
640
641
642
643
644
645
646
647
648
649
650
651
652
653
654
655
656
657
658
659
660

- 1 phytosterols (free and conjugated) is of great importance in order to address the role of these lipids
- 2 in plant biology.
- 3

661
662
663 1 **2. Lipids govern global properties of the plant PM**

664 2 **2.1 Fluidity of PM**

665 3 Confined in a restricted two-dimensional space, PM constituents are mobile and animated with
666 4 membrane fluidity reflecting the dynamic organization of biological membranes [77]. Hydrocarbon
667 5 chains perform balance and bending movements, giving elasticity to the PM. These undulations are
668 6 sources of fluidity and can be measured by atomic force microscopy that regrettably shows its real
669 7 limits of use in plants due to the presence of the cell wall. Lipids and proteins by rotating around
670 8 their axis or moving in the plane of the PM, lead to increase fluidity. Notably, lateral diffusion within
671 9 plant PM was firstly evaluated around the order of $0.02 \mu\text{m}^2.\text{sec}^{-1}$ for the agglutinin receptor of the
672 10 PM of wheat grain cells [78], whereas more recent data gives a more than ten-fold higher value of
673 11 $0.34 \mu\text{m}^2.\text{sec}^{-1}$ for the flagellin receptor FLS2 in Arabidopsis protoplast [79]. Indeed, PM proteins
674 12 exhibit distinct relatively low short-distance lateral mobility within plant PM [80, 81]. Depending on
675 13 the lipid environment, the diffusion of labeled tracer molecule also varies from 0.1 to $6 \mu\text{m}^2.\text{sec}^{-1}$ in
676 14 model membranes [82] highlighting the effect on lipid dynamics of unsaturated and saturated PC and
677 15 cholesterol. Thus, several factors affect PM fluidity, notably the steric hindrance and the interactions
678 16 of its constituents. The huge diversity of plant lipids, many of which deviate from the canonical
679 17 cylindrical form, would thus imply that the PM is bound to be very heterogenous in its geometrical
680 18 arrangement [83]. For example, PC occupies similar volumes at both its extremities *i.e.* its polar head
681 19 and its two acyl chains, corresponding to a cylinder, this geometry generates a spontaneous
682 20 organization in lamellar phase [84]. Furthermore, the level of unsaturation results in a larger steric
683 21 hindrance of the carbon chain, and therefore a greater disorder in the arrangement of the lipids.

684 22 Alterations in lipid composition during cold acclimation, such as the increase at the PM of both
685 23 unsaturated fatty acids and phospholipids have been known to be associated with increase in
686 24 tolerance of plants to cold stress [85]. In particular, accumulation of *N*-
687 25 acylphosphatidylethanolamines (NAPEs) that is related to high lipid unsaturation degree is critical to
688 26 maintain membrane fluidity. Indeed, changes in lipid composition regulate cryobehavior of the PM
689 27 [86] by contributing to maintain the membrane phase transition temperature below the chilling
690 28 temperature [87]. In cold conditions, plant cell PMs accumulate unsaturated fatty acids to decrease
691 29 membrane viscosity [88]. A similar positive effect on membrane stability is achieved by a decrease in
692 30 the unsaturation level of individual phospholipids and total lipids during water deprivation [23].

693 31
694 32 **2.2 Phytosterols are crucial regulators of membrane order**

695 33 Sterols are known to favor the packing effect in the membrane bilayer as firstly described for
696 34 cholesterol in animal membranes [89]. Phytosterols are the major component contributing to plant
697 35 PM rigidity [90-92], Interestingly, major free phytosterols differentially modulate the level of
698 36 membrane order [93-95]. Indeed, campesterol shows a high potency to organize lipid bilayers [93,
699 37 96, 97] which could be attributed to its short hydrocarbon tail. Stigmasterol exhibits a much weaker
700 38 ordering effect than other sterols [93], even if it is a somewhat controversial question [98]. This
701 39 phytosterol carries an extra carbon-carbon double-bond on the side chain in the C22 position,
702 40 similarly with α -spinasterol [99] and brassicasterol [94] that both also display a feeble ordering
703 41 capacity. Langmuir monolayer experiments (Su et al., 2007), ultrasound velocimetry studies [100]
704 42 and thermodynamic analysis [101] [102] propose a better condensing efficiency for β -sitosterol than
705 43 for stigmasterol. Such variable ability to pack lipid bilayer has been explained by differential
706 44 interactions between plant sterols and unsaturated or saturated lipids [103] [104]. It is worth noting
707 45 that phytosterols exist as a mixture within plant PM, and that such ratio of phytosterol relative

721
722
723 1 amounts allows to finely control the level of membrane order in artificial membrane [93], in model
724 2 PM of soybean [104] and in native PM of Arabidopsis mutants [105].

725 3 Properties of the conjugated forms of phytosterols, SG and ASG present in plant PM have also
726 4 been shown to have a strong ability to order membranes [93, 106]. Furthermore, free and
727 5 conjugated phytosterols work in synergy to order the membrane [93]. Regardless of the distribution
728 6 of SG and ASG between different phases of the PM, it seems very likely that the proportion of these
729 7 lipids in certain membrane domains clearly exceeds those of phospholipids and thus could locally
730 8 participate in the control of the biophysical properties of membrane domains. Regarding the scarcely
731 9 documented properties of phytosterols *i.e.* the saturated analogues of sterols reduced in the double
732 10 bond in a ring skeleton, Langmuir monolayer studies have evidenced that β -sitosterol exhibited a
733 11 similar ability to β -sitosterol in strongly interacting with saturated phospholipids [107]. Accordingly,
734 12 incorporation of β -sitosterol into artificial membranes is able to modify their packing level as well as
735 13 their behavior [108]. Overall, the multiple phytosterols are essential regulators of membrane order
736 14 and therefore play a significant role in the partitioning of the PM in order to ensure homeostasis and
737 15 dynamic functions.
738 16

739 17 **2.3. Involvement of sphingolipids in PM membrane order**

740 18 Plant sphingolipids also interact with phytosterols to increase the level of plant PM order [90-
741 19 93, 109]. In mammalian models, cholesterol appears to interact preferentially with sphingolipids over
742 20 phospholipids [110]. Several parameters have been proposed to explain such affinity: 1/ sterols
743 21 emphasize a better shielding from water by the bulky sphingolipid head group; 2/ a pairing between
744 22 the two lipids *i.e.* hydrogen bonding between these lipid species, with the low amount of water at
745 23 the PM interface increasing the stability of these bonds. The interface within the region of the
746 24 membrane of the amide bond of the sphingolipid LCB can both donate and accept a hydrogen bond
747 25 as well as the hydroxyl groups of the LCB and Fatty acids; 3/ the saturation of sphingolipid
748 26 hydrophobic tails which increases the order level [111].

749 27 In plants, GIPCs also show an ability to increase, in a sterol-dependent manner, the lipid
750 28 packing of the PM [93] and both mechanisms could be similarly proposed (Figure 3). First, the major
751 29 GIPC polar head is composed of Hexose-glucuronic acid-inositol-phosphate, and up to seven sugar
752 30 moieties can be added [45]. Thus, the volume occupied by the head group of GIPC is far much bulkier
753 31 than phospholipid head groups, and, as a general trend the volume occupied by the phospho-
754 32 inositol-sugar head group increases with the complexity of the oligosaccharide chain. Predictions
755 33 based on the geometrical properties of glycosphingolipid molecules indicated accordingly that local
756 34 enrichment of such bulkier head group strongly favors phase separation and is concomitantly
757 35 accompanied by spontaneous acquisition of a positive membrane curvature (for review [36]).
758 36 Moreover, GIPC LCB profiles are abundant in tri-hydroxylated LCB species in widely varying
759 37 proportions (for review, see [38]), and one hydroxyl residue is very often present at the 2 position of
760 38 the fatty acid. One may hypothesize that the presence of these three hydroxyl and the amide groups
761 39 at the interface between the polar phase and hydrophobic phase of the bilayer may be of
762 40 importance for sphingolipid/phytosterol interactions, see Figure 3, but also sphingolipid/sphingolipid
763 41 interactions [57]. Similar mechanisms have been experimentally confirmed, showing strong
764 42 interactions between phytoceramides and POPC (palmitoyl-oleoyl-PC) into a highly packed gel phase
765 43 ($32.1 \text{ \AA}^2/\text{molecule}$) [112], and between GIPC and sitosterols [58].
766 44

767 45 **2.4. Electrostatic charge and pH domains of the PM**

781
782
783
784
785
786
787
788
789
790
791
792
793
794
795
796
797
798
799
800
801
802
803
804
805
806
807
808
809
810
811
812
813
814
815
816
817
818
819
820
821
822
823
824
825
826
827
828
829
830
831
832
833
834
835
836
837
838
839
840

1 In all eukaryotes, the PM cytosolic-leaflet is the most electronegative compartment of the cell
2 [113]. Electrostatic territories are controlled by a combination of negatively charged lipids that are
3 organized as a gradient along the endocytic pathway. Membrane surface charge (MSC) is critical for
4 the specific recruitment to membranes of proteins with polybasic regions. Thus, PM electrostatics is
5 fundamental parameter in signaling, intracellular trafficking and polarity. For example, MSC controls
6 the PM localization and function of the polar auxin transport regulator PINOID as well as proteins
7 from the BRI1 kinase inhibitor 1 (BKI1)/Membrane-associated kinase regulator (MAKR) family, which
8 are involved in brassinosteroid and receptor-like kinase signaling [114]. MSC can be probed by
9 biosensors constituted of a fluorescent protein fused to an unstructured peptide of varying net
10 positive charges [114]. Negatively charged lipids regulate the MSC in plant PM. By contrast to yeast
11 and animals, PI4P strongly accumulates at the PM establishing a negative inner surface potential of
12 this membrane [114]. In addition, it was recently shown that PM surface potential varies according to
13 other negatively charged PM lipids such as PA and PS which are separately required to generate the
14 electrostatic signature of the plant PM [115]. Therefore, the combinatorial lipid composition of the
15 cytosolic leaflet of PM not only defines electrostatic territory but also distinguishes different
16 compartments within this territory by specifying their MSC. How the spatiotemporal pattern of PIPs
17 is established and maintained within plant cell is one of the many future challenges to tackle.

18
19 A recent study showed that the pH on both sides of the plant PM is different *in vivo*. Genetically
20 encoded fluorescent pH sensors enable access to membrane-associated pH and transmembrane
21 differential pH values from the surface of the root to the deepest cell layers beyond the Casparian
22 strip barrier [116]. This study demonstrated that the apoplastic pH close to the PM was maintained
23 at values ranging from 6.0 to 6.4 in mature root cells despite direct contact with the soil. By contrast,
24 the overall pH in the apoplastic space is far more acidic [116]. The role of lipids in this observation
25 remains to be determined.
26

3. Plant lipids are unevenly distributed within the PM and able to organize into domains

3.1 Asymmetric composition of inner and outer leaflets

During the 1970's, alongside the fluid mosaic model proposed by Singer and Nicholson (1972), experimental evidences showed that proteins and specially lipids could segregate forming a heterogeneous membrane with both lateral and transversal asymmetry. It is also well established in animal cells that there is a compositional heterogeneity of PM lipids between the two leaflets of the PM. In human erythrocyte membranes, the prototype of animal cell PMs, the outer-leaflet is composed of mostly phosphatidylcholine (PC) and sphingolipids, while the inner-leaflet of phosphatidylserine (PS), phosphatidylethanolamine (PE), and phosphatidylinositol (PI) as described in [117]. Minor lipids such as PIPs and PA are located in the inner-leaflet, whereas glycosphingolipids face the outer surface. This out-of-equilibrium is maintained by the activity of lipid translocases (namely flippases, floppases and scramblases), which compensate for the slow spontaneous diffusion of lipids. Because of the heterogeneity of lipids, the two monolayers display different physical properties: the inner-leaflet has a lower average viscosity than the outer-leaflet. The importance of membrane asymmetry is well studied in animals, see for recent reviews [118] [119].

In plants, only two publications experimentally address the asymmetry of lipids in the PM: by using a phospholipase A2 treatment, filipin labeling and immuno-labeling with antibodies against DGDG and gluCER on purified oat PM, it was shown that DGDG was exclusively located in the inner-leaflet together with 60% of phospholipids, and the GluCER and sterols were enriched in the outer-leaflet [75]. Unfortunately, GIPCs and the exact phospholipid content were not addressed in this study. GIPC are synthesized inside the Golgi apparatus, with their polar heads inside the lumen, see Figure 4, therefore it is very likely that these lipids are located in the outer-leaflet of the PM after fusion of the secretory vesicles. Moreover, the large size of the GIPCs' polar heads likely prevents spontaneous flip between the two leaflets. Immunogold labeling on tobacco PM vesicles showed that polyglycosylated GIPCs mostly locate in the outer-leaflet of the PM [39].

By taking together these scarce experimental evidences, we recently proposed a model for the distribution of lipids in the plant PM where GIPCs and GluCER are exclusively located in the outer-leaflet; sterols (free and conjugated) are enriched in this leaflet; phospholipids are enriched in the inner-leaflet with PIPs, PS, PA exclusively in this leaflet [39]. Future work should be dedicated to the in depth analysis of the lipid composition of each PM leaflet with special focus on deciphering the diversity of the various molecular species *i.e.* fatty acid content (unsaturation and length) of each class of lipids will be done and the different forms of sterols will be characterized. Numerous methods are available on RSO vs. ISO purified PM vesicles or on live protoplasts cells to address this delicate question [120].

3.3 Membrane phases in model and biological membranes

3.3.1 Membrane phases, dyes and modeling approaches

Assembly of lipids can adopt different physical states, the so-called phases. Following the nomenclature introduced by Ipsen [121], lipid organization of lamellar bilayer structures can be divided in three main phases: the solid-ordered (So), liquid-ordered (Lo) and liquid-disordered (Ld) phases depending on the lipid species, acyl chain unsaturation, temperature, pressure and several additional parameters. In So phases, lipids are tightly packed and lateral diffusion is very slow. In Ld phases, lipids are much less condensed, acyl chains are mobile and loosely packed, and lateral diffusion coefficients are high, especially at high temperatures [122]. In Lo phases, like in So phases, a high degree of acyl chain order is observed, but lateral diffusion coefficients are comparable to those

901
902
903 1 of Ld phases. Phase formation in lipid mixtures has been extensively studied *in vitro* with liposomes
904 2 and giant unilamellar vesicles (GUV) as models. In most reports, GUV membranes exhibit
905 3 micrometer-size liquid immiscibility over a wide range of temperatures. GUVs with such properties
906 4 contained a minimum of three components: high-melting temperature lipids (e.g. saturated VLCFA-
907 5 containing sphingolipids), low melting temperature lipids (e.g. not necessarily but often unsaturated
908 6 phospholipids), and sterols (for more details see review [123]). Lo phases are also referred to as
909 7 cholesterol-dependent phases because cholesterol was used in most studies on the subject, [124,
910 8 125] for reviews. In the mammalian model, lateral partitioning of Lo and Ld phases is thus explained
911 9 by a preferential interaction of sphingolipids with cholesterol over phospholipids, likely due to better
912 10 shielding from water by the sphingolipid headgroup [93].

915 11 Lo phases are also observed in the presence of various free- and conjugated-phytosterols such as
916 12 SG and ASG [93, 126, 127]. Use of environmental fluorescent probes sensitive to membrane order
917 13 such as di-4-ANEPPDHQ and Laurdan [128] allow the analysis of phase separation on GUVs made of
918 14 various mixtures of plant lipids. This reveals contrasted abilities of free-phytosterols to control phase
919 15 separation on model membranes. Although stigmasterol added to DOPC/DPPC vesicles fail to induce
920 16 the lateral segregation of lipids into domains of different order levels, GUVs containing sitosterol and
921 17 campesterol promote the formation of Lo domains at the surface of model membranes [93].
922 18 Noteworthy, SG and ASG added separately exhibit the same ability as the corresponding free sterols,
923 19 increasing the amount of Lo phase. This effect is reinforced when used in combination and increases
924 20 strikingly when free and conjugated sterols are present in the mixture [93]. The same study indicates
925 21 that GIPCs, the major plant sphingolipids [2] are not able alone to promote the formation of a liquid-
926 22 ordered phase within a phospholipid bilayer revealing no extensive phase separation in the binary
927 23 sphingolipid/phospholipid system. By contrast, this study shows the ability of GIPCs to increase the
928 24 amount of Lo phase of the membrane in presence of phytosterol and interestingly this remains still
929 25 the case even in the absence of saturated phospholipids such as DPPC. These *in vitro* studies expose
930 26 the complex association of different classes of lipids necessary to form distinct phases that are *in vivo*
931 27 linked to various membrane functions such as cell signaling or development. Yet there is a real
932 28 benefit to be able to observe this partitioning *in vivo via* fluorescent probes and dyes.
933 29

938 30 The partitioning of lipid fluorophores between coexisting Lo and Ld phases for different ternary
939 31 lipid mixtures has been extensively performed by comparing fluorescence intensities in coexisting
940 32 domains. These labeled lipids have a fluorophore (e.g. NBD, Texas Red, Bodipy, etc...) attached either
941 33 to the head group or to the hydrocarbon chain. Studies using fluorescently labeled lipid analogues in
942 34 different mixtures must be analyzed cautiously for several reasons: 1/ the fluorophore might alter
943 35 the distribution of the lipids on which it is grafted *i.e.* a large fluorophore attached to an acyl chain
944 36 might hamper the incorporation of the labeled lipids into the Lo domains, as found in the case of
945 37 fluorescent ganglioside probes [129]; 2/ It has been shown that the same fluorescent probe might
946 38 have different partitioning preferences depending on the chosen lipid mixture [130]. Nevertheless,
947 39 an important finding from this body of research is that partitioning in ordered-phases is increased for
948 40 fluorophores with saturated chains that approximately match the thickness of one leaflet of the host
949 41 membrane [131]. Fluorescent lipid probes with unsaturated chains are found to partition into the Ld
950 42 phase. These studies indicate the ability of different molecular species of lipids to partition
951 43 selectively in the different phases of a complex model membrane, according to their structure [132]
952 44 [133].

955 45 There is a current lack of such fluorescent probes designed from typical structures of plant PM

961
962
963 1 lipids. This prevents unambiguous assessing of specific lipid behaviors in different complex mixtures.
964 2 Non-perturbing specific-labeling of PM nanodomains in plant cells has been, and remains, one of the
965 3 foremost challenges in the field.
966 4

967 5
968 6 Modeling approaches based on simulation can also bring grist to the mill of such
969 7 experimental evidence. For example, very recent work by Ingolffson et al., in a pioneering *in silico*
970 8 study of PM-lipid assembly mimicking the complexity of the animal PM, confirmed the non-ideal
971 9 lateral mixing of the different lipid species [134]. Based on large-scale molecular
972 10 dynamics simulation, this study provided a high-resolution view of the lipid organization of the PM
973 11 at an unprecedented level of complexity since the model consists of 63 different lipid species, 14
974 12 types of head groups and 11 types of aliphatic moieties asymmetrically distributed across the two
975 13 leaflets. This closely mimics an idealized mammalian PM. A general non-ideal lateral mixing of the
976 14 different lipid species was observed together with the formation and disappearance on the
977 15 microsecond time scale of transient domains with liquid-ordered characteristics whereas distinct
978 16 perennial nanodomains consisting of gangliosides were observed. Nonetheless, the lack of
979 17 biophysical parameters for plant lipids necessary for the calculation of molecular dynamics impairs
980 18 the use of these approaches to modelize plant PM (see section "Conclusions").

981 19 3.3.2 Solubilization by detergents: evidences from model membranes

982 20 Detergents are amphiphilic molecules, most of them consisting of a polar head and a hydrophobic
983 21 chain. These molecules have a conical shape and spontaneously form micellar structures displaying a
984 22 positive curvature in aqueous solution. Detergents have thus the ability of incorporating themselves
985 23 into membranes and of solubilizing proteins by replacing their lipid environment. Pioneering work
986 24 evidencing correlations between resistance to detergent solubilization of a fraction of the PM and its
987 25 peculiar lipid and protein composition suggested the possible existence of lipid domains in the PM of
988 26 mammalian cells [135].

989 27 Detergent-resistant membrane fractions (DRMs) could be isolated from a variety of eukaryotic
990 28 cells and gave birth to the hypothesis that such fractions are present within native PM as a distinct
991 29 phase within the bilayer. DRMs are rich in saturated phospholipids, sphingolipids and sterols, and
992 30 display the properties of the Lo phase previously described in model membranes. Such a hypothesis
993 31 received strong support from parallel studies on lipid vesicles constructed to mimic the lipid
994 32 composition of these membranes [136]. In particular, [137] demonstrated that when mixtures of
995 33 sphingolipids, unsaturated phospholipids and cholesterol were treated in the cold with nonionic
996 34 detergents such as Triton X-100, the lower-melting phospholipids were readily solubilized while the
997 35 higher-melting sphingolipid species, and to a lesser extent cholesterol, were largely recovered in an
998 36 insolubilized and sedimentable fraction. Similar results were obtained using analogous lipid mixtures
999 37 without cholesterol, or in which long-chain saturated phospholipids replaced the sphingolipid
1000 38 component. Measurements of diphenylhexatriene fluorescence polarization have suggested that the
1001 39 existence of a DRM fraction was correlated with the presence of Lo phases in the original bilayers.
1002 40 Since that, numerous studies have addressed the differential sensitivity of Lo and Ld domains to
1003 41 detergent solubilization. Nevertheless, only a few reports, like that of [138] compared the effect of
1004 42 distinct detergents on Ld and Lo domain solubilization within model bilayers. Most works indeed
1005 43 focused solely on the impact of Triton X-100. Atomic Force Microscopy (AFM) observations on
1006 44 vesicles containing dioleoyl-PC/sphingomyelin/cholesterol provided evidence for both Triton X- 100-
1007 45 insoluble domains composed of sphingomyelin and cholesterol, and Triton X-100-soluble areas

1021
1022
1023 1 surrounding them [139]. Similarly, using real-time AFM imaging of dioleoyl-
1024 2 PC/sphingomyelin/cholesterol mixtures, [140] found that detergent did not affect
1025 3 sphingomyelin/cholesterol Lo phases, while dioleoyl-PC Ld phases were completely solubilized.
1026 4 Developing the same experimental approach on dioleoyl-PC/dipalmitoyl-PC vesicles, authors showed
1027 5 that Triton X-100 concentrations right above the critical micellar concentration (CMC) enabled the
1028 6 solubilization of the dioleoyl-PC matrix, but prevented dipalmitoyl-PC domains from solubilization
1029 7 [141]. [142] proposed a model based on equilibrium thermodynamics showing that resistance to
1030 8 solubilization only depends on the target lipid affinity with the micellar phase. The effects of
1031 9 cholesterol on the resistance of lipid mixtures to solubilization have also been investigated.
1032 10 Ahyayauch et al. demonstrated that cholesterol facilitates PC solubilization better than
1033 11 sphingomyelin [143]. Furthermore, cholesterol was found to induce higher resistance to
1034 12 solubilization of dipalmitoyl-PC vesicles, with a notable exception at 4°C. Interestingly, cholesterol
1035 13 also induced higher resistance of palmitoyl-oleoyl-PC bilayers to detergent solubilization on a
1036 14 broader range of temperatures (from 4 to 15 °C) [144]. In addition, sterols are not the only lipid
1037 15 family determining detergent insolubility. For example, it was shown that addition of 5–30 mol%
1038 16 ceramides prevented Triton X-100 from completely solubilizing sphingomyelin-containing bilayers
1039 17 [145]. It is noteworthy that microscopic observations carried out by Staneva et al. [144] revealed
1040 18 neither domain formation, nor domain coalescence in response to Triton X-100 treatment in
1041 19 heterogeneous GUV systems.

1042 20 Cholesterol is not the only sterol to induce resistance to detergent solubilization. Plant sterols,
1043 21 like campesterol, sitosterol, stigmasterol have a similar effect to cholesterol, when incorporated in
1044 22 palmitoyl-oleoyl-PC vesicles [98]. All these results, based on biophysical analysis performed on model
1045 23 membranes indicate: 1/ that animal and plant PM-mimicking lipid mixtures undergo a segregation
1046 24 between different phases corresponding to different physical states; 2/ that the different lipids
1047 25 present within the bilayer partition differentially in these phases according to their chemical
1048 26 structure; 3/ that there is a close correlation within the composition and physical characteristics of
1049 27 the DRM fraction isolated from model membranes and the ones displayed by the Lo phase.

1050 28 1051 29 3.3.3 Isolation of Detergent Resistant Membranes from PM, biochemical fractions with a specific 1052 30 lipid composition.

1053 31 Based on the conceptual framework exposed in the previous sections, a tremendously high
1054 32 number of publications (about 2000 in the last 40 years) reported the isolation and characterization
1055 33 of DRMs from biological membranes from a wide variety of animals, plants and microorganisms
1056 34 [146]. Virtually all protocols rely on a similar experimental procedure: treatment of either intact cells
1057 35 or purified membranes with a nonionic detergent (most frequently Triton X-100, but Triton X-114,
1058 36 Brij or Lubrol has also been used), generally at low temperature (4°C) followed by ultra-
1059 37 centrifugation on a sucrose (or Ficoll) gradient to recover the insoluble fraction [147]. Parameters
1060 38 which have been proven to be crucial and were carefully adapted on each material concern mainly
1061 39 the concentration of detergent and the detergent-to-membrane ratio used. The protein yield
1062 40 recovered in the insoluble fraction may vary between 5 and 20% of the initial amount of membrane
1063 41 proteins, depending on the biological material and the experimental conditions. In animal cells,
1064 42 extensive characterizations of lipids associated to DRMs consistently revealed a 3- to 5-fold
1065 43 enrichment in lipids associated to the Lo phase of model membrane, in particular cholesterol,
1066 44 saturated phospholipids, gangliosides and sphingomyelin [148] [149]. Analyses of the phospholipids
1067 45 content of DRMs classically exhibit a decrease in anionic phospholipids compared to the whole

1081
1082
1083 1 membrane [150], an increase of the proportion of saturated fatty acids [151], and a typical
1084 2 enrichment in GM1 gangliosides [152]. The biochemical analysis of such DRMs extracted from animal
1085 3 cell membranes have been extensively performed using proteomics approaches (see for review
1087 4 [153]). It emerged from this huge amount of data that some typical proteins, such as caveolin, or
1088 5 protein families, such as kinases of the Src family or small G-proteins, are in a reproducibly enriched
1089 6 in such fractions, together with some proteins harboring particular post-translational modifications
1090 7 such as GPI-anchored proteins. We can note here that some free detergent methods to isolate sub-
1091 8 fraction of the PM have also been developed. [154] [155] [156].

1093 9 In plants, DRMs were first purified in tobacco, with the first isolation reported by [157] and
1094 10 the characterization of DRM-associated proteins and lipids provided by [19]. Similar studies revealing
1095 11 by mass spectrometry the catalogue of proteins were then performed on different species such as
1096 12 *Arabidopsis thaliana* [158] [159] [160] [161] [162], *Medicago truncatula* [163] [164], *Oryza sativa*
1097 13 [165], *Avena sativa* and *Secale cereale* [166] or more recently *Beta vulgaris* [167]. According to the
1099 14 methodology used, the amount of proteins may differ between the studies but the continuous
1100 15 improvement of performance and sensitivity of the mass spectrometry approaches, led to an
1101 16 increase of the number of proteins identified which reached more than 300 proteins in the more
1102 17 recent studies [160] [161] [168]. The latest extensive analysis published on plant PM proteome,
1103 18 performed in rice, allowed the identification of more than 3900 proteins, which is quite consistent
1104 19 with the yield of PM-derived DRM proteins which is typically around 10% of total proteins in most
1106 20 studies [19] [169]. The family of proteins identified in the different studies is also quite consistent,
1107 21 with a high proportion of proteins involved in signal transduction, responses to different stress, and
1108 22 plant-microorganism interactions. Accordingly, a few studies implementing quantitative proteomics
1109 23 approaches based on different methodologies, clearly revealed a qualitative and/or quantitative
1110 24 modification of the proteins associated to DRMs upon environmental modifications, for instance in
1112 25 the early steps of plant defense signaling [168] [161] [165], or following abiotic stress [170] [167].
1113 26 Note that by contrast with proteins where genetically encoded fluorescent tags or specific antibodies
1114 27 are available, generating DRMs is the most used technique in order to study the potential
1115 28 segregation of lipids. In the next chapters, we will discuss the lipids found in DRMs purified from
1117 29 plant PMs.

1119 31 3.2.3.1. Glycerolipids in plant DRMs

1120 32 As expected from biophysical work, major structural phospholipids, *i.e.* PC, PE, PS, PA are
1121 33 markedly depleted in plant DRMs when compared to the total PM [19] [159]. The case of
1122 34 phosphoinositides (PIPs) deserves a particular attention. Despite the real challenge related to the
1123 35 detection of such a minor class of lipids in very reduced biological sample such as DRMs, the
1125 36 combined use of Thin-Layer Chromatography to separate the different classes of phosphoinositides
1126 37 prior to quantitative Gas Chromatography-Mass Spectrometry analysis [171] allows to quantify PI4P
1127 38 and PI(4,5)P₂ in DRMs isolated from tobacco leaves and BY-2 cells [31]. It was shown that both PIPs
1128 39 isomers represent less than 5 mol% of the total lipids of tobacco PM. However, their relative amount
1130 40 is 11-fold higher in DRMs compared to PM from which they originate. Hence, it is estimated that 50
1131 41 mol% of PM phosphoinositides likely segregate in BY-2 cell PM-domains. A lower increase in PI4P and
1132 42 PI(4,5)P₂ was also observed in tobacco leaf DRMs: 43 and 31 mol% of the isomers were found to
1133 43 concentrate in this fraction respectively. Moreover, PIPs display highly saturated fatty acids in both
1134 44 DRMs and PM, with 16:0, 18:0 and 18:1 being the major fatty acids, which is all the more consistent
1135 45 with the packed lipid environment or liquid-ordered phase characteristic of this fraction. This work

1141
1142
1143 1 has demonstrated that PIPs are the only glycerolipids enriched in plant DRMs, which is in agreement
1144 2 with biochemical studies performed on animal cells. In good agreement with this result, the
1145 3 nanodomain-protein marker from the potato REM group 1 isoform 3 (StREM1.3 or REM) was shown
1147 4 to cluster in the PM inner-leaflet nanodomain by specific binding to PI4P [172]. The question arises
1148 5 whether PI4P is clustered in PM-nanodomains before the anchoring of REMORIN, or whether REM's
1149 6 C-terminal anchor promotes PI4P clustering. In line with the results obtained for PIPs, striking
1150 7 evidence related to the characteristics of the fatty acyl chains associated to DRM glycerolipids have
1151 8 been obtained. Indeed, the comparative analysis of polar lipids from tobacco leaves or BY-2 cells
1152 9 revealed a very significant enrichment in saturated fatty acids (C16:0 and C18:0), in agreement with a
1154 10 DRM phospholipids double-bond index lower than that of the overall PM [19]. This was consistently
1155 11 observed in maize embryos and bean leaves with the total amount of saturated long-chain fatty acids
1156 12 being higher in the PM than in DRMs, and with the saturated/unsaturated ratio rising from 1.4 in PM
1157 13 to 6.5 in the DRMs from bean leaves and from 0.3 in the PM to 1.0 of maize embryo [173]. These
1158 14 characteristics perfectly fit with the direct relationship classically observed in model membranes
1160 15 between the proportion of lipids with saturated fatty acyl chains and the global order of the bilayer
1161 16 which has been confirmed using lipids from plant PMs [93].
1162 17

1163 18 3.2.3.2 Sterols in plant DRMs

1165 19 In all plant tissues tested, free sterols are major components of isolated DRMs. Quantitative
1166 20 analyses showed a clear increase in the sterol-to-protein ratio to around 1.7-fold in DRMs prepared
1167 21 from both tobacco leaves and *Medicago truncatula* roots [19] [163] or even 2.7- and 4-fold
1168 22 enrichment in DRM fractions from bean leaves and Arabidopsis cell cultures [158] [174]. On the
1169 23 other hand, maize embryo [174] and Arabidopsis seedlings [170] exhibited a smaller free-sterol
1170 24 accumulation with only an 1.3-fold enrichment in DRM fractions indicating a range of plant sterol
1172 25 enrichment factors as broad as that observed in animal cells. In general, relative abundances of
1173 26 individual free-sterol species such as stigmasterol, campesterol and sitosterol in DRM and PM
1174 27 fractions are similar [19] [158] [159] with the noticeable exception of maize embryo membranes
1175 28 [174]. Moreover, additional results reinforced the possible role of phytosterol in the structuration of
1176 29 plant PM domains suggested by their enrichment in DRMs. They were essentially provided by the use
1178 30 of the pharmacological compound methyl- β -cyclodextrin. This cyclic oligosaccharide able to trap
1179 31 sterols from artificial and biological membranes has been widely used to lower the content of
1180 32 membrane cholesterol in various types of animal cells and to assess sterol-associated membrane
1181 33 structuring, see for review [175] to read about the specific and nonspecific effects of cyclodextrins.
1182 34 This molecule has been proven to remove from isolated plant PM, with a comparable efficiency to
1184 35 that associated with cholesterol, the major free phytosterols (campesterol, stigmasterol, sitosterol
1185 36 and isofucosterol) [91]. Such a treatment resulted in a decrease by about 50% of BY-2 cell PM sterols,
1186 37 without affecting PM-content in conjugated sterols, phospholipids, sphingolipids and proteins.
1187 38 Importantly, methyl- β -cyclodextrin treatment totally abolished the recovery of any DRM fraction
1189 39 after PM solubilization at 4°C with Triton X-100 [91]. Moreover, the use of environment sensitive
1190 40 fluorescent probes allowed to associate this depletion in free-sterols with a decrease in liquid phase
1191 41 heterogeneities, and particularly in Lo phases [91]. This work on isolated PM has been further
1192 42 corroborated by similar results obtained on living BY-2 cells showing a clear decrease of the
1193 43 proportion of ordered PM-domains by cyclodextrin treatment that reduced by ca. 20% the amount
1195 44 of PM sterols [90]. Finally, the combination of cyclodextrin and extensive quantitative proteomic
1196 45 characterization of DRMs isolated from Arabidopsis PM identified a subset of proteins, whose
1197
1198
1199
1200

1201
1202
1203 1 association to DRMs is sterol-dependent [160] [162].

1204 2 As exposed in Section 1.3, phytosterols can be conjugated with sugars, which in turn can be
1205 3 acylated to form SG and ASG (for a review see [69]). Lipidomic analyses have shown varying amounts
1206 4 of SG and ASG in plant DRMs. In *M. truncatula* roots, the same enrichments in SG, ASG and free-
1207 5 sterols were observed in DRMs compared to PM fractions [163]. Conversely, while free-sterols did
1208 6 not show any significant enrichments in DRMs from *Arabidopsis thaliana* seedlings and plants, SG
1209 7 and ASG were found considerably enriched (more than 4-fold) in these fractions [159] [170]. In oat
1210 8 roots, conjugated-sterols were observed in similar proportions in PM and DRMs whereas a clear
1211 9 enrichment of free-sterols was reported [75]. Furthermore, total sterol amounts were markedly
1212 10 increased in tobacco leaf DRMs, mainly because of the high-enrichments in free-sterols and ASG [31].
1213 11 As exposed in section 2.1, conjugated-sterols in combination with free-phytosterols are potent
1214 12 modulators of the order level of model membranes, suggesting again a close relationship between
1215 13 the composition of the DRM fraction and the presence of a Lo phase in plant PM.
1216 14

1217 15 3.2.3.3 Sphingolipids in plant DRMs

1218 16 By contrast with DRMs extracted from animal cells, plant DRM sphingolipid content has only been
1219 17 investigated in very few studies. A first line of evidence of the enrichment of sphingolipids in DRMs
1220 18 relies on the characterization of their VLCFA content. By analyzing highly-purified PM from bean
1221 19 leaves and germinating maize embryos, a 3- to 4-fold increase of VLCFA relative amount in DRMs
1222 20 compared to PM was evidenced [173]. Moreover in the two plant species considered, VLCFAs
1223 21 harboring 20- to 32-carbon chains were present in DRMs. A significant enrichment of VLCFAs (from
1224 22 C20:0 to C26:0) in DRMs compared to PM was also observed in tobacco leaves and BY-2 cells [58].
1225 23 Among the hundreds of sphingolipid species that exist in plants many possess 2-hydroxy fatty acids,
1226 24 containing a hydroxylated C-2 position [9] which contributes to the rigid binding of sphingolipids
1227 25 between themselves and other lipids through hydrogen-bonding between hydroxyl groups,
1228 26 evidenced in artificial membranes [176, 177]. It is thus likely that 2-hydroxy sphingolipids contribute
1229 27 to the ordered structure of PM domains. Using mutant rice lines in which the levels of sphingolipids
1230 28 containing 2-hydroxy fatty acids were decreased by knocking-down two genes encoding fatty acid 2-
1231 29 hydroxylases (FAH1 and FAH2), [51] demonstrated that the DRM/PM ratio was altered in these lines.
1232 30 This result suggested a role for such lipids in structuring Lo phases within the PM, which was further
1233 31 confirmed by the observation using the environmental probe ANEPPDHQ that the PM in OsFAH1/2-
1234 32 KD1 was significantly more disordered than in the wild type.

1235 33 GluCer belongs to the monosaccharidic cerebroside family, and many GluCer species have been
1236 34 reported in plants, since lipidomics approaches showed that GluCer can exhibit a wide range of LCB
1237 35 and fatty acid composition [38]. Their relative abundance in plant PMs has not been unequivocally
1238 36 determined, varying significantly from one species to another and also according to the
1239 37 photosynthetic activity of the tissue considered [178]. In line with those observations, various
1240 38 quantitative data have been reported concerning the enrichment of GluCer in DRMs. In DRMs
1241 39 isolated from tobacco leaves and BY-2 cells [19] or *Medicago truncatula* roots [163], GluCer was only
1242 40 slightly enriched. On the other hand, GluCer was found significantly enriched in *Arabidopsis* and leek
1243 41 DRMs prepared from PM and microsomal membranes [158] [170]. DRMs isolated from leek Golgi
1244 42 membranes also showed 4-, 5-fold GluCer enrichment [159] and DRMs isolated from tobacco pollen
1245 43 tubes harbor a percentage of GluCer which increased up to two fold with the detergent/protein ratio
1246 44 [179]. Taking into account these data, it is difficult to conclude whether or not GluCer enrichment
1247 45 can be considered as an essential component of plant DRMs, even if its relative proportion increased

1261
1262
1263 1 in this fraction compared to the PM, in most studies performed.

1264 2 The first indication of an enrichment of GIPCs in plant DRMs was reported by [158], showing an
1265 3 approximately 5-fold higher LCB-to-protein ratio in DRMs extracted from Arabidopsis microsomal
1266 4 fractions. The relative decrease of (8Z)-4-hydroxy-8-sphingenine (abbreviated t18:1c) in the DRMs
1267 5 compared with microsomes and the increase of the ratio of this LCB compared with its stereoisomer
1268 6 (8E)-4-hydroxy-8-sphingenine (t18:1t) in the DRMs suggested that DRMs might contain a high
1269 7 proportion of GIPCs, which have a greater 8Z:8E ratio than cerebrosides [158]. However, although
1270 8 GIPCs belong to one of the earliest classes of plant sphingolipids that were identified [41], their study
1271 9 has for long been impaired by their limited solubility in typical lipid extraction solvents, and very
1272 10 recent progress concerning their structural characterization and role in membrane organization relies
1273 11 on the development of efficient protocols of purification [42] [53]. By taking advantage of such
1274 12 methodological developments, [39] showed that the hVLCFA and VLCFA contents were highly
1275 13 comparable between DRMs and purified GIPCs, with an even higher proportion of hVLCFAs in DRMs
1276 14 purified from BY-2 cells, suggesting that hVLCFA-containing GIPCs are most likely present in this
1277 15 fraction. Moreover, levels of the two LCBs t18:0 and t18:1, which are mostly present in GIPCs [45],
1278 16 strongly increase in DRMs when compared with PM, reaching 80% of total LCBs in DRMs. A further
1279 17 characterization indicated that series A GIPCs were found in both PM and DRM fractions of tobacco
1280 18 leaves, whereas for BY-2 series B GIPCs were 3-fold enriched in DRMs when compared with the PM,
1281 19 reaching 17% of total GIPCs in BY-2 DRMs [39]. When the global lipid composition of the PM and
1282 20 DRM fractions was recalculated taking into account these data, it appeared that GIPCs represent 45
1283 21 and 30 mol% of total PM lipids isolated from leaves and BY-2 cell suspensions, respectively, and up to
1284 22 60 mol% of the DRM fraction, suggesting that the contribution to sphingolipid-enrichment in PM Lo
1285 23 phases is mainly due to GIPCs [39].
1286 24

1292 25 **3.2.3 The use of DRMs to study the segregation of lipids in plant PM; some limits but** 1293 26 **significant contributions.**

1294 27 The “raft hypothesis” states that specific PM-lipids, mainly sterols and saturated sphingolipids,
1295 28 interact together to form dynamic nano-scale clusters by recruiting lipids and proteins that are
1296 29 present in signaling and trafficking platforms in the PM [111]. Experimentally, the nonionic detergent
1297 30 Triton X-100 is used to separate Lo phases from the rest of membrane preparation by isolation of
1298 31 DRMs isolated in the upper-phases of a sucrose density gradient after ultracentrifugation. DRMs are
1299 32 considered by many as *in vitro* counterparts of membrane rafts [147]. The characterization of lipids
1300 33 found in DRMs isolated from PM fractions of various plant species gave rise to a overall features such
1301 34 as a global decrease of glycerolipids content, with the noticeable exception of phosphoinositides; a
1302 35 strong enrichment in lipids containing saturated fatty acyl chains; an increase in free- and
1303 36 conjugated-sterols; and a strong enrichment in sphingolipids, and in particular in GIPCs. These
1304 37 characteristics are consistent with the canonical description of DRMs isolated from a plethora of
1305 38 animal PMs whilst taking into account the specificities of plant PM lipids [180]. Moreover, it appears
1306 39 that such a composition is typical of the Lo phase in model membranes, as detailed in Section 3.2.1.
1307 40 Yet, as stated in several publications (*e.g.* [181] [182] [183] [184]) the use of DRMs to evidence PM-
1308 41 associated dynamics should be accompanied with great precaution as DRM fractions should not be
1309 42 considered as direct equivalents to PM-domains. However, the numerous convergent correlations
1310 43 obtained on many different biological materials and model membranes have indicated for instance
1311
1312
1313
1314
1315
1316
1317
1318
1319
1320

1321
1322
1323 1 that 1/ a consistency between the composition of the Lo phase *in situ* and the DRM lipid content; 2/
1324 2 a relationship between the presence and abundance of DRMs and the order of biological
1325 3 membranes; 3/ the association of particular proteins to DRMs and their clustered distribution within
1326 4 the PM make them valuable tools to progress towards a better understanding of plant PM
1327 5 organization. An example of this last point is the PM-associated NADPH-oxidase RbohD, which was
1328 6 demonstrated to be responsible for the oxidative burst observed in the very early steps of the plant
1329 7 immune signaling cascade, was proved to be exclusively associated to DRMs in tobacco [19]. This
1330 8 characteristic could be related to the, immunoelectron microscopy observation that this protein is
1331 9 organized within the PM in clusters of about 20nm in diameter [185]. Upon activation, NADPH-
1332 10 oxidase products (the Reactive Oxygen Species) were also present as discrete nanometer sized
1333 11 patches along the PM [186]. Similarly, the presence of the flagellin receptor FLS2 in DRMs and its
1334 12 enrichment in this fraction observed a few minutes after treatment of Arabidopsis cells with the
1335 13 bacterial elicitor flagellin is fully consistent with recent results observed using super-resolution
1336 14 microscopy indicating its clustered distribution in the membrane, a significant modification of its
1337 15 dynamics within PM, namely an increased population of long-lived receptor clusters and a reduction
1338 16 of its lateral displacement a few minutes after elicitor treatment [187]. Moreover, group 1 Remorin
1339 17 proteins were the first biochemical markers of plant DRMs and observed as forming PM-associated
1340 18 clusters of about 75 to 100nm in diameter [188] [189]. Such nanodomain-organization was shown to
1341 19 be sterol-dependent as it was strongly impaired by the use of sterol-chelator methyl- β -cyclodextrin
1342 20 [188] or by inhibitors of sterol biosynthesis, see Table 1 [172]. More recent data have confirmed the
1343 21 confinement this protein in PM-nanodomains to be sterol- and PI4P-dependent and by using *in vivo*
1344 22 single-particle tracking microscopy that the size these Remorin-associated domains were of ca. 80nm
1345 23 in diameter [172].

1350 24 One must note that the colocalization studies of Remorins of different phylogenetic groups,
1351 25 namely groups 1, 3, 4 and 6 have shown the coexistence of highly-distinct membrane domains in the
1352 26 plane of the PM [190]. These results have demonstrated that the use of biochemical approaches such
1353 27 as DRMs cannot be sensitive enough to accurately represent the biological complexity of membrane-
1354 28 compartmentalization *in vivo*. A decisive milestone will be the ability to describe, in an extensive and
1355 29 comprehensive manner, the distribution of the various lipids together with proteins within PM, and
1356 30 to identify key causal mechanisms underlying such an organization. To do so, super-resolution
1357 31 microscopy with one or more fluorophores can be used for proteins to visualize *in vivo* whether the
1358 32 protein of interest is enriched in nanodomains; this kind of method is currently at its infancy for lipids
1359 33 due to the few fluorescently-labeled lipids available and because it is hard to insure a proper intake
1360 34 of such dyes in plant cells (see below). The use of chelator of lipids, fluorescent lipid probes or lipid-
1361 35 biosynthesis inhibitors (table 1) are the next steps to address the role of lipids in PM-nanodomain
1362 36 formation and maintenance.
1363 37

1381
1382
1383 1 **4. Spatial and multiscale segregation of lipids and proteins: a complex picture emerging from**
1384 2 **the combined use of various imaging techniques**
1385 3

1386 4
1387 5 Since the publication of the fluid mosaic model for biological membranes in 1972, a lot of
1388 6 experimental evidences revealed the outstanding complexity of the PM. Rafts characterized by tight
1389 7 lipid-packing are involved in a wide variety of cellular processes: regulation of endo- and exocytosis,
1390 8 hormone signaling, membrane trafficking in polarized epithelial cells, T-cell activation, cell migration,
1391 9 life cycle of influenza and HIV viruses [191]. As expected for biology as an experimental science,
1392 10 understanding the organization of the PM strongly relies on the evolution of microscopic methods.
1393 11 Thanks to the development of new efficient methodologies, among them imaging lipids and super-
1394 12 resolution microscopy [111], very important results have been published refining this organization
1395 13 but in the same time raising new questions. Currently, we can clearly state that the PM is organized
1396 14 in domains that differ in the nature of their components, their stability and their size from the
1397 15 nanometer to the micrometer scale. This complex remodeling is highly-dynamic and respond to
1400 16 various abiotic and biotic stresses. Particular interest of the scientific community for cell surface
1401 17 signaling processes in the past decades has led to an improved vision of the PM's membrane
1402 18 organization: a complex multi-component and multi-scale heterogeneity with a high degree of
1403 19 subcompartmentalization into micro- to nano-domains have been evidenced *in vivo* and deserve to
1404 20 be clearly qualified. Domains were originally referred as to "lipid-rafts" but the designation has very
1405 21 much evolved since. It is now known that lipid-rafts do not cover a single type of domain but rather
1406 22 include a collection of domains differing in their protein and lipid composition and their resident time
1407 23 (aggregation/disaggregation).
1408 24

1410 24 **4.1. Micro- and nano-domains coexist in the plant PM**

1411 25 **4.1.1 Microdomains in plant cells**

1412 26 Cell polarization-induced PM-microdomains (above 1 μ m) are easily observed by classical confocal
1413 27 fluorescence microscopy in leaf, root and pollen tube cells [182, 192]. The accumulation of proteins
1414 28 and lipids into microdomains is involved in defining cells' fate, functional specialization for cell
1415 29 polarity and specialization of host membranes for defense [193] [194]. These include the polar
1416 30 distribution of PINFORMED (PIN), AUX1-Auxin transporter protein 1, ABCB (ATP-binding cassette
1417 31 protein subfamily B)/P-glycoprotein, Auxin binding protein 1 (ABP1) or RAC/Rho of plants GTPases
1418 32 (ROP) that localize to the apical or basal pole of a cell [195] and the lateral and equatorial domains in
1419 33 plant endodermal cells populated by DYNAMIN-RELATED PROTEIN1A (DR1PA) or CASPARIAN STRIP
1420 34 MEMBRANE DOMAIN PROTEINs (CASPs) [182] [196]. Similarly, tip-growing cells like pollen tubes and
1421 35 root hairs are also of particular interest for the study of membrane microdomains. For instance, the
1422 36 pollen-specific H⁺-ATPase is located in the shank whereas Phospholipase C, G proteins and
1423 37 phosphoinositide kinases are located at the apex of the pollen tube (reviewed in see for review [197]).
1424 38 Lipids are also segregated into microdomains *i.e.* sterol-, phosphoinositide-, PI4,5P₂ and
1425 39 diacylglycerol-rich microdomains are shown to be especially concentrated in the apex of the pollen
1426 40 tube [179]. The presence of microdomains enriched in phosphoinositides (PIPs) plays an important
1427 41 role in polar tip growth by regulating the machinery maintaining polarity and by controlling
1428 42 cytoskeletal dynamics and the remodeling of vesicle trafficking [198]. In root endodermal cells,
1429 43 EXO70A1 exocyst subunits colocalize with PI4,5P₂ [199]. Finally, in plants, plasmodesmata (PDs),
1430 44 which are channels characterized by the apposition of the endoplasmic reticulum and the PM
1431 45 possess a specific lipid composition [200]. These PM-lined PD (PD-PM) have been shown to contain

1441
1442
1443 1 definite microdomains where not only proteins such as Plasmodesmata-located protein 1 (PDLP1)
1444 2 and PD callose binding proteins (PDCBs), but also lipids such as sterols and sphingolipids are enriched
1445 3 [201] [202] [7].

1447 4 Importantly, besides local enrichment of specific lipids and proteins within microdomains, the
1448 5 characterization of the biophysical state of pollen tube microdomains has shown that they are highly-
1449 6 segregated in the cell, *i.e.* they are especially concentrated at the PM of the cellular apex but also
1450 7 present as a ring-like distribution around the tube [72, 179]. Similarly, the cell plate of Arabidopsis
1451 8 contains highly-ordered membrane microdomains which rely on sterols and DRP1A-dependent
1452 9 endocytosis [203]. Yet, how the localization of proteins and lipids in microdomains relies on the
1454 10 cooperativity of multiple mechanisms is not yet understood [204] [205] [197].

1455 11 1456 12 4.1.2 Nanodomains in plant PM

1458 13 The development of new methods of high- and super-resolution imaging has provided the ability
1459 14 to observe membrane domains at the nanoscale level, termed nanodomains and defined by a size
1460 15 below 1 μ m [206, 207]. These methods include mainly stimulated emission depletion microscopy
1461 16 (STED), structured illumination microscopy (SIM) and single-molecule localization microscopy (SMLM,
1462 17 including methods such as Photo-Activated Localization Microscopy (PALM) and Stochastic Optical
1463 18 Reconstruction Microscopy (STORM)). These techniques have been routinely used in animal cells but
1464 19 have only recently emerged in plant studies. Super-resolution microscopy techniques allow the
1466 20 acquisition of high-density super-resolved nanoscale maps of individual fusion-protein localizations
1467 21 and trajectories in the PM [208]. Single-molecule tracking combined with photoactivated localization
1468 22 microscopy (spt-PALM) allows not only the description of the supra-molecular organization of
1469 23 proteins at the PM level far below the resolution limit of confocal microscopy but also allows the
1470 24 determination of the mobility dynamics of single molecules or particles in the PM.

1472 25 Super-resolution microscopy methods have shown that PM-associated proteins are sub-
1473 26 compartmentalized within nanodomains, to only name a few: Hypersensitive Induced Response HIR1
1474 27 [209] PIN2 [204], Borate efflux transporter (BOR1) [210], Dynamin-related protein 1a (DRP1A),
1475 28 Cellulose synthase A6 CESA6 [211], IDQ family of calmodulin-binding proteins [204] [210] [212] S-
1476 29 type anion efflux channel/ Calcium protein kinase SLAH3/CPK21 and REM1.3 [189] [172], flagellin
1478 30 receptor FLS2 [187], Brassinosteroid insensitive 1/ Somatic embryogenesis receptor kinase 1- BRI1-
1479 31 associated receptor kinase 1 BRI1/SERK1-BAK1 [213], Flotilin [214] and the NADPH oxidase [215].
1480 32 Notably, the study of group 1 REM mutants has revealed that the protein mobility rate (measured by
1481 33 the Mean Square Displacement) and protein supramolecular organization are not necessarily
1482 34 coupled. These results have shown that proteins displaying the same mobility rate can however
1483 35 assemble into clusters of different sizes [172]. Differential combinations of multiscale organizations
1485 36 have been evidenced as for instance PIN2, which is preferentially targeted in a polar fashion to PM-
1486 37 microdomains in Arabidopsis roots, locates at a lower scale into PM-nanodomains as shown by STED
1487 38 microscopy [204]. By contrast, REMORIN StREM1.3 localizes in nanodomains of ca. 80 nm observed
1488 39 by SPT-PLAM [172], but without a particular polar localization in *N. benthamiana* leaf epidermal cells.

1490 40 Lipids can also be found in nanodomains both in the inner-leaflet and in the outer-leaflet.
1491 41 Immunogold-electron microscopy has shown that PI(4,5)P₂ is found clustered in the inner-leaflet of
1492 42 the PM [31]. Interestingly this cluster formation was not significantly sensitive to sterol depletion
1493 43 [31]. More recently, immunogold-electron microscopy strategy has revealed that the distribution of
1494 44 polyglycosylated GIPCs, likely in interaction with phytosterols, form nanodomains of ca. 40 nm in the
1495 45 outer-leaflet of tobacco PM [39]. These two results strengthen the idea that lateral nano-segregation

1501
1502
1503 1 of lipids also takes place at the PM in plants. Yet, tools dedicated to the study the dynamic of plant
1504 2 lipids at the nanoscale level are still lacking, impairing progress in understanding their molecular
1505 3 distribution, behavior and dynamics of PM lipids.
1506 3
1507 4

1508 5 Therefore, the plant PM must be acknowledged as a fluid yet highly-compartmentalized mosaic
1509 6 wherein numerous membrane domains with different compositions and biophysical properties co-
1510 7 exist at different scales [192] [216]. The challenging questions now reside in clearly defining the
1511 8 essential mechanisms governing specific interactions between the different molecular species of PM
1512 9 intrinsic components. Currently microscopy methods are able to localize and track single molecules
1513 9
1514 10 with a resolution of 1 nm achieving an ultimate resolution limit in fluorescence microscopy: MINFLUX
1515 11 [217] [218], subdiffusive motion at the single trajectory level [219] or motion transition state [220].
1516 12 Such methods must be adapted to plant cells to address the specific question of plant PM biology
1517 13 and will pave the way to a better understanding of the PM's dynamic organization.
1518 13
1519 14

1520 15 **4.2 PM lipids are critical regulators of plant PM organization at the nanometer scale**

1521 16 Lipid-lipid interactions and protein-lipid interactions are believed to be key regulation parameters
1522 17 governing plant PM organization. In pollen tubes, various isoforms of the exocyst complex colocalize
1523 18 with either PI4,5P₂ or PA, resulting in the formation of PM domains [221]. The localization of
1524 18 EXO70A1 not only coincides with, but is also required for the accumulation of PI4,5P₂ [199]. The
1525 19 targeting of REMs to inner-leaflet PM nanodomains is independent of the secretory pathway,
1526 20 although it is still mediated by direct interactions with PI4P in a sterol-dependent manner [172]. This
1527 21 understanding of the anchoring mechanisms of REMs confirms the impairment of clustered
1528 22 distribution of REMs by phytosterol depletion [188] [222]. The use of raster image correlation
1529 23 spectroscopy (RICS) has shown that the lateral mobility of auxin transporters PIN is dependent on the
1530 24 amount of sterols in tobacco cell PM, arguing in favor of a sterol-dependent protein organization
1531 24 within the plant PM [80].
1532 25
1533 26

1534 27 In plasmodesmata (PD), modulations of the sterol composition alter callose-mediated PD
1535 28 permeability and reversibly impaired the PD localization of the glycosylphosphatidylinositol-anchored
1536 29 proteins Plasmodesmata Callose Binding 1 (PDCB1) and the Plasmodesmata beta-1,3-glucanase
1537 29 (PDBG2). This study emphasizes the importance of lipids in defining PD membrane microdomains and
1538 30 is in line with the lipid-raft model postulating the existence of nanoscopic assemblies of sphingolipids
1539 31 and sterols in the outer-leaflet of the PM. Finally, it is important to acknowledge that nanodomains
1540 32 exist in both leaflets and the lipid content of each of them regulates the clustering of proteins and
1541 33 lipids. The possible interaction between nanodomains across the two leaflets (a process called
1542 34 pinning or registration) will be discussed in the following section.
1543 34
1544 35
1545 36

1546 37 **4.3. PM heterogeneity might originate from a tight control along the secretory pathway**

1547 38 The neo-synthesis of lipids found at the PM results from intricate pathways that originate at the
1548 39 endoplasmic reticulum (ER), which is certainly the most ancient eukaryotic endomembrane
1549 39 compartment. From the ER, lipids are transported to the Golgi apparatus where they are further
1550 40 assembled and modified before reaching the PM, see Figure 4. At the PM, it is thought that the auto-
1551 41 association of glycerolipids, sphingolipids and sterols drives membranes close to a demixing point
1552 42 (phase separation) and induces sorting of lipids to either Lo phases or Ld phases of the membrane
1553 43 [223]. The Lo phase is enriched in sphingolipids and sterols. A higher proportion of free-hydroxyl
1554 44 groups in the long-chain-bases and acyl-chains of sphingolipids as compared to glycerophospholipids,
1555 45
1556 45
1557
1558
1559
1560

1561
1562
1563 1 allows more interactions with sterols and thereby ensuring the stabilization of sphingolipid-enriched
1564 2 membrane domains (see Section 3). The characteristic length of sphingolipid acyl-chains is a
1565 3 particularity amongst lipids that confer special physical properties to biological membranes. This
1566 4 particularity increases the melting-point of sphingolipids as compared to other lipids and causes
1567 5 strong hydrophobic mismatches between sphingolipid acyl-chains and the polar heads of other lipids
1568 6 with smaller acyl-chains. Hence, sphingolipids are segregated and more physically-ordered
1569 7 microdomains are created within the membrane [224]. Acyl-chain length also induces the formation
1570 8 of interdigitated phases (interdigitated lipid-leaflets) and plays a role in membrane stiffness and
1571 9 thickness [224] [64].

1574 10 Considering that these different phases are observed at the PM, one might ask how this
1575 11 complexity is implemented. Does this PM-lipid heterogeneity already occur within secretory
1576 12 pathways that lead to the PM and does it have a role in the secretion of proteins? In mammalian
1577 13 cells, a protein secretion model called the rapid-partitioning model, proposes a *cis*-to-*trans* gradient
1578 14 of the sphingolipid/glycerophospholipid ratio that would account for a partitioning of
1579 15 transmembrane cargos and enzymes into distinct domains of the Golgi: domains enriched in Golgi
1580 16 resident enzymes (low sphingolipid/glycerophospholipid ratio) and domains where transmembrane
1581 17 cargos are progressively enriched (high sphingolipid/glycerophospholipid ratio) at the *trans*-most
1582 18 cisterna of the Golgi until their loading into post-Golgi vesicles [225]. This model is in agreement with
1583 19 the observation that newly arrived cargos exit the Golgi with mono-exponential export kinetics.
1584 20 Moreover, alteration of sphingolipid homeostasis by treating mammalian cells with short acyl-chain
1585 21 ceramides (for further incorporation in sphingolipids at the Golgi) impacts the export of protein
1586 22 cargos from the Golgi, reduces the lipid order in Golgi membranes, and alters the ultrastructure of
1587 23 Golgi cisternae from flat to highly-curved membrane sacs, further supporting the role of very-long-
1588 24 chain sphingolipids in Golgi morpho-dynamics and sorting [226] [227].

1592 25 In plants, inhibition of the condensation of glucose with ceramides (produces GluCer) results in
1593 26 the disaggregation of Golgi cisternae into vesicular structures and in the inhibition of secretion [228].
1594 27 In animal and plant cells, the *trans*-most cisterna of the Golgi apparatus is continuous with a tubular,
1595 28 branching and reticulated Golgi structure called the *trans*-Golgi Network (TGN). In yeast, it has been
1596 29 observed that secretory vesicles budding-off of the TGN are enriched in sterols and sphingolipids and
1597 30 possess a high proportion of *Lo* phases [229]. In mammalian cells, a genetically encoded probe that
1598 31 labels sphingomyelin has revealed that sphingomyelin synthesis at the Golgi promotes sphingomyelin
1600 32 enrichment in a subset of TGN-derived secretory vesicles, where the sorting of a
1601 33 glycosylphosphatidylinositol-anchored protein is in turn also promoted [230]. In plants, extraction of
1602 34 DRMs has revealed that both PM and Golgi yield DRMs suggesting that they can be enriched in
1603 35 sterols and sphingolipids [159]. However, as stated before, this method can generate artificial
1604 36 segregations of lipids within membranes. Therefore, a combination of subcellular remodeling of
1605 37 sterols using the fluorescent probe filipin, and a novel extraction approach to specifically immuno-
1606 38 purify TGN sub-domains and Golgi apparatus without any detergents coupled with quantitative mass
1607 39 spectrometry, has opened new perspectives in defining which lipids are present in these
1608 40 compartments [231] [232]. The *in situ* subcellular remodeling of sterols by filipin has revealed that
1609 41 sterols are the most present at the PM and in sub-populations of TGN vesicles [231]. Further on,
1610 42 purification fractions of TGN sub-domains and Golgi have identified an enrichment of sterols and α -
1611 43 hydroxylated VLCFAs, a specific signature of plant sphingolipids. Moreover, this signature was
1612 44 specifically stronger in a sub-domain of TGN: Secretory Vesicles [232]. Not only an enrichment of
1613 45 sphingolipids is observed in TGN-derived vesicles, but the length of the sphingolipid acyl-chains is

1621
1622
1623 1 found to be a critical factor for the correct polarized secretory sorting of the auxin-carrier protein
1624 2 PIN2 in root epidermal cells [232]. Altogether, the enrichment of sterols and sphingolipids at TGN-
1625 3 derived secretory vesicles seems to be a conserved feature in eukaryotic cells, and appears to be
1626 4 required for protein sorting and vesicle budding. This enrichment is favorable to Lo phase lipid-
1627 5 segregation at TGN and suggests that a gradient of lipids along the secretory pathway is established
1628 6 from the ER where no enrichment of sterols and sphingolipids is observed through the TGN to the
1629 7 PM. This membrane heterogeneity is not only a structuration of pre-PM lipids but it has as well an
1630 8 important role to play in many intracellular trafficking pathways, see Figure 4.

1631 9
1632 10 The lipid heterogeneity within the secretory pathway also exists for lipids other than sterols and
1633 11 sphingolipids. In plants, the TGN-localized choline transporter like1 (CTL1) is involved in PM-recycling
1634 12 of the ion transporter NRAMP1 and the auxin efflux carrier PIN1 [233]. An interesting observation is
1635 13 that free-choline, but not phosphatidylcholine (PC), can inhibit phospholipase D (PLD) activity [233].
1636 14 PLD hydrolyses PC and phosphatidylethanolamine (PE) to produce phosphatidic acid (PA), a
1637 15 phospholipid that favors the fission of vesicles [234]. Hence, one hypothesis is that CTL1 transports
1638 16 choline inside the TGN lumen to maintain a low choline concentration on the cytoplasmic side of
1639 17 TGN in order to conserve high PLD activity converting PC and PE into PA. This mechanism would
1640 18 require further characterization, but it could be a possible way to establish membrane heterogeneity
1641 19 between the luminal and cytoplasmic leaflets of TGN membranes. Another example of phospholipid
1642 20 membrane heterogeneity is with phosphatidylserine (PS) in yeast where it has been suggested that
1643 21 PS resides primarily in the luminal leaflet of the Golgi and is flipped to the cytosolic leaflet in the
1644 22 TGN [235]. This leaflet translocation of PS is operated by PS flippases at the TGN and is thought to
1645 23 control oxysterol-binding proteins (OSBP), which exchange ER-associated sterols with TGN-associated
1646 24 PI4P in unidirectional fashion [235]. The exchange of lipids participates in creating sterol enrichment
1647 25 and membrane lipid order at the TGN [236]. An elegant model has proposed that this exchange of
1648 26 sterols for PI4P occurs at ER-TGN membrane contact sites, where PI4P is generated at the TGN by PI4
1649 27 kinases (PI4KII α) which are themselves regulated in an oscillatory (waves of PI4P consumption by
1650 28 OSBPs) fashion by sterols [236]. These studies have revealed a crucial characteristic of membrane
1651 29 heterogeneity at the TGN: its highly-dynamic and oscillatory nature.

1652 30 In plants, PIPs are localized in a gradient throughout the endomembrane system, PI4P being
1653 31 mainly located at the PM with a secondary pool at the TGN while PI3P is mainly located in late
1654 32 endosomal compartments, see Section 1 [27]. The function of PI4P at the TGN and its relationship
1655 33 with other lipids have not yet been addressed in plants and will definitely be an exciting field to
1656 34 explore in respect to plant trafficking specificity. In plants, unlike animal TGNs, at least two
1657 35 populations of TGNs are observed, one is associated to the Golgi apparatus and one is independent
1658 36 from it, as TGNs detach from the Golgi apparatus to form a highly-dynamic Golgi-independent
1659 37 structure [237] [197] [238] [239] [240]. This highly-dynamic TGN can undergo homotypic fusion and
1660 38 can associate transiently with the Golgi apparatus similarly to what is found for early endosomes and
1661 39 TGN in mammalian cells. In addition, it has been observed that the plant TGN can integrate the
1662 40 endocytic tracer FM4-64 relatively fast (a couple of minutes) during endocytosis before reaching Late
1663 41 endosomes/MVBs [241] [239]. Hence, plants have no early endosomes as described in animals, and
1664 42 endocytic vesicles converge directly to the TGN, where endocytic cargoes are sorted for recycling
1665 43 and/or degradation [239] [237] [197]. As such, plant TGNs can be viewed as a functional equivalent
1666 44 of mammalian early endosomes. Hence, it will be interesting in the future to see how the two
1667 45 systems evolve in respect to lipid heterogeneity regulation at the plant TGN.

1681
1682
1683 **1 4.3. A model for plant PM organization, interdigitation, pinning and registration**

1684 **2 4.3.1. A model for plant PM organization: mechanisms at work**

1685 **3** All these observations led to a model of plant PM organization that supposes both lipid-driven
1686 **4** phase segregation and protein-dependent protein localization. This model is based on experiments
1687 **5** on artificial membranes, composed of lipids mimicking plant PMs (lipids and/or proteins), indicating
1688 **6** that lipid-lipid interactions strongly order plant membranes [93], whereas protein-lipid interactions
1689 **7** could untighten plant PM organization [242]. Several models could explain lipid-lipid interactions.
1690 **8** The “condensed lipid complex” model has been stated following the visualization of low-energy free
1691 **9** stoichiometric cholesterol-lipid complexes occupying smaller molecular lateral zones than those
1692 **10** occupied by each lipid alone [243]. Sphingolipids, originally proposed as preferred partners of
1693 **11** cholesterol, cannot form this type of complex. The existence of cholesterol superlattice in lipid
1694 **12** bilayers highlights a parallel model proposing long-distance repulsion forces between cholesterol
1695 **13** molecules as the source for sterol-lipid interactions [244]. The “umbrella” model states that the shift
1696 **14** between the small polar head of cholesterol and its large apolar body determines its preferential
1697 **15** association with some adjacent molecules of the membrane [245]. In this model, cholesterol is
1700 **16** covered by the polar heads of neighboring phospholipids to limit the unfavorable free energy due to
1701 **17** the exposure of the apolar portion of cholesterol to water molecules. Such interactions between
1702 **18** cholesterol and “large-headed” lipids provide increased protection. In addition, the free energy
1703 **19** needed to cover a cholesterol cluster is larger than the energy required to cover a single cholesterol.
1704 **20** An essential property thus emerges from these models, namely the strong tendency of cholesterol
1705 **21** molecules not to regroup, which has been accordingly demonstrated by Monte Carlo simulations
1706 **22** [246]. By sailing between lipid molecules, proteins increase membrane line tension and modify the
1707 **23** mean size of the ordered domains as reported in Lung Surfactant Monolayers [247]. In agreement, it
1708 **24** has been demonstrated that short hydrophobic transmembrane peptides decrease the affinity of
1709 **25** sterols for neighboring phospholipids.

1710 **26** In animal, all these data led to a model that incorporates the importance of hydrophobic
1711 **27** matching between integral membrane proteins and the lipid bilayer thickness considered in the so-
1712 **28** called “mattress” model [248]. This thermodynamic model includes the elastic properties of lipids
1713 **29** and proteins, as well as indirect and direct lipid-protein interactions expressed in terms of the
1714 **30** geometrical variables. The notion of hydrophobic mismatch regions between lipids and proteins is
1715 **31** also an important component of the model. This proposal remains speculative in plants and calls for
1716 **32** further investigations.
1717 **33**

1718 **34 4.3.2. PM asymmetry, interdigitation, pinning and registration**

1719 **35** As stated before, the animal cell PM has a highly asymmetric distribution of lipids with PIPs, PE
1720 **36** and PS mostly confined to the inner-leaflet, and sterols and sphingolipids to the outer-leaflet [249].
1721 **37** The same observations seem to be true in plant PM [75] [58]. In addition, the PM contains dynamic
1722 **38** nanodomains involved in a continuous repartitioning of components between different domains.
1723 **39** Recent experimental data in the animal field have shown that transient links between lipids and
1724 **40** proteins involving both the extracellular matrix and cytoplasmic components may temporarily pin
1725 **41** membrane domains, see below. It is becoming increasingly clear that asymmetry and pinning
1726 **42** processes, also called registration, play important roles in PM nanodomain formation and coupling
1727 **43** between the two PM leaflets [250].

1728 **44** For example, a direct interaction between outer-leaflet sphingolipids Lactosylceramides
1729 **45** containing VLCFAs, and inner-leaflet nanodomain acylated-protein kinase has been shown. This

1741
1742
1743
1744
1745
1746
1747
1748
1749
1750
1751
1752
1753
1754
1755
1756
1757
1758
1759
1760
1761
1762
1763
1764
1765
1766
1767
1768
1769
1770
1771
1772
1773
1774
1775
1776
1777
1778
1779
1780
1781
1782
1783
1784
1785
1786
1787
1788
1789
1790
1791
1792
1793
1794
1795
1796
1797
1798
1799
1800

1 interleaflet pinning has been shown to specifically modulate neutrophil activity [251]. Similarly,
2 transbilayer pinning between outer-leaflet long-acyl-chain-GPI-anchored proteins and inner-leaflet
3 PSare demonstrated to be pivotal in generating actin-dependent nanoclusters of PM lipid-anchored
4 proteins [252]. These interactions may provide clues to the underlying mechanisms for the
5 registration of functional lipid domains between both leaflets of the PM. Yet, cross leaflet lipid-lipid
6 interactions seem to be the main driving force behind the formation of ordered membrane domains
7 *in vivo* [253].

8 How asymmetry, pinning, and interdigitation contribute to PM organization is only beginning to
9 be unraveled in animals. Currently, very little is known in plants but this area of research will surely
10 be developed in the next few years of membrane biology. The pending questions are of a
11 fundamentally compelling nature. One may ask whether VLCFA-containing GIPCs in PD could register
12 with acylated-proteins across the plant PM, or whether phytosterols in one leaflet influence the
13 fluidity of the other leaflet. This makes PM domains exceptionally challenging to study and even
14 then, much of what is known about membrane domains has been deduced from studies on model
15 membranes at equilibrium. However, living cells are by definition not at equilibrium, PM-lipids are
16 still distributed asymmetrically *in vivo* so model membranes may not be as biased as can be
17 expected. Moreover, each phospholipid group encompasses a wealth of species that vary according
18 to their different acyl-chain combinations, and consequently their lateral distribution is
19 heterogeneous and modulated *in vivo*. It is therefore with a combination of *in vivo* and *in vitro*
20 analyses that these questions clearly need to be tackled in plant membrane biology.
21

1 5. Lipids are key players in plant PM function

2 Proteins and lipids located in PM nanodomains serve as modulators of host-pathogen
3 interactions such as the binding of the cholera toxin to animal PM-located outer-leaflet gangliosides
4 GM1 to form a pore through the PM [254]. The discovery of a high level of saturated sphingolipids
5 and cholesterol in the viral envelope of HIV also proposed that enveloped virus budding is
6 nanodomain-mediated [255] [256]. Besides, a large number of proteins and lipids that are associated
7 with cancer, atherosclerosis and immune responses have been found in nanodomains, see the recent
8 review [111]. The example of the K-Ras protein is of particular interest as the molecular mechanisms
9 to understand its precise PM localization have been detailed in recent reviews [257] [258] [259]. In
10 the next chapter, we will focus on the role of plant PM lipids in different physiological functions.

11 5.1 Plant-microbe interactions

12 5.1.1 Membrane lipids in plant-microbe interactions

13 Plants counteract pathogenic microbes by sensing non-self and modified-self molecules by cell-
14 surface and intracellular localized immune receptors [260]. PM lipids and lipid-derived metabolites
15 have been shown to operate in plant immune signaling [261] [262]. As a result of the sensing of a
16 pathogen, enzymes hydrolyzing the polar heads of phospholipids are mobilized to trigger signaling
17 cascades essential for cellular responses. Phospholipases generate crucial messenger molecules such
18 as oxylipins, jasmonates and notably phosphatidic acid (PA) which can regulate the activity of
19 defense-associated proteins [263] [264]. For example, the activation of phosphoinositide-specific
20 phospholipase C (PI-PLC) is one of the earliest responses triggered by the recognition of several
21 microbe-associated molecular patterns (MAMPs), such as xylanase, flg22, and chitosan or of
22 pathogen effector proteins [265] [266] [267]. PI-PLC catalyzes the hydrolysis of phosphatidylinositol
23 4-phosphate and phosphatidylinositol 4,5-bisphosphate (PIP2) to generate water-soluble inositol
24 bisphosphate (IP2) or inositol triphosphate (IP3), and diacylglycerol (DAG), which remain in the
25 membrane. In plants, DAG produced by PI-PLC activity is phosphorylated by DAG kinase (DGK) to
26 produce phosphatidic acid (PA) [268] [269]. PA has been implicated specifically in the modulation of
27 immune signaling components, such as MAPKs and PHOSPHOINOSITIDE-DEPENDENT PROTEIN
28 KINASE 1, PDK1; [270] [271]). Binding of PA to proteins/enzymes has been shown to affect their
29 activity, localization, and binding to other signaling components [272] [273] (Pokotylo et al., 2018).
30 For example, PA binds to the NADPH oxidase isoforms RBOHD and RBOHF to induce ROS formation
31 during abscisic acid (ABA)-mediated stomatal closure [274]. PM-localized PI-PLC2 [275], is rapidly
32 phosphorylated upon flg22 recognition [276] and plays an important role in stomatal pre-invasion
33 immunity and non-host resistance as it associates with RBOHD [277]. This suggests a potentially
34 central regulation of the Arabidopsis NADPH oxidase and, consequently, of ROS-dependent
35 processes induced by PLC2.

36 In addition, it has been shown that PLC activity is required for ROS production during effector
37 triggered immunity (ETI) responses [278], that NPC2 is involved in the response of Arabidopsis to
38 *Pseudomonas syringae* attack, by regulating elicitor-induced ROS production [279]. Furthermore, it
39 has been demonstrated that DGK-produced PA is required for optimal ROS production in response to
40 cryptogein [280]. Nonetheless, direct regulation of Rboh isoforms by PA binding during immune
41 responses remains to be investigated. In addition, PA binding inhibits RGS1 activity to affect specific
42 immune signaling pathways in Arabidopsis. Interestingly, the central immune receptor cytoplasmic-
43 like kinase BIK1 directly linked nanodomain-localized PRRs [187] and RBOHD [281]. BIK1 regulates
44 RGS1 activity by direct phosphorylation [282] and by inhibiting PLC activity. FLS2 has been shown to
45

1861
1862
1863 1 be no longer endocytosed [283], pointing PA as a core regulatory component of plant receptor
1864 2 kinase-based immunity. Interestingly, remodeling of cortical actin network in response to elicitors is
1865 3 mediated by the negative regulation of CAPPING PROTEIN by PLD-produced PA [284].
1866

1867 4 The production of PA by Phospholipase D enzymes (PLD) is involved in ROS production in
1868 5 response to elicitation [285]. This production of PA has been also shown to be essential for
1869 6 phytoalexin biosynthesis [286] yet considering the various subcellular localizations of PLDs this may
1870 7 not be specific to PM-associated PA [287]. PLD δ has been also found to be involved in non-host
1871 8 resistance of *A. thaliana* epidermis against the barley powdery mildew fungus *Blumeria graminis* f.
1872 9 sp. *Hordei* and the pea powdery mildew fungus *Erysiphe pisi*. PM-localized PLD δ is enriched at the
1873 10 penetration sites and PA is supposedly produced and necessary for resistance considering the
1874 11 observed increase in susceptibility after treatment with n-butanol, a PLD inhibiting drug [288]. PLD-
1875 12 produced PA is also involved in plant-virus interactions by promoting the RNA replication of the Red
1876 13 clover necrotic mosaic virus. A viral auxiliary replication protein binds PA in vitro and the exogenous
1877 14 addition of PA increase replication rates. This is consistent with the observed increase of PA levels in
1878 15 infected cells [289]. PA could therefore play a central role in viral replication by tethering protein
1881 16 complexes to each other and to the membrane, thereby putatively modulating catalytic activities
1882 17 [290] and membrane curvature [291]. As PA negatively favours curved membranes [292], a local
1883 18 increase in PA levels is likely to impact membrane structure and charge. Nonetheless, stimuli-
1884 19 dependent impact of PA production on membrane organization and the dynamics of plant immune
1885 20 component remain to be studied. What are the molecular function(s) of PA in immunity is still to be
1887 21 further studied.

1888 22 In addition to PA, both phosphoinositides and lysophospholipids have been shown to play a role
1889 23 in plant defense. Lysophospholipids are derived from glycerophospholipids by the action of PLAs.
1890 24 Examples of lysophospholipids include L-PA, lysophosphatidylcholine, sphingosylphosphorylcholine,
1891 25 and sphingosine-1-phosphate [293]. The signaling activity or specificity of these compounds is
1892 26 dependent on the length and position of the acyl chain, the degree of saturation, and the presence of
1893 27 the phosphate head group. Acyl chain length and degree of saturation have been shown to influence
1894 28 plant-pathogen interactions. The accumulation of C16:1 and C16:2 fatty acids in tomato and
1895 29 eggplant, due to the overexpression of a yeast delta-9-desaturase, resulted in a heightened
1896 30 resistance to powdery mildew *Erysiphe polygoni* DC and *Verticilium dahliae*, respectively. An increase
1899 31 in C18:2 and C18:3 has also been shown to increase resistance to *Colletotrichum gloeosporioides* and
1900 32 *Pseudomonas syringae* in avocado and tomato respectively [294] [295]. Moreover, bean resistance to
1901 33 *Botrytis cinerea* induced by a non-pathogenic strain of *Pseudomonas* has been correlated with an
1902 34 increase of C18:2 and C18:3 [296].

1903 35 As stated in chapter 1, plant sterols are core components of membrane and accumulate in the
1905 36 PM. Conversely, PM sterols are conserved regulators of membrane organization. Mutants altered in
1906 37 sterol biosynthesis and the use of sterol-biosynthesis inhibiting drugs, affect cell wall composition
1907 38 and induce abnormal callose and lignin deposits (cell wall compounds involved in biotic stress) [297].
1908 39 Cryptogein is able to induce an increase in PM-fluidity via sterol-binding [109]. Highly-hydroxylated
1910 40 sphingolipids increase membrane stability and decrease membrane permeability which are both
1911 41 associated to increased defence against phytopathogenic fungi [35] [298]. Rice *fah1/2* knock-down
1912 42 mutants, displaying the lack of an α -hydroxyl group on the fatty-acid moiety of sphingolipids, exhibit
1913 43 a decrease in PM order level [51]. These mutants show reduced resistance to the rice blast fungus
1914 44 *Magnaporthe oryzae*, with the delocalization of major actors of innate immunity such as NB-LRRs,
1915 45 NADPH oxidases, Small GTPases and Calcium-dependent kinases [51]. On the contrary, Arabidopsis

1921
1922
1923 1 fah1/2 knock-out mutants display an increased resistance to obligate biotrophic fungi *Golovinomyces*
1924 2 *cichoracearum* potentially due to a consequential increase in intracellular ceramides and salicylate
1925 3 [299]. Interestingly, a sphingosine analogue produced by the fungal pathogen *Alternaria alternata* f.
1926 4 sp. *Lycopersici* (AAL), serves as a virulence factor that induces PCD in plants and animals [300].
1928 5

1929 6 5.1.2 Sphingolipids as receptors of necrotrophic toxins and plant-pathogen 1930 7 elicitors

1932 8 Glycosylated lipids are often receptors in insect host binding to microbial toxins [301]. One very
1933 9 important glycosylated lipids of the animal kingdom are gangliosides. Their polar heads act as surface
1934 10 recognition markers and surface receptors for bacterial toxins such as cholera and Bt toxins [254].
1935 11 They are recognized and used by virus to enter and infect cells [302]. Plant GIPCs bear structural
1936 12 similarities with gangliosides because they contain negatively charged glycan polar heads located in
1937 13 the outer-leaflet of the PM [303].

1939 14 A recent study has shown that GIPCs were located in the outer-leaflet of plant PM are receptors
1940 15 to Necrosis and ethylene-inducing peptide 1-like (NLP) proteins [40]. In the study of Lenarčič et al
1941 16 2017, microbial NLP proteins are used for the identification and characterization of NLP receptors.
1942 17 NLPs are part of a superfamily of cytotoxins produced by plant pathogens such as bacteria, fungi and
1943 18 oomycetes [304]. They can be cytolytic, inducing symptoms on eudicot plants but not monocot
1944 19 plants where no necrotic and cytolytic effects are observed [305]. The secretion of NLPs occurs in the
1946 20 extracellular environment of host plants with the toxins targeting the PM outer-leaflet [304] [306]. *In*
1947 21 *vitro*, NLPs were shown to specifically bind to purified GIPCs from tobacco and Arabidopsis but not to
1948 22 phospholipids, GluCer or sphingomyelin. Moreover, NLPs also bind to all GIPCs, irrespective of the
1949 23 plant clade, with similar affinities [40]. Upon binding to the hexose moieties of the GIPC polar heads,
1950 24 NLPs undergo structural changes triggering the conformational modification of their L3 loop and the
1951 25 incorporation of a Mg²⁺ ion responsible for its cytotoxicity. This results in the interaction of the W155
1952 26 residue of the L3 loop with the membrane, crucial for cytolysis [40]. The study has also showed that
1954 27 sugar residues exposed on the plant outer membrane surface are important for NLP toxicity, such
1955 28 that Glucosamine, Man/Glucose being GIPC terminal sugars of tobacco and Arabidopsis respectively,
1956 29 induces membrane damage upon binding to NLPs. Plant mutants impaired in the GIPC biosynthetic
1958 30 pathway, are less sensitive to NLPs, implying the importance of intact GIPCs for NLP cytotoxicity [40].
1959 31 The sensitivity to NLP toxicity occurs only for eudicots but not monocots with the exception of a
1960 32 monocot *Phalaenopsis* species (an orchid). This intriguing fact could be explained by the presence of
1961 33 different GIPC series in these two plant clades. While both have similar terminal hexose sugars with
1962 34 similar affinity to NLPs; eudicots GIPCs contain two hexoses linked to IPC (series A GIPC) whereas
1963 35 monocot GIPCs contain three hexoses (series A GIPC), with the exception of *Phalaenopsis* containing
1965 36 both series A and B. Biophysical characterization of GIPC series in monolayer artificial membranes
1966 37 suggests a perpendicular arrangement of the polar head of both series A and B GIPC, such that the
1967 38 terminal hexose in series B GIPC, is located further away from the membrane surface compared to
1968 39 series A GIPC. Hence, NLPs binding to series B GIPC terminal sugars have their L3 loop positioned
1970 40 farther from the plant membrane, preventing NLP contact with the membrane and thereby,
1971 41 cytolysis. Both, the length of GIPC head groups and the structural design of the NLP sugar-binding
1972 42 sites explain the differential sensitivity of host plants to NLP toxins.
1973 43

1974 44 5.1.3. Lipid domain-associated proteins in plant microbe interaction

1975
1976
1977
1978
1979
1980

1981
1982
1983
1984
1985
1986
1987
1988
1989
1990
1991
1992
1993
1994
1995
1996
1997
1998
1999
2000
2001
2002
2003
2004
2005
2006
2007
2008
2009
2010
2011
2012
2013
2014
2015
2016
2017
2018
2019
2020
2021
2022
2023
2024
2025
2026
2027
2028
2029
2030
2031
2032
2033
2034
2035
2036
2037
2038
2039
2040

1 Remorins (REM) are plant-specific nanodomain-organized proteins notably involved in plant-
2 microbe interactions. REMs are anchored by their C-terminal domain to the cytosolic leaflet of the
3 PM. The anchoring and lateral segregation in the PM is PI4P- and sterol-mediated [172]. REM1.3 was
4 shown to be delocalized after sterol disrupting treatments, such as methyl- β -D-cyclodextrin [189]
5 [222] [160] [188] [172] or fenpropimorph [172]. Both their presence at the PM and their correct
6 partitioning within their cognate nanodomains, are essential for their cellular function, e.g.
7 StREM1.3's role in hindering Potato Virus X cell-to-cell movement [172] [307]. Other REM-group
8 proteins have been evidenced as key players in biotic interactions such as SYMREM1 (MtREM2.2)
9 involved in the nodulation process of *M. truncatula* with *Sinorhizobium meliloti* [308] Its role was also
10 shown to be essential in the dynamic stabilization of the LYK3-FLOT4-SYMREM1 PM-nanodomains,
11 important for root bacterial symbiosis [309]. Remorins are found in DRM, the closest biochemical
12 counterpart to PM-nanodomains known today, in virtually all clades of land plants: Poplar [310], Oat
13 and Rye [166], Tobacco [169], Arabidopsis [162]. The role of REMs as actors involved in a wide range
14 of biotic interactions has been established throughout the years: ranging from susceptibility factors
15 to viral infections [311], to oomycetes [312] or on the contrary as resistance factors to Potato Virus X
16 [188]. Their capacity to impact PD permeability [172] [313] also demonstrates their implication in
17 innate immunity. Super-resolution microscopy has been used to understand the role of nanodomain
18 dynamics in the context of viral infection, revealing that an optimal partition (*i.e.* size of
19 nanodomains, number of molecules in and out domains, and mobility) of REM-associated
20 nanodomains was necessary for the function of REMs [172].

21 PM receptors involved in the oxidative-burst response to the perception of Pathogen-Associated
22 Molecular Patterns (PAMPs) are key players in plant innate immunity [314]. Their PM localization
23 gives them the role of gatekeepers capable of dynamically associating to co-receptors complexes and
24 triggering signaling pathways to prepare the cell for immediate and short-to-mid-term defense
25 responses [314]. The best example is FLS2, an LRR receptor-like kinase involved in the perception of
26 the bacterial elicitor flagellin (flg22) in Arabidopsis [315]. PM-subcompartmentalization via raft-like
27 domains is an essential phenomenon in the PAMP perception and response processes. Upon
28 cryptogein treatment on tobacco cells, a quantitative proteomics approach has evidenced the
29 delocalization of various Dynamin and 14-3-3 proteins into the DRM fraction, both involved in PM-
30 based signaling [168]. The reorganization of the PM in response to elicitors is not only observed via
31 its protein composition but also via the biophysical properties conferred by lipids: upon elicitation
32 with flg22 or cryptogein, PM order and fluidity are altered [90]. As regards to flg22's cognate
33 receptor FLS2, it was shown to relocate to DRM fractions upon flg22 treatment as well as many other
34 key proteins involved in immunity-associated signaling [161], revealing that PM-remodeling, at both
35 the lipid and protein level, is important for a functional immune response.

36 In good agreement, perception of flg22 in BY-2 cells induces global increase of the order level of
37 the PM. While this modification of the PM properties correlates with signal initiation [316], the
38 potential functional implication and molecular basis of such membrane modification remains to be
39 elucidated. Cryptogein is shown to be able to induce an increase in PM-fluidity via sterol-binding
40 [109]. Sterols and their associated micro-environments appear to be crucial for immune responses at
41 the cellular level to the extent that both mutants for sterol biosynthesis and sterol-biosynthesis
42 inhibiting drugs affect cell wall composition and induce abnormal callose and lignin deposits *i.e.* cell
43 wall compounds involved in biotic stress [297].

44 45 5.1.4. GPI-anchored proteins & outer-leaflet PM domains

2041
2042
2043 1 The importance of outer-leaflet PM-nanodomains enriched in sphingolipids and sterols is also
2044 2 underscored by the presence of GPI-anchored proteins in these domains, many of which are
2045 3 implicated in host responses to invading microbes. GPI-anchored β -1,3-glucanases (BGs), responsible
2046 4 for callose degradation, are found in DRM fractions alongside callose synthases [310]. Their presence
2047 5 in microdomains around PD enable a turnover of callose deposits when proper signaling occurs. The
2048 6 localization of BGs at PD is regulated by the presence of sterol-enriched domains at the PM, which
2049 7 share a virtually identical lipid composition with the PD-PM interface to the extent that sterol-
2050 8 biosynthesis inhibitors abolish this targeting [7]. The PD-enriched GPI-anchored protein LYM2 has
2051 9 been found to impact PD conductance in response to chitin treatments [317]. Several GPI-anchored
2052 10 BGs have been shown to associate to PD thanks to their GPI-anchoring motif [318] in a salicylic acid-
2053 11 dependent fashion [319] consolidating the idea that addressing proteins to PM-PD microdomains via
2054 12 GPI-anchoring plays a significant role in host responses to pathogens.
2055
2056
2057
2058

2059 14 5.1.5 Extracellular Vesicles & host-induced gene silencing

2060 15 Extracellular vesicles (EVs) are PM-derived vesicles secreted in the extracellular matrix involved in
2061 16 inter-cellular communication and in response to stress, notably biotic stimuli. The existence of these
2062 17 vesicles has been first observed in plants in the 1960's [320] yet EVs have only recently been better
2063 18 characterized [321] regarding their function during plant-pathogen interactions. They are observed
2064 19 upon xylanase treatment [322] and in response to hormone treatments [323]. EVs are believed to be
2065 20 derived from multi-vesicular bodies (MVB) which accumulate around appressorium and haustoria
2066 21 during defense against fungal pathogens [324] [325]. They have recently been shown to contain a
2067 22 number of biotic stress-related compounds such as phytoalexins like glucosinolates [323], small-
2068 23 interfering RNAs that can effectively silence pathogen-associated virulence and/or housekeeping
2069 24 genes [326] [327] [328] and signaling-associated enzymes, such as PLD and PLC [329]. The presence
2070 25 of these phospholipases hints to the possibility of EVs being involved in lipid signaling pathways.

2071 26 Plant EVs contain phospholipids such as PI4P [322] [330], PI and PA [323]. The lipid composition
2072 27 may vary upon which organ they are secreted, and upon different stimuli applied to the secreting
2073 28 cells. For example, upon jasmonic acid treatment, sunflower seed-derived EVs will be enriched in
2074 29 PI4P and depleted in PI [323]. The lipidome of plant EVs, in different conditions, has yet to be
2075 30 published and it will surely reveal crucial information on their biogenesis and activity.
2076
2077
2078
2079

2080 32 5.2 Hormone signaling and transport

2081 33 Lipid-mediated protein sorting mechanisms at TGN have strong impact on plant development
2082 34 since they are involved in directing the secretion and endosomal recycling pathways of a set of
2083 35 proteins that includes hormone transporters. Higher plants are multi-cellular organisms able to
2084 36 respond and quickly adapt to their environment. In particular, the plant hormone auxin plays a
2085 37 fundamental role in the regulation of a variety of developmental processes enabling plants to adapt
2086 38 to their environment, including directional growth as gravitropism [331] [332] [333] [334] [335] [336]
2087 39 [337]. Auxin mediated control of plant development relies on establishment of concentration
2088 40 gradient of auxin that are generated by the activity of plasma membrane localized auxin carriers
2089 41 [335] [336] [337] [338] [339]. Therefore, the mechanisms that control the remodeling of auxin
2090 42 carriers represent a key control point for signals that control plant development and response to
2091 43 abiotic stress. Several studies have shown that the TGN is involved in auxin-carrier trafficking but the
2092 44 sorting mechanisms are poorly understood [340] [341] [342]. Several elements related to G proteins
2093 45 (guanine nucleotide-binding proteins) are known to be involved in TGN-mediated auxin-carriers'

2101
2102
2103
2104
2105
2106
2107
2108
2109
2110
2111
2112
2113
2114
2115
2116
2117
2118
2119
2120
2121
2122
2123
2124
2125
2126
2127
2128
2129
2130
2131
2132
2133
2134
2135
2136
2137
2138
2139
2140
2141
2142
2143
2144
2145
2146
2147
2148
2149
2150
2151
2152
2153
2154
2155
2156
2157
2158
2159
2160

1 trafficking. Our goal in this review is not to create an exhaustive list of all these elements but we can
2 name a few: the small GTPase protein RAB-A1b, the ECHIDNA protein which interacts with YPT/RAB
3 GTPase interacting protein 4a (YIP4a) and YIP4b, the ADP ribosylation factor (ARF) ARF1 as well as
4 the ARF-guanine exchange factors (ARF-GEFs) GNOM and BIG1-5, and finally the ARF-GTPase
5 activating proteins (ARF-GAPs) SCARFACE/VAN3[342] [343] [344] [345] [346] [347]. On the lipid side,
6 sphingolipids represent a class of lipids particularly interesting since VLCFAs, an imprint of
7 sphingolipids, are enriched at TGN [232]. Shortening of the acyl-chain using pharmacological and
8 genetic tools reveal that the length of sphingolipid acyl-chains is involved in the secretory sorting of
9 the efflux auxin carrier PIN2 (but not in PIN1 or AUX1 trafficking), auxin redistribution during root
10 response to gravity (root gravitropism) and root gravitropism *per se* [232]. Interestingly, it had been
11 shown before that VLCFA-containing sphingolipids are involved in PIN1 and AUX1 trafficking (but not
12 PIN2 trafficking) and lateral root formation [55]. These results are not necessarily contradictory.
13 Indeed, the structural diversity of sphingolipids is wide and has been described in chapter 1 and in
14 several reviews [298] [35]. LCBs are not always found included in a ceramide molecule but can also
15 be freely found at non-negligible proportion inside the cell as sphinganine and phytosphingosines.
16 Finally, aside from sphingolipids, VLCFAs can also be included in some phospholipids. On this topic, it
17 has been shown that the *pas2* mutant displays a reduced level of VLCFA-containing
18 phosphatidylethanolamine (PE) and show endocytic trafficking defects [348]. Decrease of VLCFA-
19 containing PE in the *pas2* mutant targets the RAB-A2a compartment and the plasma membrane
20 endocytic recycling of the auxin efflux-carrier PIN1 but has no effect on PIN2 localization [349] [348].

21 Coming back on sphingolipids, it has been shown that the *loh1/loh2* double mutant, which is
22 defective in ceramide synthases LOH1 and LOH2, are involved in endocytosis and plasma membrane
23 recycling of the auxin carriers PIN1 and AUX1, but not PIN2, potentially through RAB-A2a
24 compartments [55]. Hence, it is possible that VLCFA-containing sphingolipids are important for
25 endocytic/recycling of certain subset of proteins from plasma membrane through a RAB-A2a-positive
26 subdomain of TGN that would host the recycling pathway. In contrast, the herbicide metazachlor,
27 that drastically modifies both GluCer and GIPCs fatty acids composition by replacing VLCFAs in GluCer
28 and GIPCs pools by LCFAs without modifying the global quantity of either GluCer or GIPCs, alters PIN2
29 polarity at plasma membrane while it neither affects PIN1 polarity nor AUX1 localization [232].
30 Importantly, metazachlor blocks PIN2 predominantly at SYP61/secretory vesicles (SVs)
31 compartments as compared to RAB-A2a/CCVs [232]. Concomitantly, metazachlor treatment neither
32 alters endocytosis nor plasma membrane recycling of PIN2 but rather blocks the secretion of *de novo*
33 synthesized PIN2 at SYP61/SVs compartments. From these studies, it can be postulated that TGN-
34 associated RAB-A2a/Clathrin-coated vesicles (CCVs) compartments could host the ceramide-
35 dependent PM recycling of auxin carriers PIN1 and AUX1 while TGN-associated SYP61/SVs
36 compartments could host VLCFA-containing GluCer and GIPC-dependent secretory sorting of PIN2.
37 However, future challenges on this topic need to address TGN sub-domains' dynamics, interactions
38 and maturation, which could involve a tight regulation of lipid homeostasis and crosstalk to define
39 the identity of each sub-domain.

40 The VLCFAs of sphingolipids determine a specific physical property of sphingolipids, which is the
41 ability to insert their acyl-chain within the opposing leaflet of the membrane, a phenomenon known
42 as interdigitation, see Figure 4. Interestingly, it has been shown in animal cells that the coupling of
43 membrane leaflets is cholesterol-dependent [64]. In yeast and in plants, it has been shown by
44 immuno-purification of intact compartments coupled with lipid mass spectrometry analyses, that
45 TGN-derived secretory vesicles are enriched in both sphingolipids and sterols [229] [232]. Currently,

2161
2162
2163 1 it is not clear whether the pool of sterols at the TGN would play a role in the trafficking of auxin
2164 2 carriers. Previously, it has been shown that sterols are involved in endocytosis and recycling at
2165 3 plasma membrane of the PINs auxin carriers [350] [351] [352]. Sterol-mediated endocytosis is
2166 4 involved in PIN2 polarity establishment after cytokinesis by removing PIN2 from the new basal
2167 5 membrane of daughter cells, while PIN2 at the new apical membrane remains [351]. Sterol-mediated
2168 6 auxin carriers' sub-cellular localization impacts auxin distribution at the tissue-level, which has
2169 7 repercussions on plant development such as the graviresponse of the root [351]. Interestingly, not
2170 8 only are the major sterols: sitosterol, stigmasterol and campesterol involved in plant development,
2171 9 but also some very rare intermediate-sterol compounds such as derivatives of cycloartanol (4-
2172 10 carboxy-4-methyl-24-methylenecycloartanol) and 4 α -methyl sterols (24-ethyl-ionophenol and 24-
2173 11 ethylidene-ionophenol) [353] [354]. Future studies will reveal how sterols interplay with other lipids
2174 12 such as sphingolipids and anionic phospholipids to regulate hormone transport.
2175
2176
2177
2178

2179 14 **5.3 Abiotic stress**

2180 15 Lipids have been involved as second messengers in many responses to abiotic stress, see for
2181 16 review [262, 355-357] [358]. PLD and PLC/DGK-mediated PA formation and its subsequent
2182 17 phosphorylation to form Diacylglycerol Pyrophosphate (DGPP) are key players in this response
2183 18 [359]. Other lipids participate to the response: oxylipins, PIPs, sphingolipids, fatty acids,
2184 19 lysophospholipids, N-acylethanolamines and galactolipids, see for reviews [1] [360]. Studies have
2185 20 started deciphering the different isoforms of enzymes involved in these transduction pathways as
2186 21 well as their tight regulations, for recent reviews see [361]. For example, PA displays different modes
2187 22 of action, including direct target protein binding and biophysical effects on cell membranes. It is
2188 23 puzzling that PA production can be triggered by opposite stressors, such as cold and heat. How PA
2189 24 regulates this diversity of response is discussed in this recent review [264].

2190 25 PLD-derived PA was shown to recruit the ABA-regulated ABI1 phosphatase 2C (PP2C) to the PM
2191 26 [362]. The identification of ABI1 as a direct target of the PA provides a functional link between the
2192 27 two families of important signaling enzymes, PLD and PP2C. Recently, a study on the regulation of
2193 28 ion transport in plants showed that C2-domain ABA-related (CAR) family of small proteins is involved
2194 29 in the Ca²⁺-dependent recruitment of the pyrabactin resistance 1/PYR1-like (PYR/PYL) ABA receptors
2195 30 to the PM. CARs are peripheral membrane proteins that cluster at the PM and generate strong
2196 31 positive membrane curvature. These features represent a mechanism for the generation,
2197 32 stabilization, and/or specific recognition of PM discontinuities involved in the recruitment of PYR/PYL
2198 33 receptors and other signaling components in cell responses to salt stress [363].
2199
2200
2201
2202
2203

2204 35 **5.4 Plasmodesmata function**

2205 36 Plasmodesmata (PD) are specialized nano-sized membrane-lined channels, which cross the walls
2206 37 of plants and of some algal cells. PDs enable direct, regulated, symplastic transport of small RNAs and
2207 38 molecules between cells. They are also hijacked by phytoviruses to allow their propagation from cell-
2208 39 to-cell. Ultrastructure of PD has been deciphered. They are lined by the PM forming what is termed
2209 40 the PD-PM subcompartment (PD-PM) and contain a strand of tubular modified endoplasmic
2210 41 reticulum (ER) called desmotubule, and the space between these two membranes is thought to
2211 42 control PD permeability [200]. A recent study has reconstructed PD three-dimensional ultrastructure
2212 43 with an unprecedented resolution using electron tomography, showing that ER-PM contact sites
2213 44 undergo substantial remodeling events during cell differentiation [364]. Post-cytokinesis PD, called
2214 45 type I PD, present an intimate ER-PM contact along the entire length of the pores whereas during cell

2221
2222
2223 1 expansion, the PD pore widens and the two membranes separate, leaving a cytosolic sleeve spanned
2224 2 by tethers whose presence correlates with the appearance of the intermembrane gaps, called type II
2225 3 PD. Surprisingly, the type II PD allow diffusion of macromolecules despite the apparent lack of an
2226 4 open cytoplasmic sleeve, forcing the reassessment of the mechanisms that control plant cell-to-cell
2227 5 communication [364].

2228 6 The membrane organization of PDs is therefore characterized by the close apposition of the ER-
2229 7 derived desmotubule and the PM with spoke-like structures linking the two membranes likely
2230 8 defining microdomains of the PM, PD-PM and desmotubules has been recently proposed to be
2231 9 membrane contact sites (MCS). MCS control close appositions between two membranes that form
2232 10 microdomains involved in the control of lipid exchanges or in coupling events (review in [365]). MCS-
2233 11 subdomains are likely to display specific biophysical properties and may cluster proteins and
2234 12 negatively-charged lipids like phosphoinositides, promoting specific physicochemical membrane
2235 13 properties taking part in shaping local membrane electronegativity gradients [365].

2236 14 Firmly anchored within the cell wall, PDs are difficult to purify. A two-step simple purification
2237 15 procedure (consisting in isolating cell wall fragments containing intact PD and an enzymatic
2238 16 degradation of the wall matrix to release of PD) has been successfully design to obtain highly-purified
2239 17 PD preparations [366]. Hence, analyses of PD fractions have provided valuable information on the
2240 18 functional and structural elements that define PD, particularly for lipids. PD membranes display
2241 19 enrichment in sterols and sphingolipids with saturated VLCFAs (likely GIPCs) when compared with
2242 20 the bulk of the PM. This profile is reminiscent of DRMs although the isolation procedure is detergent-
2243 21 free and suggest that lipids are laterally segregated the PD-PM cell-to-cell junction in *Arabidopsis*
2244 22 *thaliana* [7]. This study identifies a role for sterols in modulating cell-to-cell connectivity, possibly by
2245 23 establishing and maintaining the positional specificity of callose-modifying GPI-anchored proteins at
2246 24 PD and emphasizes the importance of lipids in defining PD-associated nanodomains. The role played
2247 25 by the other major lipid constituents, such as GIPCs and glycerolipids in defining specialized
2248 26 membrane domains in PD, remains to be further studied. This change of paradigm regarding the
2249 27 membrane organization of PD will likely pave the way to a deep understanding of cell-to-cell
2250 28 communication in plants.
2251 29

2281
2282
2283 **1 Conclusions and perspectives: How to get a comprehensive membrane organization in plants?**
2284

2285 2 The deep-seated understanding of how the plant PM is organized in terms of the involvement of
2286 3 lipids and proteins clearly necessitates multiple approaches. Our community needs to develop new
2287 4 dedicated methodologies and dare multidisciplinary even further that what we have been
2288 5 accustomed to. For example, the extensive use of biophysical approaches to study lipid/protein
2289 6 interactions as reviewed in [367], among them: 1/ surface plasmon resonance [40], isothermal
2290 7 titration calorimetry (ITC), Langmuir monolayer tensiometry, liposomes binding and lipid strips and
2291 8 arrays [114] to study the interaction of proteins with lipids; 2/ liposome leakage and lipid-mixing
2292 9 assays [307] to investigate how proteins can destabilize membrane bilayers; 3/ Circular dichroism
2293 10 [307], Fourier-transform infrared spectroscopy [172], solid-state NMR with labeled lipids or proteins
2294 11 [368] to obtain 3D structures of the membrane-bound interaction-complexes; 4/ Atomic force
2295 12 microscopy (AFM) to scan the surface of bilayers and access the topology of different membrane
2296 13 organizations. A deep understanding of the structural aspects of protein/lipid interactions will allow
2297 14 the targeted-mutagenesis of key residues, the biological role of which could be further addressed by
2300 15 reverse genetics approaches.

2301 16 In all the methods described above, there is an urgent need for biochemistry to obtain purified
2302 17 proteins and lipids, in order to reconstitute proteoliposomes. Concerning proteins, the problem of
2303 18 insolubility of highly hydrophobic proteins could be solved by using different expression systems
2304 19 [369]. As for lipids, most of plant lipids are commercially available with the notable exception of
2305 20 GIPCs. The lack of commercially-available GIPCs strongly impairs any serious *in vitro* reconstitutions
2306 21 of true plant PM-like vesicles. One must undertake hardcore preparative biochemistry as described
2307 22 during the 1970's to obtain milligrams of purified GIPCs from living material [52, 54]. Purification of
2308 23 mg amount of GIPCs will also pave the way to the development of fluorescently labeled sphingolipid
2309 24 analogs by conjugating a hydrophilic fluorophore to the headgroup or a hydrophobic fluorophore to
2310 25 the amidified fatty acids e.g. [370]. Unfortunately, very few plant lipids labeled with a fluorochrome
2311 26 or deuterated are available. Similarly, none of the great diversity of free- and conjugated-
2312 27 phytosterols are commercialized in a labeled form, which strongly impairs NMR studies that would
2313 28 enable to further enquire about the role of each molecular species individually. From purified lipids,
2314 29 the preparation of asymmetrical liposomes will also be very challenging. To have access to the
2315 30 properties of asymmetric vesicles that mimic the plant PM would provide means to understand lipid
2316 31 raft formation or transmembrane helix orientation [371],

2320 32 Molecular dynamics (MD) is a method that computes the physical movements of atoms and
2321 33 molecules in order to give a view of the dynamic evolution of a virtual chemical system. It can
2322 34 therefore study the interaction dynamics of lipids and proteins, or the conformational changes of
2323 35 molecules, for a fixed period of time. MD computes lipid-lipid and lipid-protein interactions and
2324 36 provides a comprehensive atomistic model of a typical lipid bilayer and gather information on
2325 37 membrane domain formations [372] [373]. MD has been used in plant membrane biology to
2326 38 decipher the structural basis of the unconventional lipid-binding motif of REM that confers
2327 39 nanodomain organization [172]. Such approach of "computational microscopy" captures the
2328 40 molecular interactions within a complex system at a spatiotemporal resolution, unmatched by any
2329 41 other conventional experimental methods e.g. [134, 374]. MD can be of particular interest in
2330 42 grasping the intricacies of plant PM dynamics because the control of the thermodynamic parameters
2331 43 permitted by MD can be used to mimic the constantly varying environmental conditions sustained by
2332 44 plants in their natural habitats, and thereby to understand the biophysical implications of these
2333 45 variations on the PM. Unfortunately, neither plant sphingolipids (GluCER, GIPCs), nor phytosterols

2341
2342
2343 1 (free or conjugated) have been, to this day, modeled in the force field, preventing all MD studies
2344 2 with plant PM lipids. The force field refers to the functional form and parameter sets used to
2345 3 calculate the potential energy of a system of atoms or coarse-grained particles; it is the necessary
2346 4 step for MD simulations. The parameters of the energy functions may be derived from experiments
2348 5 in physics (solid-state NMR, Langmuir monolayer, calorimetry...) or chemistry (chemical structure,
2349 6 liquid-state NMR...) [375]. All-atom force fields provide parameters for every type of atom in a
2350 7 system. Coarse-grained potentials, which are often used in long-time simulations of macromolecules
2351 8 and multi-component complexes, provide even cruder representations for higher computing
2352 9 efficiency. Such modelization must be carried for plant sphingolipids and phytosterols as it was
2354 10 described for animal gangliosides in [376].

2355 11 Other aspects still missing in the plant membrane biology field, are the methods to image lipids *in*
2356 12 *vivo* necessary to follow their segregation at the nanoscale level, their dynamics and interactions
2357 13 with proteins. Two reasons can be given: firstly, as stated before, very few fluorescently-labeled
2359 14 lipids are available, and secondly, the cell wall strongly impairs the intake of fluorescently labeled
2360 15 molecules. Nevertheless, the use of *in vivo* bioorthogonal click chemistry could be an elegant
2361 16 approach to circumvent this problem in plants [377] [378]. Although genetically encoded biosensors
2362 17 for PIPs, PA, DAG and PS have already been developed [27, 114] [115]), biosensors of plant
2363 18 sphingolipids and phytosterols are crucially missing and will surely be developed using lipid-binding
2365 19 domains found in plant proteins. Inhibitors of lipid synthesis (table 1), and genetically-modified lipid-
2366 20 using enzymes (phosphoinositides kinase, lipase phosphatase) able to target the PM and specifically
2367 21 modify *in vivo* pools of lipids, are used to address the question of the role of lipids in nanodomain
2368 22 formation and dynamics [115, 172, 379]. Similarly, membrane surface charge or pH biosensors must
2369 23 be improved as described in animal literature with intramolecular FRET sensors [380, 381]. The
2370 24 development of environmentally-sensitive probes to label the outer- or inner-leaflet and measure
2372 25 independently the fluidity of plant PM leaflets, must also be engaged (see examples of available
2373 26 probes in [382]). Furthermore, super-resolution microscopy will continue to allow a deep
2374 27 understanding of segregation and dynamics of proteins and lipids at the nanometer scale. The
2375 28 development of fluorescent bimolecular tracking in the live-cell PM will reveal whether proteins and
2377 29 lipids may directly or indirectly interact with each other [208].

2378 30 Finally, state of the art lipidomics [383] and proteomics approaches must be further developed
2379 31 including phosphoproteomics and lipid-modification of proteins (myristoylation, palmitoylation,
2380 32 isoprenylation and GPI-anchoring, review in [384]).

2382 34 The study of K-RAS protein which controls cell proliferation in animal cells should be exemplified
2383 35 for the combinations of approaches mobilized by Hancock's group to tackle its function in relation to
2385 36 its organization within PM [257-259, 385-387]. K-Ras controls cell proliferation, and when mutated,
2386 37 cells continuously proliferate and often develop into cancer. This group tackled the role of K-Ras in
2387 38 PM nanodomains by using in parallel biochemistry, biophysics, modeling, high-resolution imagery,
2388 39 mutagenesis, structural biology, model membranes, transcriptomics, cancerology and genetics
2390 40 techniques. This form of multidisciplinary approach has led to a deep understanding of the
2391 41 anchoring, the clustering of K-Ras with PM lipids, as well as the integration of these molecular
2392 42 mechanisms into higher levels of cell biology, hence determining their consequences on the fate of
2393 43 the cell. For example, a recent paper of this group has shown that K-Ras anchoring sequences can
2394 44 create lipid nanodomains with a remarkable specificity [258], and that lipid nanodomains are not
2396 45 preexisting. A matter of the chicken or the egg causality dilemma! Similarly the works of Katharina

2401
2402
2403
2404
2405
2406
2407
2408
2409
2410
2411
2412
2413
2414
2415
2416
2417
2418
2419
2420
2421
2422
2423
2424
2425
2426
2427
2428
2429
2430
2431
2432
2433
2434
2435
2436
2437
2438
2439
2440
2441
2442
2443
2444
2445
2446
2447
2448
2449
2450
2451
2452
2453
2454
2455
2456
2457
2458
2459
2460

1 Gaus' [380, 381, 388] [389] [390, 391] or Akihiro Kusumi's labs [129, 392-394] are exemplary to
2 understand, by developing single-molecule imaging methods, how T-cells initiate an immune
3 response and to better fathom the intricate complexity between cytoskeleton and protein/lipid
4 segregation. These two research groups have been remarkable by developing, in collaboration with
5 biophysicists, state of the art technology to follow single-molecules in the PM.

6
7 Taken together, tools and methods must be developed by the plant membrane biology
8 community in the near future to pave the way towards the better understanding of the intimate
9 molecular relationships between lipids and proteins at the basis of domain segregation, dynamics,
10 signaling and function.

11

2461
2462
2463
2464
2465
2466
2467
2468
2469
2470
2471
2472
2473
2474
2475
2476
2477
2478
2479
2480
2481
2482
2483
2484
2485
2486
2487
2488
2489
2490
2491
2492
2493
2494
2495
2496
2497
2498
2499
2500
2501
2502
2503
2504
2505
2506
2507
2508
2509
2510
2511
2512
2513
2514
2515
2516
2517
2518
2519
2520

1 **Acknowledgements**

2 We apologize to researchers whose work could not be cited here because of space limitations. AMC
3 and PG are supported by the Ministère de l'Enseignement Supérieur et de la Recherche, France
4 (MERS, doctoral grants). This work was supported by the Bordeaux Metabolome Facility-MetaboHUB
5 (grant no. ANR-11-INBS-0010). We acknowledge the platform Metabolome-Fluxome-Lipidome of
6 Bordeaux (<http://www.biomemb.cnrs.fr/INDEX.html>) for contribution to lipid analysis.

7
8 No conflict of interest declared.
9

2521
2522
2523
2524
2525
2526
2527
2528
2529
2530
2531
2532
2533
2534
2535
2536
2537
2538
2539
2540
2541
2542
2543
2544
2545
2546
2547
2548
2549
2550
2551
2552
2553
2554
2555
2556
2557
2558
2559
2560
2561
2562
2563
2564
2565
2566
2567
2568
2569
2570
2571
2572
2573
2574
2575
2576
2577
2578
2579
2580

1 **Figure legends :**

2 **Figure 1: Determined structures of GIPC glycosidic polar head from tobacco and maize.**

3 A, tobacco GIPC of series A are major in tobacco leaves (top) with glucuronic acid (GlcA) and either
4 glucosamine (GlcN) or N-acetyl glucosamine (GlcNAc). Other minor polar head of series B and higher
5 glycosylated GIPC with arabinose (Ara), galactose (Gal) and Manose (Man) have been identified, but
6 the precise structure remains to be determined. Grey part is the conserved glycan moiety of
7 glucuronic-Hex. Cer indicates the ceramide moiety, in tobacco, with t18:0 and t18:1 for LCB, and
8 VLCFA mostly alpha 2-hydroxylated ; B, GIPC found in corn seeds with branched polar head

9
10 **Figure 2: Structures of specific plasma membrane phytosterols compared with animal cholesterol.**

11 A, free phytosterols ; B, phytostanol ; C, conjugated phytosterols.

12
13 **Figure 3: Biophysical features involved between a GIPC of series A and three molecules of sitosterols.**

14
15 These interactions are important for nanodomain formations in the PM. LCB, Long Chain Base;
16 VLCFA, Very Long Chain Fatty Acid.

17
18 **Figure 4: Formation of GIPC- and sterol-enriched domains along the secretory pathway.**

19 GIPCs are synthesized in the lumen of the trans Golgi network (TGN) by grafting on the ceramide
20 sequentially inositol-phosphate (IPCS, inositolphosphorylceramide synthase), glucuronic acid (IPUT1,
21 inositol phosphorylceramide glucuronosyltransferase) and mannose (GMT1, GIPC mannosyl-
22 transferase1). Golgi-localized nucleotide sugar transporter (GONST1) is responsible for the import of
23 GDP-mannose to fuel GIPC synthesis. After vesicular fusion to the PM, GIPC polar heads face the
24 apoplasm. Polyglycosylated GIPCs form nanodomains in the PM (in red).

2581
2582
2583
2584
2585
2586
2587
2588
2589
2590
2591
2592
2593
2594
2595
2596
2597
2598
2599
2600
2601
2602
2603
2604
2605
2606
2607
2608
2609
2610
2611
2612
2613
2614
2615
2616
2617
2618
2619
2620
2621
2622
2623
2624
2625
2626
2627
2628
2629
2630
2631
2632
2633
2634
2635
2636
2637
2638
2639
2640

1 **REFERENCES**

2 [1] Xue HW, Chen X, Mei Y. Function and regulation of phospholipid signalling in plants. *The*
3 *Biochemical journal*. 2009;421:145-56.
4 [2] Cacas JL BC, Grosjean K, Gerbeau-Pissot P, Lherminier J, Rombouts Y, Maes E, Bossard C,
5 Gronnier J, Furt F, Fouillen L, Germain¹, Bayer E, Cluzet S, Robert F, Schmitter JM, Deleu M,
6 Lins M, Simon-Plas F, Mongrand S. Re-visiting plant plasma membrane lipids in tobacco: a
7 focus on sphingolipids. *Plant physiology*. 2015;in press.
8 [3] Yetukuri L, Ekroos K, Vidal-Puig A, Oresic M. Informatics and computational strategies for
9 the study of lipids. *Molecular bioSystems*. 2008;4:121-7.
10 [4] Larsson C, Sommarin, M., Widell, S. Isolation of highly purified plant plasma membranes
11 and separation of inside-out and right-side-out vesicles. *Methods in Enzymology*.
12 1994;228:451-69.
13 [5] Samarakoon T, Shiva S, Lowe K, Tamura P, Roth MR, Welti R. *Arabidopsis thaliana*
14 membrane lipid molecular species and their mass spectral analysis. *Methods in molecular*
15 *biology*. 2012;918:179-268.
16 [6] Yu D, Rupasinghe TWT, Boughton BA, Natera SHA, Hill CB, Tarazona P, et al. A high-
17 resolution HPLC-QqTOF platform using parallel reaction monitoring for in-depth lipid
18 discovery and rapid profiling. *Anal Chim Acta*. 2018;1026:87-100.
19 [7] Grison MS, Brocard L, Fouillen L, Nicolas W, Wewer V, Dormann P, et al. Specific
20 membrane lipid composition is important for plasmodesmata function in *Arabidopsis*. *The*
21 *Plant cell*. 2015;27:1228-50.
22 [8] Doignon F, Laquel P, Testet E, Tuphile K, Fouillen L, Bessoule JJ. Requirement of
23 Phosphoinositides Containing Stearic Acid To Control Cell Polarity. *Molecular and cellular*
24 *biology*. 2015;36:765-80.
25 [9] Markham JE, Jaworski JG. Rapid measurement of sphingolipids from *Arabidopsis thaliana*
26 by reversed-phase high-performance liquid chromatography coupled to electrospray
27 ionization tandem mass spectrometry. *Rapid communications in mass spectrometry : RCM*.
28 2007;21:1304-14.
29 [10] Markham JE, Li J, Cahoon EB, Jaworski JG. Separation and identification of major plant
30 sphingolipid classes from leaves. *The Journal of biological chemistry*. 2006;281:22684-94.
31 [11] Schrick K, Shiva S, Arpin JC, Delimont N, Isaac G, Tamura P, et al. Steryl glucoside and
32 acyl steryl glucoside analysis of *Arabidopsis* seeds by electrospray ionization tandem mass
33 spectrometry. *Lipids*. 2012;47:185-93.
34 [12] Wewer V, Dombrink I, vom Dorp K, Dormann P. Quantification of sterol lipids in plants
35 by quadrupole time-of-flight mass spectrometry. *Journal of lipid research*. 2011;52:1039-54.
36 [13] Wenk MR. Lipidomics: new tools and applications. *Cell*. 2010;143:888-95.
37 [14] Horn PJ, Korte AR, Neogi PB, Love E, Fuchs J, Strupat K, et al. Spatial mapping of lipids at
38 cellular resolution in embryos of cotton. *The Plant cell*. 2012;24:622-36.
39 [15] Woodfield HK, Sturtevant D, Borisjuk L, Munz E, Guschina IA, Chapman K, et al. Spatial
40 and Temporal Mapping of Key Lipid Species in *Brassica napus* Seeds. *Plant physiology*.
41 2017;173:1998-2009.
42 [16] Ellis SR, Paine MRL, Eijkel GB, Pauling JK, Husen P, Jervelund MW, et al. Automated,
43 parallel mass spectrometry imaging and structural identification of lipids. *Nat Methods*.
44 2018.
45 [17] Frisz JF, Klitzing HA, Lou K, Hutcheon ID, Weber PK, Zimmerberg J, et al. Sphingolipid
46 domains in the plasma membranes of fibroblasts are not enriched with cholesterol. *The*
47 *Journal of biological chemistry*. 2013;288:16855-61.

2641
2642
2643
2644
2645
2646
2647
2648
2649
2650
2651
2652
2653
2654
2655
2656
2657
2658
2659
2660
2661
2662
2663
2664
2665
2666
2667
2668
2669
2670
2671
2672
2673
2674
2675
2676
2677
2678
2679
2680
2681
2682
2683
2684
2685
2686
2687
2688
2689
2690
2691
2692
2693
2694
2695
2696
2697
2698
2699
2700

1 [18] Frisz JF, Lou K, Klitzing HA, Hanafin WP, Lizunov V, Wilson RL, et al. Direct chemical
2 evidence for sphingolipid domains in the plasma membranes of fibroblasts. Proceedings of
3 the National Academy of Sciences of the United States of America. 2013;110:E613-22.
4 [19] Mongrand S, Morel J, Laroche J, Claverol S, Carde JP, Hartmann MA, et al. Lipid rafts in
5 higher plant cells: purification and characterization of Triton X-100-insoluble microdomains
6 from tobacco plasma membrane. The Journal of biological chemistry. 2004;279:36277-86.
7 [20] Uemura M, Joseph RA, Steponkus PL. Cold Acclimation of Arabidopsis thaliana (Effect on
8 Plasma Membrane Lipid Composition and Freeze-Induced Lesions). Plant physiology.
9 1995;109:15-30.
10 [21] Bohn M, Heinz E, Luthje S. Lipid composition and fluidity of plasma membranes isolated
11 from corn (*Zea mays* L.) roots. Archives of biochemistry and biophysics. 2001;387:35-40.
12 [22] Uemura M, Steponkus PL. A Contrast of the Plasma Membrane Lipid Composition of Oat
13 and Rye Leaves in Relation to Freezing Tolerance. Plant physiology. 1994;104:479-96.
14 [23] Quartacci MF, Glisic O, Stevanovic B, Navari-Izzo F. Plasma membrane lipids in the
15 resurrection plant *Ramonda serbica* following dehydration and rehydration. Journal of
16 experimental botany. 2002;53:2159-66.
17 [24] Berglund AH, Quartacci MF, Calucci L, Navari-Izzo F, Pinzino C, Liljenberg C. Alterations
18 of wheat root plasma membrane lipid composition induced by copper stress result in
19 changed physicochemical properties of plasma membrane lipid vesicles. Biochimica et
20 biophysica acta. 2002;1564:466-72.
21 [25] Vermeer JE, Munnik T. Using genetically encoded fluorescent reporters to image lipid
22 signalling in living plants. Methods in molecular biology. 2013;1009:283-9.
23 [26] Tejos R, Sauer M, Vanneste S, Palacios-Gomez M, Li H, Heilmann M, et al. Bipolar Plasma
24 Membrane Distribution of Phosphoinositides and Their Requirement for Auxin-Mediated
25 Cell Polarity and Patterning in Arabidopsis. The Plant cell. 2014;26:2114-28.
26 [27] Simon ML, Platre MP, Assil S, van Wijk R, Chen WY, Chory J, et al. A multi-colour/multi-
27 affinity marker set to visualize phosphoinositide dynamics in Arabidopsis. The Plant journal :
28 for cell and molecular biology. 2014;77:322-37.
29 [28] Yamaoka Y, Yu Y, Mizoi J, Fujiki Y, Saito K, Nishijima M, et al. PHOSPHATIDYLSERINE
30 SYNTHASE1 is required for microspore development in Arabidopsis thaliana. The Plant
31 journal : for cell and molecular biology. 2011;67:648-61.
32 [29] Hirano T, Stecker K, Munnik T, Xu H, Sato MH. Visualization of Phosphatidylinositol 3,5-
33 Bisphosphate Dynamics by a Tandem ML1N-Based Fluorescent Protein Probe in Arabidopsis.
34 Plant Cell Physiol. 2017;58:1185-95.
35 [30] van Leeuwen W, Vermeer JE, Gadella TW, Jr., Munnik T. Visualization of
36 phosphatidylinositol 4,5-bisphosphate in the plasma membrane of suspension-cultured
37 tobacco BY-2 cells and whole Arabidopsis seedlings. The Plant journal : for cell and molecular
38 biology. 2007;52:1014-26.
39 [31] Furt F, Konig S, Bessoule JJ, Sargueil F, Zallot R, Stanislas T, et al. Polyphosphoinositides
40 are enriched in plant membrane rafts and form microdomains in the plasma membrane.
41 Plant physiology. 2010;152:2173-87.
42 [32] Andersson MX, Stridh MH, Larsson KE, Liljenberg C, Sandelius AS. Phosphate-deficient
43 oat replaces a major portion of the plasma membrane phospholipids with the galactolipid
44 digalactosyldiacylglycerol. FEBS letters. 2003;537:128-32.
45 [33] Andersson MX, Larsson KE, Tjellstrom H, Liljenberg C, Sandelius AS. Phosphate-limited
46 oat. The plasma membrane and the tonoplast as major targets for phospholipid-to-glycolipid

2701
2702
2703
2704
2705
2706
2707
2708
2709
2710
2711
2712
2713
2714
2715
2716
2717
2718
2719
2720
2721
2722
2723
2724
2725
2726
2727
2728
2729
2730
2731
2732
2733
2734
2735
2736
2737
2738
2739
2740
2741
2742
2743
2744
2745
2746
2747
2748
2749
2750
2751
2752
2753
2754
2755
2756
2757
2758
2759
2760

1 replacement and stimulation of phospholipases in the plasma membrane. *The Journal of*
2 *biological chemistry*. 2005;280:27578-86.

3 [34] Vermeer JEM, van Wijk R, Goedhart J, Geldner N, Chory J, Gadella TWJ, Jr., et al. *In Vivo*
4 *Imaging of Diacylglycerol at the Cytoplasmic Leaflet of Plant Membranes*. *Plant Cell Physiol*.
5 2017;58:1196-207.

6 [35] Lynch. D DT. An introduction to plant sphingolipids and a review of recent advances in
7 understanding their metabolism and function. *New Phytologist*. 2004;16:677-702.

8 [36] Sonnino S, Prinetti A. Gangliosides as regulators of cell membrane organization and
9 functions. *Advances in experimental medicine and biology*. 2010;688:165-84.

10 [37] Moreau P, Bessoule JJ, Mongrand S, Testet E, Vincent P, Cassagne C. Lipid trafficking in
11 plant cells. *Progress in lipid research*. 1998;37:371-91.

12 [38] Pata MO, Hannun YA, Ng CK. Plant sphingolipids: decoding the enigma of the Sphinx.
13 *The New phytologist*. 2010;185:611-30.

14 [39] Cacas JL, Bure C, Grosjean K, Gerbeau-Pissot P, Lherminier J, Rombouts Y, et al.
15 *Revisiting Plant Plasma Membrane Lipids in Tobacco: A Focus on Sphingolipids*. *Plant*
16 *physiology*. 2016;170:367-84.

17 [40] Lenarčič T AI, Böhm H, Hodnik V, Pirc K, Zavec AP, Podobnik M, Greimel P, Yamaji AH,
18 Kobayashi T, Feussner I, Mortimer JC, Mamode--Cassim A, Mongrand S, Oecking C, Anderluh
19 G, Nürnberger T. Eudicot plant--specific sphingolipids determine host selectivity of microbial
20 NLP cytolysins. 2017.

21 [41] Carter HE, Gigg RH, Law JH, Nakayama T, Weber E. *Biochemistry of the sphingolipides*.
22 XI. Structure of phytoglycolipide. *The Journal of biological chemistry*. 1958;233:1309-14.

23 [42] Bure C, Cacas JL, Mongrand S, Schmitter JM. Characterization of glycosyl inositol
24 phosphoryl ceramides from plants and fungi by mass spectrometry. *Analytical and*
25 *bioanalytical chemistry*. 2014;406:995-1010.

26 [43] Hsieh TC, Lester RL, Laine RA. Glycophosphoceramides from plants. Purification and
27 characterization of a novel tetrasaccharide derived from tobacco leaf glycolipids. *The Journal*
28 *of biological chemistry*. 1981;256:7747-55.

29 [44] Sperling P, Heinz E. Plant sphingolipids: structural diversity, biosynthesis, first genes and
30 functions. *Biochimica et biophysica acta*. 2003;1632:1-15.

31 [45] Bure C, Cacas JL, Wang F, Gaudin K, Domergue F, Mongrand S, et al. Fast screening of
32 highly glycosylated plant sphingolipids by tandem mass spectrometry. *Rapid*
33 *communications in mass spectrometry : RCM*. 2011;25:3131-45.

34 [46] Cacas JL, Bure C, Furt F, Maalouf JP, Badoc A, Cluzet S, et al. Biochemical survey of the
35 polar head of plant glycosylinositolphosphoceramides unravels broad diversity.
36 *Phytochemistry*. 2013;96:191-200.

37 [47] Mortimer JC, Yu X, Albrecht S, Sicilia F, Huichalaf M, Ampuero D, et al. Abnormal
38 glycosphingolipid mannosylation triggers salicylic acid-mediated responses in *Arabidopsis*.
39 *The Plant cell*. 2013;25:1881-94.

40 [48] Bure C, Cacas JL, Mongrand S, Schmitter JM. Characterization of glycosyl inositol
41 phosphoryl ceramides from plants and fungi by mass spectrometry. *Analytical and*
42 *bioanalytical chemistry*. 2013.

43 [49] Fang L, Ishikawa T, Rennie EA, Murawska GM, Lao J, Yan J, et al. Loss of Inositol
44 Phosphorylceramide Sphingolipid Mannosylation Induces Plant Immune Responses and
45 Reduces Cellulose Content in *Arabidopsis*. *The Plant cell*. 2016;28:2991-3004.

2761
2762
2763
2764
2765
2766
2767
2768
2769
2770
2771
2772
2773
2774
2775
2776
2777
2778
2779
2780
2781
2782
2783
2784
2785
2786
2787
2788
2789
2790
2791
2792
2793
2794
2795
2796
2797
2798
2799
2800
2801
2802
2803
2804
2805
2806
2807
2808
2809
2810
2811
2812
2813
2814
2815
2816
2817
2818
2819
2820

1 [50] Luttgeharm KD, Kimberlin AN, Cahoon RE, Cerny RL, Napier JA, Markham JE, et al.
2 Sphingolipid metabolism is strikingly different between pollen and leaf in Arabidopsis as
3 revealed by compositional and gene expression profiling. *Phytochemistry*. 2015;115:121-9.
4 [51] Nagano M, Ishikawa T, Fujiwara M, Fukao Y, Kawano Y, Kawai-Yamada M, et al. Plasma
5 Membrane Microdomains Are Essential for Rac1-RbohB/H-Mediated Immunity in Rice. *The*
6 *Plant cell*. 2016;28:1966-83.
7 [52] Kaul K, Lester RL. Characterization of Inositol-containing Phosphosphingolipids from
8 Tobacco Leaves: Isolation and Identification of Two Novel, Major Lipids: N-
9 Acetylglucosamidoglucuronidoinositol Phosphorylceramide and
10 Glucosamidoglucuronidoinositol Phosphorylceramide. *Plant physiology*. 1975;55:120-9.
11 [53] Blaas N, Humpf HU. Structural profiling and quantitation of glycosyl inositol
12 phosphoceramides in plants with Fourier transform mass spectrometry. *Journal of*
13 *agricultural and food chemistry*. 2013;61:4257-69.
14 [54] Hsieh TC, Kaul K, Laine RA, Lester RL. Structure of a major glycoposphoceramide from
15 tobacco leaves, PSL-I: 2-deoxy-2-acetamido-D-glucopyranosyl(alpha1 leads to 4)-D-
16 glucuronopyranosyl(alpha1 leads to 2)myoinositol-1-O-phosphoceramide. *Biochemistry*.
17 1978;17:3575-81.
18 [55] Markham JE, Molino D, Gissot L, Bellec Y, Hematy K, Marion J, et al. Sphingolipids
19 containing very-long-chain Fatty acids define a secretory pathway for specific polar plasma
20 membrane protein targeting in Arabidopsis. *The Plant cell*. 2011;23:2362-78.
21 [56] Liang H, Yao N, Song JT, Luo S, Lu H, Greenberg JT. Ceramides modulate programmed
22 cell death in plants. *Genes & development*. 2003;17:2636-41.
23 [57] Marques JT, Marinho HS, de Almeida RFM. Sphingolipid hydroxylation in mammals,
24 yeast and plants - An integrated view. *Progress in lipid research*. 2018;71:18-42.
25 [58] Cacas JL, Bure C, Grosjean K, Gerbeau-Pissot P, Lherminier J, Rombouts Y, et al. Re-
26 Visiting Plant Plasma Membrane Lipids in Tobacco: A Focus on Sphingolipids. *Plant*
27 *physiology*. 2015.
28 [59] Hillig I, Leipelt M, Ott C, Zahringer U, Warnecke D, Heinz E. Formation of
29 glucosylceramide and sterol glucoside by a UDP-glucose-dependent glucosylceramide
30 synthase from cotton expressed in *Pichia pastoris*. *FEBS letters*. 2003;553:365-9.
31 [60] Wang W, Yang X, Tangchaiburana S, Ndeh R, Markham JE, Tsegaye Y, et al. An
32 inositolphosphorylceramide synthase is involved in regulation of plant programmed cell
33 death associated with defense in Arabidopsis. *The Plant cell*. 2008;20:3163-79.
34 [61] Rennie EA, Ebert B, Miles GP, Cahoon RE, Christiansen KM, Stonebloom S, et al.
35 Identification of a sphingolipid alpha-glucuronosyltransferase that is essential for pollen
36 function in Arabidopsis. *The Plant cell*. 2014;26:3314-25.
37 [62] Ishikawa T, Fang L, Rennie EA, Sechet J, Yan J, Jing B, et al. GLUCOSAMINE
38 INOSITOLPHOSPHORYLCERAMIDE TRANSFERASE1 (GINT1) Is a GlcNAc-Containing
39 Glycosylinositol Phosphorylceramide Glycosyltransferase. *Plant physiology*. 2018;177:938-
40 52.
41 [63] Blachutzik JO, Demir F, Kreuzer I, Hedrich R, Harms GS. Methods of staining and
42 visualization of sphingolipid enriched and non-enriched plasma membrane regions of
43 Arabidopsis thaliana with fluorescent dyes and lipid analogues. *Plant Methods*. 2012;8:28.
44 [64] Rog T, Orłowski A, Llorente A, Skotland T, Sylvanne T, Kauhanen D, et al. Interdigitation
45 of long-chain sphingomyelin induces coupling of membrane leaflets in a cholesterol
46 dependent manner. *Biochimica et biophysica acta*. 2016;1858:281-8.

2821
2822
2823
2824
2825
2826
2827
2828
2829
2830
2831
2832
2833
2834
2835
2836
2837
2838
2839
2840
2841
2842
2843
2844
2845
2846
2847
2848
2849
2850
2851
2852
2853
2854
2855
2856
2857
2858
2859
2860
2861
2862
2863
2864
2865
2866
2867
2868
2869
2870
2871
2872
2873
2874
2875
2876
2877
2878
2879
2880

1 [65] Guo DA, Venkatramesh M, Nes WD. Developmental regulation of sterol biosynthesis in
2 *Zea mays*. *Lipids*. 1995;30:203-19.

3 [66] Schaller H. New aspects of sterol biosynthesis in growth and development of higher
4 plants. *Plant Physiol Biochem*. 2004;42:465-76.

5 [67] Moreau RA, Nystrom L, Whitaker BD, Winkler-Moser JK, Baer DJ, Gebauer SK, et al.
6 Phytosterols and their derivatives: Structural diversity, distribution, metabolism, analysis,
7 and health-promoting uses. *Progress in lipid research*. 2018;70:35-61.

8 [68] Webb MS, Uemura M, Steponkus PL. A Comparison of Freezing Injury in Oat and Rye:
9 Two Cereals at the Extremes of Freezing Tolerance. *Plant physiology*. 1994;104:467-78.

10 [69] Ferrer A, Altabella T, Arro M, Boronat A. Emerging roles for conjugated sterols in plants.
11 *Progress in lipid research*. 2017;67:27-37.

12 [70] Boutte Y, Men S, Grebe M. Fluorescent in situ visualization of sterols in *Arabidopsis*
13 roots. *Nat Protoc*. 2011;6:446-56.

14 [71] Ovecka M, Berson T, Beck M, Derksen J, Samaj J, Baluska F, et al. Structural sterols are
15 involved in both the initiation and tip growth of root hairs in *Arabidopsis thaliana*. *The Plant*
16 *cell*. 2010;22:2999-3019.

17 [72] Liu P, Li RL, Zhang L, Wang QL, Niehaus K, Baluska F, et al. Lipid microdomain
18 polarization is required for NADPH oxidase-dependent ROS signaling in *Picea meyeri* pollen
19 tube tip growth. *The Plant journal : for cell and molecular biology*. 2009;60:303-13.

20 [73] Bonneau L, Gerbeau-Pissot P, Thomas D, Der C, Lherminier J, Bourque S, et al. Plasma
21 membrane sterol complexation, generated by filipin, triggers signaling responses in tobacco
22 cells. *Biochimica et biophysica acta*. 2010;1798:2150-9.

23 [74] Stanislas T, Grebe M, Boutte Y. Sterol dynamics during endocytic trafficking in
24 *Arabidopsis*. *Methods in molecular biology*. 2014;1209:13-29.

25 [75] Tjellstrom H, Hellgren LI, Wieslander A, Sandelius AS. Lipid asymmetry in plant plasma
26 membranes: phosphate deficiency-induced phospholipid replacement is restricted to the
27 cytosolic leaflet. *FASEB journal : official publication of the Federation of American Societies*
28 *for Experimental Biology*. 2010;24:1128-38.

29 [76] Liu SL, Sheng R, Jung JH, Wang L, Stec E, O'Connor MJ, et al. Orthogonal lipid sensors
30 identify transbilayer asymmetry of plasma membrane cholesterol. *Nat Chem Biol*.
31 2017;13:268-74.

32 [77] Hazel JR, Williams EE. The role of alterations in membrane lipid composition in enabling
33 physiological adaptation of organisms to their physical environment. *Progress in lipid*
34 *research*. 1990;29:167-227.

35 [78] Jacobson K, Derzko Z, Wu ES, Hou Y, Poste G. Measurement of the lateral mobility of cell
36 surface components in single, living cells by fluorescence recovery after photobleaching. *J*
37 *Supramol Struct*. 1976;5:565(417)-576(428).

38 [79] Ali GS, Prasad KV, Day I, Reddy AS. Ligand-dependent reduction in the membrane
39 mobility of FLAGELLIN SENSITIVE2, an *arabidopsis* receptor-like kinase. *Plant Cell Physiol*.
40 2007;48:1601-11.

41 [80] Lankova M, Humpolickova J, Vosolsobe S, Cit Z, Lacek J, Covan M, et al. Determination
42 of Dynamics of Plant Plasma Membrane Proteins with Fluorescence Recovery and Raster
43 Image Correlation Spectroscopy. *Microsc Microanal*. 2016;22:290-9.

44 [81] Martiniere A, Lavagi I, Nageswaran G, Rolfe DJ, Maneta-Peyret L, Luu DT, et al. Cell wall
45 constrains lateral diffusion of plant plasma-membrane proteins. *Proceedings of the National*
46 *Academy of Sciences of the United States of America*. 2012;109:12805-10.

2881
2882
2883
2884
2885
2886
2887
2888
2889
2890
2891
2892
2893
2894
2895
2896
2897
2898
2899
2900
2901
2902
2903
2904
2905
2906
2907
2908
2909
2910
2911
2912
2913
2914
2915
2916
2917
2918
2919
2920
2921
2922
2923
2924
2925
2926
2927
2928
2929
2930
2931
2932
2933
2934
2935
2936
2937
2938
2939
2940

1 [82] Machan R, Hof M. Lipid diffusion in planar membranes investigated by fluorescence
2 correlation spectroscopy. *Biochimica et biophysica acta*. 2010;1798:1377-91.

3 [83] Janmey PA, Kinnunen PK. Biophysical properties of lipids and dynamic membranes.
4 *Trends Cell Biol*. 2006;16:538-46.

5 [84] Lentz BR, Barenholz Y, Thompson TE. Fluorescence depolarization studies of phase
6 transitions and fluidity in phospholipid bilayers. 1. Single component phosphatidylcholine
7 liposomes. *Biochemistry*. 1976;15:4521-8.

8 [85] Moellering ER, Muthan B, Benning C. Freezing tolerance in plants requires lipid
9 remodeling at the outer chloroplast membrane. *Science*. 2010;330:226-8.

10 [86] Uemura M TY, Nakagawara c, Shigematsu s, Minami A, Kawamura Y. Responses of the
11 plasma membrane to low temperatures. *Physiologia Plantarum*. 2005;126:81-9.

12 [87] Thomashow MF. PLANT COLD ACCLIMATION: Freezing Tolerance Genes and Regulatory
13 Mechanisms. *Annu Rev Plant Physiol Plant Mol Biol*. 1999;50:571-99.

14 [88] Martiniere A, Shvedunova M, Thomson AJ, Evans NH, Penfield S, Runions J, et al.
15 Homeostasis of plasma membrane viscosity in fluctuating temperatures. *The New
16 phytologist*. 2011;192:328-37.

17 [89] Van Blitterswijk WJ, Van Hoeven RP, Emmelot P. On the lipid fluidity of malignant
18 lymphoid cell membranes. *Cancer research*. 1981;41:3670-1.

19 [90] Gerbeau-Pissot P, Der C, Thomas D, Anca IA, Grosjean K, Roche Y, et al. Modification of
20 plasma membrane organization in tobacco cells elicited by cryptogein. *Plant physiology*.
21 2014;164:273-86.

22 [91] Roche Y, Gerbeau-Pissot P, Buhot B, Thomas D, Bonneau L, Gresti J, et al. Depletion of
23 phytosterols from the plant plasma membrane provides evidence for disruption of lipid
24 rafts. *FASEB journal : official publication of the Federation of American Societies for
25 Experimental Biology*. 2008;22:3980-91.

26 [92] Roche Y, Klymchenko AS, Gerbeau-Pissot P, Gervais P, Mely Y, Simon-Plas F, et al.
27 Behavior of plant plasma membranes under hydrostatic pressure as monitored by
28 fluorescent environment-sensitive probes. *Biochimica et biophysica acta*. 2010;1798:1601-7.

29 [93] Grosjean K, Mongrand S, Beney L, Simon-Plas F, Gerbeau-Pissot P. Differential effect of
30 plant lipids on membrane organization: hot features and specificities of phytosphingolipids
31 and phytosterols. *The Journal of biological chemistry*. 2015.

32 [94] Shaghghi M, Chen MT, Hsueh YW, Zuckermann MJ, Thewalt JL. Effect of Sterol
33 Structure on the Physical Properties of 1-Palmitoyl-2-oleoyl-sn-glycero-3-phosphocholine
34 Membranes Determined Using (2)H Nuclear Magnetic Resonance. *Langmuir : the ACS journal
35 of surfaces and colloids*. 2016;32:7654-63.

36 [95] Mouritsen OG, Bagatolli LA, Duelund L, Garvik O, Ipsen JH, Simonsen AC. Effects of
37 seaweed sterols fucosterol and desmosterol on lipid membranes. *Chem Phys Lipids*.
38 2017;205:1-10.

39 [96] Bruckdorfer KR, Demel RA, De Gier J, van Deenen LL. The effect of partial replacements
40 of membrane cholesterol by other steroids on the osmotic fragility and glycerol permeability
41 of erythrocytes. *Biochimica et biophysica acta*. 1969;183:334-45.

42 [97] Edwards PA, Green C. Incorporation of plant sterols into membranes and its relation to
43 sterol absorption. *FEBS letters*. 1972;20:97-9.

44 [98] Halling KK, Slotte JP. Membrane properties of plant sterols in phospholipid bilayers as
45 determined by differential scanning calorimetry, resonance energy transfer and detergent-
46 induced solubilization. *Biochimica et biophysica acta*. 2004;1664:161-71.

2941
2942
2943
2944
2945
2946
2947
2948
2949
2950
2951
2952
2953
2954
2955
2956
2957
2958
2959
2960
2961
2962
2963
2964
2965
2966
2967
2968
2969
2970
2971
2972
2973
2974
2975
2976
2977
2978
2979
2980
2981
2982
2983
2984
2985
2986
2987
2988
2989
2990
2991
2992
2993
2994
2995
2996
2997
2998
2999
3000

1 [99] Haralampiev I, Scheidt HA, Huster D, Muller P. The Potential of alpha-Spinasterol to
2 Mimic the Membrane Properties of Natural Cholesterol. *Molecules*. 2017;22.
3 [100] Hodzic A, Rappolt M, Amenitsch H, Laggner P, Pabst G. Differential modulation of
4 membrane structure and fluctuations by plant sterols and cholesterol. *Biophysical journal*.
5 2008;94:3935-44.
6 [101] Hac-Wydro K, Wydro P, Dynarowicz-Latka P, Paluch M. Cholesterol and phytosterols
7 effect on sphingomyelin/phosphatidylcholine model membranes--thermodynamic analysis
8 of the interactions in ternary monolayers. *Journal of colloid and interface science*.
9 2009;329:265-72.
10 [102] Mannock DA, Benesch MG, Lewis RN, McElhaney RN. A comparative calorimetric and
11 spectroscopic study of the effects of cholesterol and of the plant sterols beta-sitosterol and
12 stigmasterol on the thermotropic phase behavior and organization of
13 dipalmitoylphosphatidylcholine bilayer membranes. *Biochimica et biophysica acta*.
14 2015;1848:1629-38.
15 [103] Bernsdorff CW, R. Differential Properties of the Sterols Cholesterol, Ergosterol, β -
16 Sitosterol, trans-7-Dehydrocholesterol, Stigmasterol and Lanosterol on DPPC Bilayer Order. *J*
17 *Phys Chem B* 2003;107:10658-64.
18 [104] Zhuang X, Ou A, Klauda JB. Simulations of simple linoleic acid-containing lipid
19 membranes and models for the soybean plasma membranes. *J Chem Phys*.
20 2017;146:215103.
21 [105] Sena F, Sotelo-Silveira M, Astrada S, Botella MA, Malacrida L, Borsani O. Spectral
22 phasor analysis reveals altered membrane order and function of root hair cells in
23 *Arabidopsis dry2/sqe1-5* drought hypersensitive mutant. *Plant Physiol Biochem*.
24 2017;119:224-31.
25 [106] Mudd JB, McManus TT. Effect of steryl glycosides on the phase transition of
26 dipalmitoyl lecithin. *Plant physiology*. 1980;65:78-80.
27 [107] Hac-Wydro K, Flasiński M, Broniatowski M, Dynarowicz-Latka P, Majewski J. Properties
28 of beta-sitostanol/DPPC monolayers studied with Grazing Incidence X-ray Diffraction (GIXD)
29 and Brewster Angle Microscopy. *Journal of colloid and interface science*. 2011;364:133-9.
30 [108] Hac-Wydro K, Lenartowicz R, Dynarowicz-Latka P. The influence of plant stanol (beta-
31 sitostanol) on inner leaflet of human erythrocytes membrane modeled with the Langmuir
32 monolayer technique. *Colloids Surf B Biointerfaces*. 2013;102:178-88.
33 [109] Sandor R, Der C, Grosjean K, Anca I, Noirot E, Leborgne-Castel N, et al. Plasma
34 membrane order and fluidity are diversely triggered by elicitors of plant defence. *Journal of*
35 *experimental botany*. 2016;67:5173-85.
36 [110] Lonnfors M, Doux JP, Killian JA, Nyholm TK, Slotte JP. Sterols have higher affinity for
37 sphingomyelin than for phosphatidylcholine bilayers even at equal acyl-chain order.
38 *Biophysical journal*. 2011;100:2633-41.
39 [111] Sezgin E, Levental I, Mayor S, Eggeling C. The mystery of membrane organization:
40 composition, regulation and roles of lipid rafts. *Nature reviews Molecular cell biology*.
41 2017;18:361-74.
42 [112] Marques JT, Cordeiro AM, Viana AS, Herrmann A, Marinho HS, de Almeida RF.
43 Formation and Properties of Membrane-Ordered Domains by Phytoceramide: Role of
44 Sphingoid Base Hydroxylation. *Langmuir : the ACS journal of surfaces and colloids*.
45 2015;31:9410-21.
46 [113] Platre MP, Jaillais Y. Anionic lipids and the maintenance of membrane electrostatics in
47 eukaryotes. *Plant signaling & behavior*. 2017;12:e1282022.

3001
3002
3003
3004
3005
3006
3007
3008
3009
3010
3011
3012
3013
3014
3015
3016
3017
3018
3019
3020
3021
3022
3023
3024
3025
3026
3027
3028
3029
3030
3031
3032
3033
3034
3035
3036
3037
3038
3039
3040
3041
3042
3043
3044
3045
3046
3047
3048
3049
3050
3051
3052
3053
3054
3055
3056
3057
3058
3059
3060

1 [114] Simon ML, Platre MP, Marques-Bueno MM, Armengot L, Stanislas T, Bayle V, et al. A
2 PtdIns(4)P-driven electrostatic field controls cell membrane identity and signalling in plants.
3 Nat Plants. 2016;2:16089.
4 [115] Platre MP, Noack LC, Doumane M, Bayle V, Simon MLA, Maneta-Peyret L, et al. A
5 Combinatorial Lipid Code Shapes the Electrostatic Landscape of Plant Endomembranes. Dev
6 Cell. 2018;45:465-80 e11.
7 [116] Martiniere A, Gibrat R, Sentenac H, Dumont X, Gaillard I, Paris N. Uncovering pH at
8 both sides of the root plasma membrane interface using noninvasive imaging. Proceedings
9 of the National Academy of Sciences of the United States of America. 2018.
10 [117] Zachowski A. Phospholipids in animal eukaryotic membranes: transverse asymmetry
11 and movement. The Biochemical journal. 1993;294 (Pt 1):1-14.
12 [118] Devaux PF, Morris R. Transmembrane asymmetry and lateral domains in biological
13 membranes. Traffic. 2004;5:241-6.
14 [119] Nickels JD, Smith JC, Cheng X. Lateral organization, bilayer asymmetry, and inter-leaflet
15 coupling of biological membranes. Chem Phys Lipids. 2015.
16 [120] Murate M, Kobayashi T. Revisiting transbilayer distribution of lipids in the plasma
17 membrane. Chem Phys Lipids. 2016;194:58-71.
18 [121] Ipsen JH, Mouritsen OG, Zuckermann MJ. Theory of thermal anomalies in the specific
19 heat of lipid bilayers containing cholesterol. Biophysical journal. 1989;56:661-7.
20 [122] Mouritsen OG. Theoretical models of phospholipid phase transitions. Chem Phys
21 Lipids. 1991;57:179-94.
22 [123] Veatch SL, Keller SL. Separation of liquid phases in giant vesicles of ternary mixtures of
23 phospholipids and cholesterol. Biophysical journal. 2003;85:3074-83.
24 [124] Almeida PF. Thermodynamics of lipid interactions in complex bilayers. Biochimica et
25 biophysica acta. 2009;1788:72-85.
26 [125] London E. How principles of domain formation in model membranes may explain
27 ambiguities concerning lipid raft formation in cells. Biochimica et biophysica acta.
28 2005;1746:203-20.
29 [126] Beck JG, Mathieu D, Loudet C, Buchoux S, Dufourc EJ. Plant sterols in "rafts": a better
30 way to regulate membrane thermal shocks. FASEB journal : official publication of the
31 Federation of American Societies for Experimental Biology. 2007;21:1714-23.
32 [127] Dufourc EJ. Sterols and membrane dynamics. J Chem Biol. 2008;1:63-77.
33 [128] Klymchenko AS, Kreder R. Fluorescent probes for lipid rafts: from model membranes to
34 living cells. Chem Biol. 2014;21:97-113.
35 [129] Komura N, Suzuki KG, Ando H, Konishi M, Koikeda M, Imamura A, et al. Raft-based
36 interactions of gangliosides with a GPI-anchored receptor. Nat Chem Biol. 2016;12:402-10.
37 [130] Fidorra M, Garcia A, Ipsen JH, Hartel S, Bagatolli LA. Lipid domains in giant unilamellar
38 vesicles and their correspondence with equilibrium thermodynamic phases: a quantitative
39 fluorescence microscopy imaging approach. Biochimica et biophysica acta. 2009;1788:2142-
40 9.
41 [131] Klausner RD, Wolf DE. Selectivity of fluorescent lipid analogues for lipid domains.
42 Biochemistry. 1980;19:6199-203.
43 [132] Mesquita RM, Melo E, Thompson TE, Vaz WL. Partitioning of amphiphiles between
44 coexisting ordered and disordered phases in two-phase lipid bilayer membranes. Biophysical
45 journal. 2000;78:3019-25.

3061
3062
3063
3064
3065
3066
3067
3068
3069
3070
3071
3072
3073
3074
3075
3076
3077
3078
3079
3080
3081
3082
3083
3084
3085
3086
3087
3088
3089
3090
3091
3092
3093
3094
3095
3096
3097
3098
3099
3100
3101
3102
3103
3104
3105
3106
3107
3108
3109
3110
3111
3112
3113
3114
3115
3116
3117
3118
3119
3120

1 [133] Baumgart T, Hunt G, Farkas ER, Webb WW, Feigenson GW. Fluorescence probe
2 partitioning between Lo/Ld phases in lipid membranes. *Biochimica et biophysica acta*.
3 2007;1768:2182-94.

4 [134] Ingolfsson HI, Melo MN, van Eerden FJ, Arnarez C, Lopez CA, Wassenaar TA, et al. Lipid
5 organization of the plasma membrane. *J Am Chem Soc*. 2014;136:14554-9.

6 [135] Brown DA, Rose JK. Sorting of GPI-anchored proteins to glycolipid-enriched membrane
7 subdomains during transport to the apical cell surface. *Cell*. 1992;68:533-44.

8 [136] London E, Brown DA. Insolubility of lipids in triton X-100: physical origin and
9 relationship to sphingolipid/cholesterol membrane domains (rafts). *Biochimica et biophysica*
10 *acta*. 2000;1508:182-95.

11 [137] Schroeder R, London E, Brown D. Interactions between saturated acyl chains confer
12 detergent resistance on lipids and glycosylphosphatidylinositol (GPI)-anchored proteins: GPI-
13 anchored proteins in liposomes and cells show similar behavior. *Proceedings of the National*
14 *Academy of Sciences of the United States of America*. 1994;91:12130-4.

15 [138] Garner AE, Smith DA, Hooper NM. Visualization of detergent solubilization of
16 membranes: implications for the isolation of rafts. *Biophysical journal*. 2008;94:1326-40.

17 [139] Rinia HA, de Kruijff B. Imaging domains in model membranes with atomic force
18 microscopy. *FEBS letters*. 2001;504:194-9.

19 [140] El Kirat K, Morandat S. Cholesterol modulation of membrane resistance to Triton X-100
20 explored by atomic force microscopy. *Biochimica et biophysica acta*. 2007;1768:2300-9.

21 [141] Morandat S, El Kirat K. Membrane resistance to Triton X-100 explored by real-time
22 atomic force microscopy. *Langmuir : the ACS journal of surfaces and colloids*. 2006;22:5786-
23 91.

24 [142] Keller S, Tsamaloukas A, Heerklotz H. A quantitative model describing the selective
25 solubilization of membrane domains. *J Am Chem Soc*. 2005;127:11469-76.

26 [143] Ahyayauch H, Collado MI, Goni FM, Lichtenberg D. Cholesterol reverts Triton X-100
27 preferential solubilization of sphingomyelin over phosphatidylcholine: a ³¹P-NMR study.
28 *FEBS letters*. 2009;583:2859-64.

29 [144] Staneva G, Seigneuret M, Koumanov K, Trugnan G, Angelova MI. Detergents induce
30 raft-like domains budding and fission from giant unilamellar heterogeneous vesicles: a direct
31 microscopy observation. *Chem Phys Lipids*. 2005;136:55-66.

32 [145] Sot J, Bagatolli LA, Goni FM, Alonso A. Detergent-resistant, ceramide-enriched domains
33 in sphingomyelin/ceramide bilayers. *Biophysical journal*. 2006;90:903-14.

34 [146] Babychuk EB, Draeger A. Biochemical characterization of detergent-resistant
35 membranes: a systematic approach. *The Biochemical journal*. 2006;397:407-16.

36 [147] Lingwood D, Simons K. Detergent resistance as a tool in membrane research. *Nat*
37 *Protoc*. 2007;2:2159-65.

38 [148] Rietveld A, Simons K. The differential miscibility of lipids as the basis for the formation
39 of functional membrane rafts. *Biochimica et biophysica acta*. 1998;1376:467-79.

40 [149] Salzer U, Prohaska R. Stomatin, flotillin-1, and flotillin-2 are major integral proteins of
41 erythrocyte lipid rafts. *Blood*. 2001;97:1141-3.

42 [150] Pike LJ, Han X, Chung KN, Gross RW. Lipid rafts are enriched in arachidonic acid and
43 plasmenylethanolamine and their composition is independent of caveolin-1 expression: a
44 quantitative electrospray ionization/mass spectrometric analysis. *Biochemistry*.
45 2002;41:2075-88.

3121
3122
3123
3124
3125
3126
3127
3128
3129
3130
3131
3132
3133
3134
3135
3136
3137
3138
3139
3140
3141
3142
3143
3144
3145
3146
3147
3148
3149
3150
3151
3152
3153
3154
3155
3156
3157
3158
3159
3160
3161
3162
3163
3164
3165
3166
3167
3168
3169
3170
3171
3172
3173
3174
3175
3176
3177
3178
3179
3180

1 [151] Schuck S, Honsho M, Ekroos K, Shevchenko A, Simons K. Resistance of cell membranes
2 to different detergents. *Proceedings of the National Academy of Sciences of the United*
3 *States of America*. 2003;100:5795-800.

4 [152] Pinaud F, Michalet X, Iyer G, Margeat E, Moore HP, Weiss S. Dynamic partitioning of a
5 glycosyl-phosphatidylinositol-anchored protein in glycosphingolipid-rich microdomains
6 imaged by single-quantum dot tracking. *Traffic*. 2009;10:691-712.

7 [153] Foster LJ, Chan QW. Lipid raft proteomics: more than just detergent-resistant
8 membranes. *Subcell Biochem*. 2007;43:35-47.

9 [154] Ayuyan AG, Cohen FS. Raft composition at physiological temperature and pH in the
10 absence of detergents. *Biophysical journal*. 2008;94:2654-66.

11 [155] Persaud-Sawin DA, Lightcap S, Harry GJ. Isolation of rafts from mouse brain tissue by a
12 detergent-free method. *Journal of lipid research*. 2009;50:759-67.

13 [156] Lee SC, Knowles TJ, Postis VL, Jamshad M, Parslow RA, Lin YP, et al. A method for
14 detergent-free isolation of membrane proteins in their local lipid environment. *Nat Protoc*.
15 2016;11:1149-62.

16 [157] Peskan T, Westermann M, Oelmüller R. Identification of low-density Triton X-100-
17 insoluble plasma membrane microdomains in higher plants. *European journal of*
18 *biochemistry / FEBS*. 2000;267:6989-95.

19 [158] Borner GH, Sherrier DJ, Weimar T, Michaelson LV, Hawkins ND, Macaskill A, et al.
20 Analysis of detergent-resistant membranes in Arabidopsis. Evidence for plasma membrane
21 lipid rafts. *Plant physiology*. 2005;137:104-16.

22 [159] Laloi M, Perret AM, Chatre L, Melser S, Cantrel C, Vaultier MN, et al. Insights into the
23 role of specific lipids in the formation and delivery of lipid microdomains to the plasma
24 membrane of plant cells. *Plant physiology*. 2007;143:461-72.

25 [160] Kierszniowska S, Seiwert B, Schulze WX. Definition of Arabidopsis sterol-rich
26 membrane microdomains by differential treatment with methyl-beta-cyclodextrin and
27 quantitative proteomics. *Molecular & cellular proteomics : MCP*. 2009;8:612-23.

28 [161] Keinath NF, Kierszniowska S, Lorek J, Bourdais G, Kessler SA, Shimosato-Asano H, et al.
29 PAMP (pathogen-associated molecular pattern)-induced changes in plasma membrane
30 compartmentalization reveal novel components of plant immunity. *The Journal of biological*
31 *chemistry*. 2010;285:39140-9.

32 [162] Zauber H, Szymanski W, Schulze WX. Unraveling sterol-dependent membrane
33 phenotypes by analysis of protein abundance-ratio distributions in different membrane
34 fractions under biochemical and endogenous sterol depletion. *Molecular & cellular*
35 *proteomics : MCP*. 2013;12:3732-43.

36 [163] Lefebvre B, Furt F, Hartmann MA, Michaelson LV, Carde JP, Sargueil-Boiron F, et al.
37 Characterization of lipid rafts from *Medicago truncatula* root plasma membranes: a
38 proteomic study reveals the presence of a raft-associated redox system. *Plant physiology*.
39 2007;144:402-18.

40 [164] Guillier C, Cacas JL, Recorbet G, Depretre N, Mounier A, Mongrand S, et al. Direct
41 purification of detergent-insoluble membranes from *Medicago truncatula* root microsomes:
42 comparison between floatation and sedimentation. *BMC plant biology*. 2014;14:255.

43 [165] Fujiwara M, Hamada S, Hiratsuka M, Fukao Y, Kawasaki T, Shimamoto K. Proteome
44 analysis of detergent-resistant membranes (DRMs) associated with OsRac1-mediated innate
45 immunity in rice. *Plant Cell Physiol*. 2009;50:1191-200.

3181
3182
3183
3184
3185
3186
3187
3188
3189
3190
3191
3192
3193
3194
3195
3196
3197
3198
3199
3200
3201
3202
3203
3204
3205
3206
3207
3208
3209
3210
3211
3212
3213
3214
3215
3216
3217
3218
3219
3220
3221
3222
3223
3224
3225
3226
3227
3228
3229
3230
3231
3232
3233
3234
3235
3236
3237
3238
3239
3240

1 [166] Takahashi D, Kawamura Y, Uemura M. Detergent-resistant plasma membrane
2 proteome to elucidate microdomain functions in plant cells. *Frontiers in plant science*.
3 2013;4:27.

4 [167] Gutierrez-Carbonell E, Takahashi D, Luthje S, Gonzalez-Reyes JA, Mongrand S,
5 Contreras-Moreira B, et al. A Shotgun Proteomic Approach Reveals That Fe Deficiency
6 Causes Marked Changes in the Protein Profiles of Plasma Membrane and Detergent-
7 Resistant Microdomain Preparations from *Beta vulgaris* Roots. *J Proteome Res*.
8 2016;15:2510-24.

9 [168] Stanislas T, Bouyssie D, Rossignol M, Vesa S, Fromentin J, Morel J, et al. Quantitative
10 proteomics reveals a dynamic association of proteins to detergent-resistant membranes
11 upon elicitor signaling in tobacco. *Molecular & cellular proteomics : MCP*. 2009;8:2186-98.

12 [169] Morel J, Claverol S, Mongrand S, Furt F, Fromentin J, Bessoule JJ, et al. Proteomics of
13 plant detergent-resistant membranes. *Molecular & cellular proteomics : MCP*. 2006;5:1396-
14 411.

15 [170] Minami A, Fujiwara M, Furuto A, Fukao Y, Yamashita T, Kamo M, et al. Alterations in
16 detergent-resistant plasma membrane microdomains in *Arabidopsis thaliana* during cold
17 acclimation. *Plant Cell Physiol*. 2009;50:341-59.

18 [171] Konig S, Hoffmann M, Mosblech A, Heilmann I. Determination of content and fatty acid
19 composition of unlabeled phosphoinositide species by thin-layer chromatography and gas
20 chromatography. *Anal Biochem*. 2008;378:197-201.

21 [172] Gronnier J, Crowet JM, Habenstein B, Nasir MN, Bayle V, Hosy E, et al. Structural basis
22 for plant plasma membrane protein dynamics and organization into functional
23 nanodomains. *Elife*. 2017;6.

24 [173] Carmona-Salazar L, El Hafidi M, Gutierrez-Najera N, Noyola-Martinez L, Gonzalez-Solis
25 A, Gavilanes-Ruiz M. Fatty acid profiles from the plasma membrane and detergent resistant
26 membranes of two plant species. *Phytochemistry*. 2015;109:25-35.

27 [174] Carmona-Salazar L, El Hafidi M, Enriquez-Arredondo C, Vazquez-Vazquez C, Gonzalez
28 de la Vara LE, Gavilanes-Ruiz M. Isolation of detergent-resistant membranes from plant
29 photosynthetic and non-photosynthetic tissues. *Anal Biochem*. 2011;417:220-7.

30 [175] Zidovetzki R, Levitan I. Use of cyclodextrins to manipulate plasma membrane
31 cholesterol content: evidence, misconceptions and control strategies. *Biochimica et*
32 *biophysica acta*. 2007;1768:1311-24.

33 [176] Nyholm PG, Pascher I, Sundell S. The effect of hydrogen bonds on the conformation of
34 glycosphingolipids. Methylated and unmethylated cerebroside studied by X-ray single crystal
35 analysis and model calculations. *Chem Phys Lipids*. 1990;52:1-10.

36 [177] Lofgren H, Pascher I. Molecular arrangements of sphingolipids. The monolayer
37 behaviour of ceramides. *Chem Phys Lipids*. 1977;20:273-84.

38 [178] Sperling P, Franke S, Luthje S, Heinz E. Are glucocerebrosides the predominant
39 sphingolipids in plant plasma membranes? *Plant Physiol Biochem*. 2005;43:1031-8.

40 [179] Moscatelli A, Gagliardi A, Maneta-Peyret L, Bini L, Stroppa N, Onelli E, et al.
41 Characterisation of detergent-insoluble membranes in pollen tubes of *Nicotiana tabacum*
42 (L.). *Biol Open*. 2015;4:378-99.

43 [180] Lingwood D, Simons K. Lipid rafts as a membrane-organizing principle. *Science*.
44 2010;327:46-50.

45 [181] Lichtenberg D, Goni FM, Heerklotz H. Detergent-resistant membranes should not be
46 identified with membrane rafts. *Trends Biochem Sci*. 2005;30:430-6.

3241
3242
3243
3244
3245
3246
3247
3248
3249
3250
3251
3252
3253
3254
3255
3256
3257
3258
3259
3260
3261
3262
3263
3264
3265
3266
3267
3268
3269
3270
3271
3272
3273
3274
3275
3276
3277
3278
3279
3280
3281
3282
3283
3284
3285
3286
3287
3288
3289
3290
3291
3292
3293
3294
3295
3296
3297
3298
3299
3300

1 [182] Malinsky J, Opekarova M, Grossmann G, Tanner W. Membrane microdomains, rafts,
2 and detergent-resistant membranes in plants and fungi. *Annu Rev Plant Biol.* 2013;64:501-
3 29.

4 [183] Munro S. Lipid rafts: elusive or illusive? *Cell.* 2003;115:377-88.

5 [184] Tanner W, Malinsky J, Opekarova M. In plant and animal cells, detergent-resistant
6 membranes do not define functional membrane rafts. *The Plant cell.* 2011;23:1191-3.

7 [185] Noirot E, Der C, Lherminier J, Robert F, Moricova P, Kieu K, et al. Dynamic changes in
8 the subcellular distribution of the tobacco ROS-producing enzyme RBOHD in response to the
9 oomycete elicitor cryptogein. *Journal of experimental botany.* 2014;65:5011-22.

10 [186] Lherminier J, Elmayan T, Fromentin J, Elaraqui KT, Vesa S, Morel J, et al. NADPH
11 oxidase-mediated reactive oxygen species production: subcellular localization and
12 reassessment of its role in plant defense. *Molecular plant-microbe interactions : MPMI.*
13 2009;22:868-81.

14 [187] Bucherl CA, Jarsch IK, Schudoma C, Segonzac C, Mbengue M, Robatzek S, et al. Plant
15 immune and growth receptors share common signalling components but localise to distinct
16 plasma membrane nanodomains. *Elife.* 2017;6.

17 [188] Raffaele S, Bayer E, Lafarge D, Cluzet S, German Retana S, Boubekour T, et al. Remorin,
18 a solanaceae protein resident in membrane rafts and plasmodesmata, impairs potato virus X
19 movement. *The Plant cell.* 2009;21:1541-55.

20 [189] Demir F, Horntrich C, Blachutzik JO, Scherzer S, Reinders Y, Kierszniowska S, et al.
21 *Arabidopsis* nanodomain-delimited ABA signaling pathway regulates the anion channel
22 SLAH3. *Proceedings of the National Academy of Sciences of the United States of America.*
23 2013;110:8296-301.

24 [190] Jarsch IK, Konrad SS, Stratil TF, Urbanus SL, Szymanski W, Braun P, et al. Plasma
25 Membranes Are Subcompartmentalized into a Plethora of Coexisting and Diverse
26 Microdomains in *Arabidopsis* and *Nicotiana benthamiana*. *The Plant cell.* 2014;26:1698-711.

27 [191] Simons K, Gerl MJ. Revitalizing membrane rafts: new tools and insights. *Nature reviews*
28 *Molecular cell biology.* 2010;11:688-99.

29 [192] Ott T. Membrane nanodomains and microdomains in plant-microbe interactions.
30 *Current opinion in plant biology.* 2017;40:82-8.

31 [193] Nakamura M, Grebe M. Outer, inner and planar polarity in the *Arabidopsis* root.
32 *Current opinion in plant biology.* 2018;41:46-53.

33 [194] Faulkner C. A cellular backline: specialization of host membranes for defence. *Journal*
34 *of experimental botany.* 2015;66:1565-71.

35 [195] Galweiler L, Guan C, Muller A, Wisman E, Mendgen K, Yephremov A, et al. Regulation
36 of polar auxin transport by AtPIN1 in *Arabidopsis* vascular tissue. *Science.* 1998;282:2226-30.

37 [196] Geldner N. Casparian strips. *Current biology : CB.* 2013;23:R1025-6.

38 [197] Noack LC, Jaillais Y. Precision targeting by phosphoinositides: how PIs direct
39 endomembrane trafficking in plants. *Current opinion in plant biology.* 2017;40:22-33.

40 [198] Ischebeck T, Seiler S, Heilmann I. At the poles across kingdoms: phosphoinositides and
41 polar tip growth. *Protoplasma.* 2010;240:13-31.

42 [199] Kalmbach L, Hematy K, De Bellis D, Barberon M, Fujita S, Ursache R, et al. Transient
43 cell-specific EXO70A1 activity in the CASP domain and Casparian strip localization. *Nat*
44 *Plants.* 2017;3:17058.

45 [200] Tilsner J, Nicolas W, Rosado A, Bayer EM. Staying Tight: Plasmodesmal Membrane
46 Contact Sites and the Control of Cell-to-Cell Connectivity in Plants. *Annu Rev Plant Biol.*
47 2016;67:337-64.

3301
3302
3303
3304
3305
3306
3307
3308
3309
3310
3311
3312
3313
3314
3315
3316
3317
3318
3319
3320
3321
3322
3323
3324
3325
3326
3327
3328
3329
3330
3331
3332
3333
3334
3335
3336
3337
3338
3339
3340
3341
3342
3343
3344
3345
3346
3347
3348
3349
3350
3351
3352
3353
3354
3355
3356
3357
3358
3359
3360

1 [201] Thomas CL, Bayer EM, Ritzenthaler C, Fernandez-Calvino L, Maule AJ. Specific targeting
2 of a plasmodesmal protein affecting cell-to-cell communication. *PLoS Biol.* 2008;6:e7.
3 [202] Simpson C, Thomas C, Findlay K, Bayer E, Maule AJ. An Arabidopsis GPI-anchor
4 plasmodesmal neck protein with callose binding activity and potential to regulate cell-to-cell
5 trafficking. *The Plant cell.* 2009;21:581-94.
6 [203] Frescatada-Rosa M, Stanislas T, Backues SK, Reichardt I, Men S, Boutte Y, et al. High
7 lipid order of Arabidopsis cell-plate membranes mediated by sterol and DYNAMIN-RELATED
8 PROTEIN1A function. *The Plant journal : for cell and molecular biology.* 2014;80:745-57.
9 [204] Kleine-Vehn J, Wabnik K, Martiniere A, Langowski L, Willig K, Naramoto S, et al.
10 Recycling, clustering, and endocytosis jointly maintain PIN auxin carrier polarity at the
11 plasma membrane. *Mol Syst Biol.* 2011;7:540.
12 [205] Rodriguez-Boulan E, Kreitzer G, Musch A. Organization of vesicular trafficking in
13 epithelia. *Nature reviews Molecular cell biology.* 2005;6:233-47.
14 [206] Burnette DT, Sengupta P, Dai Y, Lippincott-Schwartz J, Kachar B. Bleaching/blinking
15 assisted localization microscopy for superresolution imaging using standard fluorescent
16 molecules. *Proceedings of the National Academy of Sciences of the United States of*
17 *America.* 2011;108:21081-6.
18 [207] Kusumi A, Tsunoyama TA, Hirosawa KM, Kasai RS, Fujiwara TK. Tracking single
19 molecules at work in living cells. *Nat Chem Biol.* 2014;10:524-32.
20 [208] Curthoys NM, Parent M, Mlodzianoski M, Nelson AJ, Lilieholm J, Butler MB, et al.
21 Dances with Membranes: Breakthroughs from Super-resolution Imaging. *Curr Top Membr.*
22 2015;75:59-123.
23 [209] Lv X, Jing Y, Xiao J, Zhang Y, Zhu Y, Julian R, et al. Membrane microdomains and the
24 cytoskeleton constrain AtHIR1 dynamics and facilitate the formation of an AtHIR1-associated
25 immune complex. *The Plant journal : for cell and molecular biology.* 2017;90:3-16.
26 [210] Yoshinari A, Fujimoto M, Ueda T, Inada N, Naito S, Takano J. DRP1-Dependent
27 Endocytosis is Essential for Polar Localization and Boron-Induced Degradation of the Borate
28 Transporter BOR1 in Arabidopsis thaliana. *Plant Cell Physiol.* 2016;57:1985-2000.
29 [211] Gutierrez R, Lindeboom JJ, Paredez AR, Emons AM, Ehrhardt DW. Arabidopsis cortical
30 microtubules position cellulose synthase delivery to the plasma membrane and interact with
31 cellulose synthase trafficking compartments. *Nature cell biology.* 2009;11:797-806.
32 [212] Burstenbinder K, Moller B, Plotner R, Stamm G, Hause G, Mitra D, et al. The IQD Family
33 of Calmodulin-Binding Proteins Links Calcium Signaling to Microtubules, Membrane
34 Subdomains, and the Nucleus. *Plant physiology.* 2017;173:1692-708.
35 [213] Hutten SJ, Hamers DS, Aan den Toorn M, van Esse W, Nolles A, Bucherl CA, et al.
36 Visualization of BRI1 and SERK3/BAK1 Nanoclusters in Arabidopsis Roots. *PloS one.*
37 2017;12:e0169905.
38 [214] Li R, Liu P, Wan Y, Chen T, Wang Q, Mettbach U, et al. A membrane microdomain-
39 associated protein, Arabidopsis Flot1, is involved in a clathrin-independent endocytic
40 pathway and is required for seedling development. *The Plant cell.* 2012;24:2105-22.
41 [215] Hao H, Fan L, Chen T, Li R, Li X, He Q, et al. Clathrin and Membrane Microdomains
42 Cooperatively Regulate RbohD Dynamics and Activity in Arabidopsis. *The Plant cell.*
43 2014;26:1729-45.
44 [216] Gronnier JG-PP, Germain. V, Mongrand. S, Simon-Plas, F. Divide and Rule: plant plasma
45 membrane organization. *Trends in plant science.* 2018.
46 [217] Pertsinidis A, Zhang Y, Chu S. Subnanometre single-molecule localization, registration
47 and distance measurements. *Nature.* 2010;466:647-51.

3361
3362
3363
3364
3365
3366
3367
3368
3369
3370
3371
3372
3373
3374
3375
3376
3377
3378
3379
3380
3381
3382
3383
3384
3385
3386
3387
3388
3389
3390
3391
3392
3393
3394
3395
3396
3397
3398
3399
3400
3401
3402
3403
3404
3405
3406
3407
3408
3409
3410
3411
3412
3413
3414
3415
3416
3417
3418
3419
3420

1 [218] Balzarotti F, Eilers Y, Gwosch KC, Gynna AH, Westphal V, Stefani FD, et al. Nanometer
2 resolution imaging and tracking of fluorescent molecules with minimal photon fluxes.
3 Science. 2017;355:606-12.
4 [219] Golan Y, Sherman E. Resolving mixed mechanisms of protein subdiffusion at the T cell
5 plasma membrane. Nat Commun. 2017;8:15851.
6 [220] Persson F, Linden M, Unoson C, Elf J. Extracting intracellular diffusive states and
7 transition rates from single-molecule tracking data. Nat Methods. 2013;10:265-9.
8 [221] Sekeres J, Pejchar P, Santrucek J, Vukasinovic N, Zarsky V, Potocky M. Analysis of
9 Exocyst Subunit EXO70 Family Reveals Distinct Membrane Polar Domains in Tobacco Pollen
10 Tubes. Plant physiology. 2017;173:1659-75.
11 [222] Konrad SS, Popp C, Stratil TF, Jarsch IK, Thallmair V, Folgmann J, et al. S-acylation
12 anchors remorin proteins to the plasma membrane but does not primarily determine their
13 localization in membrane microdomains. The New phytologist. 2014;203:758-69.
14 [223] Sorre B, Callan-Jones A, Manneville JB, Nassoy P, Joanny JF, Prost J, et al. Curvature-
15 driven lipid sorting needs proximity to a demixing point and is aided by proteins.
16 Proceedings of the National Academy of Sciences of the United States of America.
17 2009;106:5622-6.
18 [224] Pinto SN, Laviad EL, Stiban J, Kelly SL, Merrill AH, Jr., Prieto M, et al. Changes in
19 membrane biophysical properties induced by sphingomyelinase depend on the sphingolipid
20 N-acyl chain. Journal of lipid research. 2014;55:53-61.
21 [225] Patterson GH, Hirschberg K, Polishchuk RS, Gerlich D, Phair RD, Lippincott-Schwartz J.
22 Transport through the Golgi apparatus by rapid partitioning within a two-phase membrane
23 system. Cell. 2008;133:1055-67.
24 [226] Duran JM, Campelo F, van Galen J, Sachsenheimer T, Sot J, Egorov MV, et al.
25 Sphingomyelin organization is required for vesicle biogenesis at the Golgi complex. EMBO J.
26 2012;31:4535-46.
27 [227] Campelo F, van Galen J, Turacchio G, Parashuraman S, Kozlov MM, Garcia-Parajo MF,
28 et al. Sphingomyelin metabolism controls the shape and function of the Golgi cisternae.
29 Elife. 2017;6.
30 [228] Melser S, Batailler B, Peypelut M, Poujol C, Bellec Y, Wattelet-Boyer V, et al.
31 Glucosylceramide biosynthesis is involved in Golgi morphology and protein secretion in plant
32 cells. Traffic. 2010;11:479-90.
33 [229] Klemm RW, Ejsing CS, Surma MA, Kaiser HJ, Gerl MJ, Sampaio JL, et al. Segregation of
34 sphingolipids and sterols during formation of secretory vesicles at the trans-Golgi network. J
35 Cell Biol. 2009;185:601-12.
36 [230] Deng Y, Rivera-Molina FE, Toomre DK, Burd CG. Sphingomyelin is sorted at the trans
37 Golgi network into a distinct class of secretory vesicle. Proceedings of the National Academy
38 of Sciences of the United States of America. 2016;113:6677-82.
39 [231] Boutte Y, Frescatada-Rosa M, Men S, Chow CM, Ebine K, Gustavsson A, et al.
40 Endocytosis restricts Arabidopsis KNOLLE syntaxin to the cell division plane during late
41 cytokinesis. EMBO J. 2010;29:546-58.
42 [232] Wattelet-Boyer V, Brocard L, Jonsson K, Esnay N, Joubes J, Domergue F, et al.
43 Enrichment of hydroxylated C24- and C26-acyl-chain sphingolipids mediates PIN2 apical
44 sorting at trans-Golgi network subdomains. Nat Commun. 2016;7:12788.
45 [233] Gao YQ, Chen JG, Chen ZR, An D, Lv QY, Han ML, et al. A new vesicle trafficking
46 regulator CTL1 plays a crucial role in ion homeostasis. PLoS Biol. 2017;15:e2002978.

3421
3422
3423
3424
3425
3426
3427
3428
3429
3430
3431
3432
3433
3434
3435
3436
3437
3438
3439
3440
3441
3442
3443
3444
3445
3446
3447
3448
3449
3450
3451
3452
3453
3454
3455
3456
3457
3458
3459
3460
3461
3462
3463
3464
3465
3466
3467
3468
3469
3470
3471
3472
3473
3474
3475
3476
3477
3478
3479
3480

1 [234] Siddhanta A, Shields D. Secretory vesicle budding from the trans-Golgi network is
2 mediated by phosphatidic acid levels. *The Journal of biological chemistry*. 1998;273:17995-8.

3 [235] Hankins HM, Sere YY, Diab NS, Menon AK, Graham TR. Phosphatidylserine
4 translocation at the yeast trans-Golgi network regulates protein sorting into exocytic
5 vesicles. *Molecular biology of the cell*. 2015;26:4674-85.

6 [236] Mesmin B, Bigay J, Polidori J, Jamecna D, Lacas-Gervais S, Antonny B. Sterol transfer,
7 PI4P consumption, and control of membrane lipid order by endogenous OSBP. *EMBO J*.
8 2017;36:3156-74.

9 [237] Gendre D, Jonsson K, Boutte Y, Bhalerao RP. Journey to the cell surface--the central
10 role of the trans-Golgi network in plants. *Protoplasma*. 2015;252:385-98.

11 [238] Rosquete MR, Davis DJ, Drakakaki G. The Plant Trans-Golgi Network: Not Just a Matter
12 of Distinction. *Plant physiology*. 2018;176:187-98.

13 [239] Viotti C, Bubeck J, Stierhof YD, Krebs M, Langhans M, van den Berg W, et al. Endocytic
14 and secretory traffic in Arabidopsis merge in the trans-Golgi network/early endosome, an
15 independent and highly dynamic organelle. *The Plant cell*. 2010;22:1344-57.

16 [240] Uemura T, Suda Y, Ueda T, Nakano A. Dynamic behavior of the trans-golgi network in
17 root tissues of Arabidopsis revealed by super-resolution live imaging. *Plant Cell Physiol*.
18 2014;55:694-703.

19 [241] Dettmer J, Hong-Hermesdorf A, Stierhof YD, Schumacher K. Vacuolar H⁺-ATPase
20 activity is required for endocytic and secretory trafficking in Arabidopsis. *The Plant cell*.
21 2006;18:715-30.

22 [242] Grosjean K, Der C, Robert F, Thomas D, Mongrand S, Simon-Plas F, et al. Interactions
23 between Lipids and Proteins are Critical for Plasma Membrane Ordered Domain
24 Organization in BY-2 Cells. *Journal of experimental botany*. 2018.

25 [243] Radhakrishnan A, McConnell HM. Condensed complexes of cholesterol and
26 phospholipids. *Biophysical journal*. 1999;77:1507-17.

27 [244] Somerharju PJ, Virtanen JA, Eklund KK, Vainio P, Kinnunen PK. 1-Palmitoyl-2-
28 pyrenedecanoyl glycerophospholipids as membrane probes: evidence for regular
29 distribution in liquid-crystalline phosphatidylcholine bilayers. *Biochemistry*. 1985;24:2773-
30 81.

31 [245] Huang J. Exploration of molecular interactions in cholesterol superlattices: effect of
32 multibody interactions. *Biophysical journal*. 2002;83:1014-25.

33 [246] Huang J, Feigenson GW. A microscopic interaction model of maximum solubility of
34 cholesterol in lipid bilayers. *Biophysical journal*. 1999;76:2142-57.

35 [247] Dhar P, Eck E, Israelachvili JN, Lee DW, Min Y, Ramachandran A, et al. Lipid-protein
36 interactions alter line tensions and domain size distributions in lung surfactant monolayers.
37 *Biophysical journal*. 2012;102:56-65.

38 [248] Mouritsen OG, Bloom M. Mattress model of lipid-protein interactions in membranes.
39 *Biophysical journal*. 1984;46:141-53.

40 [249] Nickels JD, Smith JC, Cheng X. Lateral organization, bilayer asymmetry, and inter-leaflet
41 coupling of biological membranes. *Chem Phys Lipids*. 2015;192:87-99.

42 [250] Fujimoto T, Parmryd I. Interleaflet Coupling, Pinning, and Leaflet Asymmetry-Major
43 Players in Plasma Membrane Nanodomain Formation. *Front Cell Dev Biol*. 2016;4:155.

44 [251] Chiricozzi E, Ciampa MG, Brasile G, Compostella F, Prinetti A, Nakayama H, et al. Direct
45 interaction, instrumental for signaling processes, between LacCer and Lyn in the lipid rafts of
46 neutrophil-like cells. *Journal of lipid research*. 2015;56:129-41.

3481
3482
3483
3484
3485
3486
3487
3488
3489
3490
3491
3492
3493
3494
3495
3496
3497
3498
3499
3500
3501
3502
3503
3504
3505
3506
3507
3508
3509
3510
3511
3512
3513
3514
3515
3516
3517
3518
3519
3520
3521
3522
3523
3524
3525
3526
3527
3528
3529
3530
3531
3532
3533
3534
3535
3536
3537
3538
3539
3540

1 [252] Raghupathy R, Anilkumar AA, Polley A, Singh PP, Yadav M, Johnson C, et al.
2 Transbilayer lipid interactions mediate nanoclustering of lipid-anchored proteins. *Cell*.
3 2015;161:581-94.
4 [253] Argos M, Rahman M, Parvez F, Dignam J, Islam T, Quasem I, et al. Baseline
5 comorbidities in a skin cancer prevention trial in Bangladesh. *Eur J Clin Invest*. 2013;43:579-
6 88.
7 [254] Yilmaz N, Kobayashi T. Assemblies of pore-forming toxins visualized by atomic force
8 microscopy. *Biochimica et biophysica acta*. 2016;1858:500-11.
9 [255] Lorizate M, Brugger B, Akiyama H, Glass B, Muller B, Anderluh G, et al. Probing HIV-1
10 membrane liquid order by Laurdan staining reveals producer cell-dependent differences.
11 *The Journal of biological chemistry*. 2009;284:22238-47.
12 [256] Brugger B, Glass B, Haberkant P, Leibrecht I, Wieland FT, Krausslich HG. The HIV
13 lipidome: a raft with an unusual composition. *Proceedings of the National Academy of
14 Sciences of the United States of America*. 2006;103:2641-6.
15 [257] Prior IA, Muncke C, Parton RG, Hancock JF. Direct visualization of Ras proteins in
16 spatially distinct cell surface microdomains. *J Cell Biol*. 2003;160:165-70.
17 [258] Zhou Y, Prakash P, Liang H, Cho KJ, Gorfe AA, Hancock JF. Lipid-Sorting Specificity
18 Encoded in K-Ras Membrane Anchor Regulates Signal Output. *Cell*. 2017;168:239-51 e16.
19 [259] Zhou Y, Wong CO, Cho KJ, van der Hoeven D, Liang H, Thakur DP, et al. SIGNAL
20 TRANSDUCTION. Membrane potential modulates plasma membrane phospholipid dynamics
21 and K-Ras signaling. *Science*. 2015;349:873-6.
22 [260] Jones JD, Dangl JL. The plant immune system. *Nature*. 2006;444:323-9.
23 [261] Laxalt AM, Munnik T. Phospholipid signalling in plant defence. *Current opinion in plant
24 biology*. 2002;5:332-8.
25 [262] Munnik T, Vermeer JE. Osmotic stress-induced phosphoinositide and inositol
26 phosphate signalling in plants. *Plant Cell Environ*. 2010;33:655-69.
27 [263] Canonne J, Froidure-Nicolas S, Rivas S. Phospholipases in action during plant defense
28 signaling. *Plant signaling & behavior*. 2011;6:13-8.
29 [264] Pokotylo I, Kravets V, Martinec J, Ruelland E. The phosphatidic acid paradox: Too many
30 actions for one molecule class? *Lessons from plants. Progress in lipid research*. 2018;71:43-
31 53.
32 [265] van der Luit AH, Piatti T, van Doorn A, Musgrave A, Felix G, Boller T, et al. Elicitation of
33 suspension-cultured tomato cells triggers the formation of phosphatidic acid and
34 diacylglycerol pyrophosphate. *Plant physiology*. 2000;123:1507-16.
35 [266] Laxalt AM, Raho N, Have AT, Lamattina L. Nitric oxide is critical for inducing
36 phosphatidic acid accumulation in xylanase-elicited tomato cells. *The Journal of biological
37 chemistry*. 2007;282:21160-8.
38 [267] Raho N, Ramirez L, Lanteri ML, Gonorazky G, Lamattina L, ten Have A, et al.
39 Phosphatidic acid production in chitosan-elicited tomato cells, via both phospholipase D and
40 phospholipase C/diacylglycerol kinase, requires nitric oxide. *J Plant Physiol*. 2011;168:534-9.
41 [268] Arisz SA, Testerink C, Munnik T. Plant PA signaling via diacylglycerol kinase. *Biochimica
42 et biophysica acta*. 2009;1791:869-75.
43 [269] Testerink C, Munnik T. Molecular, cellular, and physiological responses to phosphatidic
44 acid formation in plants. *Journal of experimental botany*. 2011;62:2349-61.
45 [270] Farmer PK, Choi JH. Calcium and phospholipid activation of a recombinant calcium-
46 dependent protein kinase (DcCPK1) from carrot (*Daucus carota* L.). *Biochimica et biophysica
47 acta*. 1999;1434:6-17.

3541
3542
3543
3544
3545
3546
3547
3548
3549
3550
3551
3552
3553
3554
3555
3556
3557
3558
3559
3560
3561
3562
3563
3564
3565
3566
3567
3568
3569
3570
3571
3572
3573
3574
3575
3576
3577
3578
3579
3580
3581
3582
3583
3584
3585
3586
3587
3588
3589
3590
3591
3592
3593
3594
3595
3596
3597
3598
3599
3600

1 [271] Szczegieliński J, Klimecka M, Liwosz A, Ciesielski A, Kaczanowski S, Dobrowolska G, et al.
2 A wound-responsive and phospholipid-regulated maize calcium-dependent protein kinase.
3 *Plant physiology*. 2005;139:1970-83.
4 [272] Munnik T, Testerink C. Plant phospholipid signaling: "in a nutshell". *Journal of lipid*
5 *research*. 2009;50 Suppl:S260-5.
6 [273] Munnik T, Laxalt AM. Measuring PLD activity in vivo. *Methods in molecular biology*.
7 2013;1009:219-31.
8 [274] Camehl I, Drzewiecki C, Vadassery J, Shahollari B, Sherameti I, Forzani C, et al. The OX11
9 kinase pathway mediates *Piriformospora indica*-induced growth promotion in *Arabidopsis*.
10 *PLoS pathogens*. 2011;7:e1002051.
11 [275] Pokotylo I, Kolesnikov Y, Kravets V, Zachowski A, Ruelland E. Plant phosphoinositide-
12 dependent phospholipases C: variations around a canonical theme. *Biochimie*. 2014;96:144-
13 57.
14 [276] Nuhse TS, Bottrill AR, Jones AM, Peck SC. Quantitative phosphoproteomic analysis of
15 plasma membrane proteins reveals regulatory mechanisms of plant innate immune
16 responses. *The Plant journal : for cell and molecular biology*. 2007;51:931-40.
17 [277] D'Ambrosio JM, Couto D, Fabro G, Scuffi D, Lamattina L, Munnik T, et al. Phospholipase
18 C2 Affects MAMP-Triggered Immunity by Modulating ROS Production. *Plant physiology*.
19 2017;175:970-81.
20 [278] Andersson MX, Kourtchenko O, Dangl JL, Mackey D, Ellerstrom M. Phospholipase-
21 dependent signalling during the AvrRpm1- and AvrRpt2-induced disease resistance
22 responses in *Arabidopsis thaliana*. *The Plant journal : for cell and molecular biology*.
23 2006;47:947-59.
24 [279] Krčková. Z KZ, Daněk. M, Brouzdová. J, Janda. PPM, Pokotylo. I, Ott. PG, Valentová. O,
25 Martinec. J. The *Arabidopsis thaliana* non-specific phospholipase C2 is involved in the
26 response to *Pseudomonas syringae* attack. *Annals of Botany*. 2017;121:297-310.
27 [280] Cacas JL, Gerbeau-Pissot P, Fromentin J, Cantrel C, Thomas D, Jeannette E, et al.
28 Diacylglycerol kinases activate tobacco NADPH oxidase-dependent oxidative burst in
29 response to cryptogein. *Plant Cell Environ*. 2017;40:585-98.
30 [281] Kadota Y, Shirasu K, Zipfel C. Regulation of the NADPH Oxidase RBOHD During Plant
31 Immunity. *Plant Cell Physiol*. 2015;56:1472-80.
32 [282] Liang X, Ma M, Zhou Z, Wang J, Yang X, Rao S, et al. Ligand-triggered de-repression of
33 *Arabidopsis* heterotrimeric G proteins coupled to immune receptor kinases. *Cell research*.
34 2018;28:529-43.
35 [283] Abd-El-Haliem AM, Vossen JH, van Zeijl A, Dezhsetan S, Testerink C, Seidl MF, et al.
36 Biochemical characterization of the tomato phosphatidylinositol-specific phospholipase C
37 (PI-PLC) family and its role in plant immunity. *Biochimica et biophysica acta*.
38 2016;1861:1365-78.
39 [284] Li J, Henty-Ridilla JL, Staiger BH, Day B, Staiger CJ. Capping protein integrates multiple
40 MAMP signalling pathways to modulate actin dynamics during plant innate immunity. *Nat*
41 *Commun*. 2015;6:7206.
42 [285] Sang Y, Zheng S, Li W, Huang B, Wang X. Regulation of plant water loss by manipulating
43 the expression of phospholipase Dalpha. *The Plant journal : for cell and molecular biology*.
44 2001;28:135-44.
45 [286] Yamaguchi T, Minami E, Ueki J, Shibuya N. Elicitor-induced activation of
46 phospholipases plays an important role for the induction of defense responses in
47 suspension-cultured rice cells. *Plant Cell Physiol*. 2005;46:579-87.

3601
3602
3603
3604
3605
3606
3607
3608
3609
3610
3611
3612
3613
3614
3615
3616
3617
3618
3619
3620
3621
3622
3623
3624
3625
3626
3627
3628
3629
3630
3631
3632
3633
3634
3635
3636
3637
3638
3639
3640
3641
3642
3643
3644
3645
3646
3647
3648
3649
3650
3651
3652
3653
3654
3655
3656
3657
3658
3659
3660

1 [287] Fan L, Zheng S, Cui D, Wang X. Subcellular distribution and tissue expression of
2 phospholipase Dalpha, Dbeta, and Dgamma in Arabidopsis. *Plant physiology*. 1999;119:1371-
3 8.

4 [288] Pinosa F, Buhot N, Kwaaitaal M, Fahlberg P, Thordal-Christensen H, Ellerstrom M, et al.
5 Arabidopsis phospholipase ddelta is involved in basal defense and nonhost resistance to
6 powdery mildew fungi. *Plant physiology*. 2013;163:896-906.

7 [289] Hyodo K, Taniguchi T, Manabe Y, Kaido M, Mise K, Sugawara T, et al. Phosphatidic acid
8 produced by phospholipase D promotes RNA replication of a plant RNA virus. *PLoS*
9 *pathogens*. 2015;11:e1004909.

10 [290] Guo L, Wang X. Crosstalk between Phospholipase D and Sphingosine Kinase in Plant
11 Stress Signaling. *Frontiers in plant science*. 2012;3:51.

12 [291] Kooijmam. E CV, de Kruijff. B, Burger. KNJ. Modulation of Membrane Curvature by
13 Phosphatidic Acid and Lysophosphatidic Acid. *Traffic*. 2003;4:162-74.

14 [292] Roth M. Molecular Mechanisms of PLD Function in Membrane Traffic. *Traffic*.
15 2008;9:1233-9.

16 [293] Lim GH, Singhal R, Kachroo A, Kachroo P. Fatty Acid- and Lipid-Mediated Signaling in
17 Plant Defense. *Annu Rev Phytopathol*. 2017;55:505-36.

18 [294] Yaeno T, Matsuda O, Iba K. Role of chloroplast trienoic fatty acids in plant disease
19 defense responses. *The Plant journal : for cell and molecular biology*. 2004;40:931-41.

20 [295] Madi LWX, Kobiler, L. Lichter, A. Prusky, D. Stress on avocado fruits regulates $\Delta 9$ -
21 stearoyl ACP desaturase expression, fatty acid composition, antifungal diene level and
22 resistance to *Colletotrichum gloeosporioides* attack. *Physiological and Molecular Plant*
23 *Pathology*. 2003;62:277-83.

24 [296] Ongena M, Duby F, Rossignol F, Fauconnier ML, Dommès J, Thonart P. Stimulation of
25 the lipoxygenase pathway is associated with systemic resistance induced in bean by a
26 nonpathogenic *Pseudomonas* strain. *Molecular plant-microbe interactions : MPMI*.
27 2004;17:1009-18.

28 [297] Schrick K, Fujioka S, Takatsuto S, Stierhof YD, Stransky H, Yoshida S, et al. A link
29 between sterol biosynthesis, the cell wall, and cellulose in Arabidopsis. *The Plant journal : for*
30 *cell and molecular biology*. 2004;38:227-43.

31 [298] Michaelson LV, Napier JA, Molino D, Faure JD. Plant sphingolipids: Their importance in
32 cellular organization and adaptation. *Biochimica et biophysica acta*. 2016;1861:1329-35.

33 [299] König S, Feussner K, Schwarz M, Kaefer A, Iven T, Landesfeind M, et al. Arabidopsis
34 mutants of sphingolipid fatty acid alpha-hydroxylases accumulate ceramides and salicylates.
35 *The New phytologist*. 2012;196:1086-97.

36 [300] Abbas HK, Tanaka T, Shier WT. Biological activities of synthetic analogues of *Alternaria*
37 *alternata* toxin (AAL-toxin) and fumonisin in plant and mammalian cell cultures.
38 *Phytochemistry*. 1995;40:1681-9.

39 [301] Griffiths JS, Haslam SM, Yang T, Garczynski SF, Mulloy B, Morris H, et al. Glycolipids as
40 receptors for *Bacillus thuringiensis* crystal toxin. *Science*. 2005;307:922-5.

41 [302] Yu X, Feizpour A, Ramirez NG, Wu L, Akiyama H, Xu F, et al. Glycosphingolipid-
42 functionalized nanoparticles recapitulate CD169-dependent HIV-1 uptake and trafficking in
43 dendritic cells. *Nat Commun*. 2014;5:4136.

44 [303] Gronnier J, Germain V, Gouguet P, Cacas JL, Mongrand S. GIPC: Glycosyl Inositol
45 Phospho Ceramides, the major sphingolipids on earth. *Plant signaling & behavior*.
46 2016;11:e1152438.

3661
3662
3663
3664
3665
3666
3667
3668
3669
3670
3671
3672
3673
3674
3675
3676
3677
3678
3679
3680
3681
3682
3683
3684
3685
3686
3687
3688
3689
3690
3691
3692
3693
3694
3695
3696
3697
3698
3699
3700
3701
3702
3703
3704
3705
3706
3707
3708
3709
3710
3711
3712
3713
3714
3715
3716
3717
3718
3719
3720

1 [304] Oome S, Van den Ackerveken G. Comparative and functional analysis of the widely
2 occurring family of Nep1-like proteins. *Molecular plant-microbe interactions* : MPMI.
3 2014;27:1081-94.

4 [305] Gijzen M, Nurnberger T. Nep1-like proteins from plant pathogens: recruitment and
5 diversification of the NPP1 domain across taxa. *Phytochemistry*. 2006;67:1800-7.

6 [306] Qutob D, Kemmerling B, Brunner F, Kufner I, Engelhardt S, Gust AA, et al. Phytotoxicity
7 and innate immune responses induced by Nep1-like proteins. *The Plant cell*. 2006;18:3721-
8 44.

9 [307] Perraki A, Cacas JL, Crowet JM, Lins L, Castroviejo M, German-Retana S, et al. Plasma
10 membrane localization of *Solanum tuberosum* remorin from group 1, homolog 3 is mediated
11 by conformational changes in a novel C-terminal anchor and required for the restriction of
12 potato virus X movement]. *Plant physiology*. 2012;160:624-37.

13 [308] Lefebvre B, Timmers T, Mbengue M, Moreau S, Herve C, Toth K, et al. A remorin
14 protein interacts with symbiotic receptors and regulates bacterial infection. *Proceedings of*
15 *the National Academy of Sciences of the United States of America*. 2010;107:2343-8.

16 [309] Liang P, Stratil TF, Popp C, Marin M, Folgmann J, Mysore KS, et al. Symbiotic root
17 infections in *Medicago truncatula* require remorin-mediated receptor stabilization in
18 membrane nanodomains. *Proceedings of the National Academy of Sciences of the United*
19 *States of America*. 2018;115:5289-94.

20 [310] Srivastava V, Malm E, Sundqvist G, Bulone V. Quantitative proteomics reveals that
21 plasma membrane microdomains from poplar cell suspension cultures are enriched in
22 markers of signal transduction, molecular transport, and callose biosynthesis. *Molecular &*
23 *cellular proteomics* : MCP. 2013;12:3874-85.

24 [311] Son S, Oh CJ, An CS. *Arabidopsis thaliana* Remorins Interact with SnRK1 and Play a Role
25 in Susceptibility to Beet Curly Top Virus and Beet Severe Curly Top Virus. *The plant pathology*
26 *journal*. 2014;30:269-78.

27 [312] Bozkurt TO, Richardson A, Dagdas YF, Mongrand S, Kamoun S, Raffaele S. The Plant
28 Membrane-Associated REMORIN1.3 Accumulates in Discrete Perhaustorial Domains and
29 Enhances Susceptibility to *Phytophthora infestans*. *Plant physiology*. 2014;165:1005-18.

30 [313] Gui J, Liu C, Shen J, Li L. Grain setting defect1, encoding a remorin protein, affects the
31 grain setting in rice through regulating plasmodesmatal conductance. *Plant physiology*.
32 2014;166:1463-78.

33 [314] Zipfel C, Oldroyd GE. Plant signalling in symbiosis and immunity. *Nature*. 2017;543:328-
34 36.

35 [315] Gomez-Gomez L, Boller T. FLS2: an LRR receptor-like kinase involved in the perception
36 of the bacterial elicitor flagellin in *Arabidopsis*. *Mol Cell*. 2000;5:1003-11.

37 [316] Couto D, Niebergall R, Liang X, Bucherl CA, Sklenar J, Macho AP, et al. The *Arabidopsis*
38 Protein Phosphatase PP2C38 Negatively Regulates the Central Immune Kinase BIK1. *PLoS*
39 *pathogens*. 2016;12:e1005811.

40 [317] Faulkner C, Petutschnig E, Benitez-Alfonso Y, Beck M, Robatzek S, Lipka V, et al. LYM2-
41 dependent chitin perception limits molecular flux via plasmodesmata. *Proceedings of the*
42 *National Academy of Sciences of the United States of America*. 2013;110:9166-70.

43 [318] Zavaliev R, Dong X, Epel BL. Glycosylphosphatidylinositol (GPI) Modification Serves as a
44 Primary Plasmodesmal Sorting Signal. *Plant physiology*. 2016;172:1061-73.

45 [319] Zavaliev R, Levy A, Gera A, Epel BL. Subcellular dynamics and role of *Arabidopsis beta*-
46 *1,3-glucanases* in cell-to-cell movement of tobamoviruses. *Molecular plant-microbe*
47 *interactions* : MPMI. 2013;26:1016-30.

3721
3722
3723
3724
3725
3726
3727
3728
3729
3730
3731
3732
3733
3734
3735
3736
3737
3738
3739
3740
3741
3742
3743
3744
3745
3746
3747
3748
3749
3750
3751
3752
3753
3754
3755
3756
3757
3758
3759
3760
3761
3762
3763
3764
3765
3766
3767
3768
3769
3770
3771
3772
3773
3774
3775
3776
3777
3778
3779
3780

1 [320] Halperin W, Jensen WA. Ultrastructural changes during growth and embryogenesis in
2 carrot cell cultures. *J Ultrastruct Res.* 1967;18:428-43.

3 [321] Rutter BD, Innes RW. Extracellular vesicles as key mediators of plant-microbe
4 interactions. *Current opinion in plant biology.* 2018;44:16-22.

5 [322] Gonorazky G, Laxalt AM, Testerink C, Munnik T, de la Canal L. Phosphatidylinositol 4-
6 phosphate accumulates extracellularly upon xylanase treatment in tomato cell suspensions.
7 *Plant Cell Environ.* 2008;31:1051-62.

8 [323] Regente M, Pinedo M, San Clemente H, Balliau T, Jamet E, de la Canal L. Plant
9 extracellular vesicles are incorporated by a fungal pathogen and inhibit its growth. *Journal of*
10 *experimental botany.* 2017;68:5485-95.

11 [324] Micali CO, Neumann U, Grunewald D, Panstruga R, O'Connell R. Biogenesis of a
12 specialized plant-fungal interface during host cell internalization of *Golovinomyces orontii*
13 haustoria. *Cell Microbiol.* 2011;13:210-26.

14 [325] An Q, Huckelhoven R, Kogel KH, van Bel AJ. Multivesicular bodies participate in a cell
15 wall-associated defence response in barley leaves attacked by the pathogenic powdery
16 mildew fungus. *Cell Microbiol.* 2006;8:1009-19.

17 [326] Wang M, Weiberg A, Lin FM, Thomma BP, Huang HD, Jin H. Bidirectional cross-
18 kingdom RNAi and fungal uptake of external RNAs confer plant protection. *Nat Plants.*
19 2016;2:16151.

20 [327] Zhang T, Zhao YL, Zhao JH, Wang S, Jin Y, Chen ZQ, et al. Cotton plants export
21 microRNAs to inhibit virulence gene expression in a fungal pathogen. *Nat Plants.*
22 2016;2:16153.

23 [328] Cai Q, Qiao L, Wang M, He B, Lin FM, Palmquist J, et al. Plants send small RNAs in
24 extracellular vesicles to fungal pathogen to silence virulence genes. *Science.* 2018;360:1126-
25 9.

26 [329] Rutter BD, Innes RW. Extracellular Vesicles Isolated from the Leaf Apoplast Carry
27 Stress-Response Proteins. *Plant physiology.* 2017;173:728-41.

28 [330] Gonorazky G, Laxalt AM, Dekker HL, Rep M, Munnik T, Testerink C, et al.
29 Phosphatidylinositol 4-phosphate is associated to extracellular lipoproteic fractions and is
30 detected in tomato apoplastic fluids. *Plant Biol (Stuttg).* 2012;14:41-9.

31 [331] Sabatini S, Beis D, Wolkenfelt H, Murfett J, Guilfoyle T, Malamy J, et al. An auxin-
32 dependent distal organizer of pattern and polarity in the *Arabidopsis* root. *Cell.* 1999;99:463-
33 72.

34 [332] Benkova E, Michniewicz M, Sauer M, Teichmann T, Seifertova D, Jurgens G, et al. Local,
35 efflux-dependent auxin gradients as a common module for plant organ formation. *Cell.*
36 2003;115:591-602.

37 [333] Friml J, Benkova E, Mayer U, Palme K, Muster G. Automated whole mount localisation
38 techniques for plant seedlings. *The Plant journal : for cell and molecular biology.*
39 2003;34:115-24.

40 [334] Grieneisen VA, Xu J, Maree AF, Hogeweg P, Scheres B. Auxin transport is sufficient to
41 generate a maximum and gradient guiding root growth. *Nature.* 2007;449:1008-13.

42 [335] Bennett MJ, Marchant A, Green HG, May ST, Ward SP, Millner PA, et al. *Arabidopsis*
43 *AUX1* gene: a permease-like regulator of root gravitropism. *Science.* 1996;273:948-50.

44 [336] Luschnig C, Gaxiola RA, Grisafi P, Fink GR. *EIR1*, a root-specific protein involved in auxin
45 transport, is required for gravitropism in *Arabidopsis thaliana*. *Genes & development.*
46 1998;12:2175-87.

3781
3782
3783
3784
3785
3786
3787
3788
3789
3790
3791
3792
3793
3794
3795
3796
3797
3798
3799
3800
3801
3802
3803
3804
3805
3806
3807
3808
3809
3810
3811
3812
3813
3814
3815
3816
3817
3818
3819
3820
3821
3822
3823
3824
3825
3826
3827
3828
3829
3830
3831
3832
3833
3834
3835
3836
3837
3838
3839
3840

1 [337] Petrasek J, Mravec J, Bouchard R, Blakeslee JJ, Abas M, Seifertova D, et al. PIN proteins
2 perform a rate-limiting function in cellular auxin efflux. *Science*. 2006;312:914-8.

3 [338] Wisniewska J, Xu J, Seifertova D, Brewer PB, Ruzicka K, Blilou I, et al. Polar PIN
4 localization directs auxin flow in plants. *Science*. 2006;312:883.

5 [339] Yang Y, Hammes UZ, Taylor CG, Schachtman DP, Nielsen E. High-affinity auxin
6 transport by the AUX1 influx carrier protein. *Current biology : CB*. 2006;16:1123-7.

7 [340] Boutte Y, Jonsson K, McFarlane HE, Johnson E, Gendre D, Swarup R, et al. ECHIDNA-
8 mediated post-Golgi trafficking of auxin carriers for differential cell elongation. *Proceedings*
9 *of the National Academy of Sciences of the United States of America*. 2013;110:16259-64.

10 [341] Wang JG, Li S, Zhao XY, Zhou LZ, Huang GQ, Feng C, et al. HAPLESS13, the Arabidopsis
11 mu1 adaptin, is essential for protein sorting at the trans-Golgi network/early endosome.
12 *Plant physiology*. 2013;162:1897-910.

13 [342] Feraru E, Feraru MI, Asaoka R, Paciorek T, De Rycke R, Tanaka H, et al. BEX5/RabA1b
14 regulates trans-Golgi network-to-plasma membrane protein trafficking in Arabidopsis. *The*
15 *Plant cell*. 2012;24:3074-86.

16 [343] Gendre D, Oh J, Boutte Y, Best JG, Samuels L, Nilsson R, et al. Conserved Arabidopsis
17 ECHIDNA protein mediates trans-Golgi-network trafficking and cell elongation. *Proceedings*
18 *of the National Academy of Sciences of the United States of America*. 2011;108:8048-53.

19 [344] Gendre D, McFarlane HE, Johnson E, Mouille G, Sjodin A, Oh J, et al. Trans-Golgi
20 network localized ECHIDNA/Ypt interacting protein complex is required for the secretion of
21 cell wall polysaccharides in Arabidopsis. *The Plant cell*. 2013;25:2633-46.

22 [345] Naramoto S, Otegui MS, Kutsuna N, de Rycke R, Dainobu T, Karampelias M, et al.
23 Insights into the localization and function of the membrane trafficking regulator GNOM ARF-
24 GEF at the Golgi apparatus in Arabidopsis. *The Plant cell*. 2014;26:3062-76.

25 [346] Jonsson K, Boutte Y, Singh RK, Gendre D, Bhalerao RP. Ethylene Regulates Differential
26 Growth via BIG ARF-GEF-Dependent Post-Golgi Secretory Trafficking in Arabidopsis. *The*
27 *Plant cell*. 2017;29:1039-52.

28 [347] Sieburth LE, Muday GK, King EJ, Benton G, Kim S, Metcalf KE, et al. SCARFACE encodes
29 an ARF-GAP that is required for normal auxin efflux and vein patterning in Arabidopsis. *The*
30 *Plant cell*. 2006;18:1396-411.

31 [348] Bach L, Michaelson LV, Haslam R, Bellec Y, Gissot L, Marion J, et al. The very-long-chain
32 hydroxy fatty acyl-CoA dehydratase PASTICCINO2 is essential and limiting for plant
33 development. *Proceedings of the National Academy of Sciences of the United States of*
34 *America*. 2008;105:14727-31.

35 [349] Roudier F, Gissot L, Beaudoin F, Haslam R, Michaelson L, Marion J, et al. Very-long-
36 chain fatty acids are involved in polar auxin transport and developmental patterning in
37 Arabidopsis. *The Plant cell*. 2010;22:364-75.

38 [350] Willemsen V, Friml J, Grebe M, van den Toorn A, Palme K, Scheres B. Cell polarity and
39 PIN protein positioning in Arabidopsis require STEROL METHYLTRANSFERASE1 function. *The*
40 *Plant cell*. 2003;15:612-25.

41 [351] Men S, Boutte Y, Ikeda Y, Li X, Palme K, Stierhof YD, et al. Sterol-dependent
42 endocytosis mediates post-cytokinetic acquisition of PIN2 auxin efflux carrier polarity.
43 *Nature cell biology*. 2008;10:237-44.

44 [352] Kleine-Vehn J, Dhonukshe P, Swarup R, Bennett M, Friml J. Subcellular trafficking of the
45 Arabidopsis auxin influx carrier AUX1 uses a novel pathway distinct from PIN1. *The Plant cell*.
46 2006;18:3171-81.

3841
3842
3843
3844
3845
3846
3847
3848
3849
3850
3851
3852
3853
3854
3855
3856
3857
3858
3859
3860
3861
3862
3863
3864
3865
3866
3867
3868
3869
3870
3871
3872
3873
3874
3875
3876
3877
3878
3879
3880
3881
3882
3883
3884
3885
3886
3887
3888
3889
3890
3891
3892
3893
3894
3895
3896
3897
3898
3899
3900

1 [353] Mialoundama AS, Jadid N, Brunel J, Di Pascoli T, Heintz D, Erhardt M, et al. Arabidopsis
2 ERG28 tethers the sterol C4-demethylation complex to prevent accumulation of a
3 biosynthetic intermediate that interferes with polar auxin transport. *The Plant cell*.
4 2013;25:4879-93.

5 [354] Zhang X, Sun S, Nie X, Boutte Y, Grison M, Li P, et al. Sterol Methyl Oxidases Affect
6 Embryo Development via Auxin-Associated Mechanisms. *Plant physiology*. 2016;171:468-82.

7 [355] Darwish E, Testerink C, Khalil M, El-Shihy O, Munnik T. Phospholipid signaling
8 responses in salt-stressed rice leaves. *Plant Cell Physiol*. 2009;50:986-97.

9 [356] Mishkind M, Vermeer JE, Darwish E, Munnik T. Heat stress activates phospholipase D
10 and triggers PIP accumulation at the plasma membrane and nucleus. *The Plant journal : for
11 cell and molecular biology*. 2009;60:10-21.

12 [357] Meijer HJ, van Himbergen JA, Musgrave A, Munnik T. Acclimation to salt modifies the
13 activation of several osmotic stress-activated lipid signalling pathways in *Chlamydomonas*.
14 *Phytochemistry*. 2017;135:64-72.

15 [358] Hou Q, Ufer G, Bartels D. Lipid signalling in plant responses to abiotic stress. *Plant Cell
16 Environ*. 2016;39:1029-48.

17 [359] Li M, Hong Y, Wang X. Phospholipase D- and phosphatidic acid-mediated signaling in
18 plants. *Biochimica et biophysica acta*. 2009;1791:927-35.

19 [360] Heilmann M, Heilmann I. Plant phosphoinositides-complex networks controlling
20 growth and adaptation. *Biochimica et biophysica acta*. 2015;1851:759-69.

21 [361] Wang X, Chapman KD. Lipid signaling in plants. *Frontiers in plant science*. 2013;4:216.

22 [362] Zhang W, Qin C, Zhao J, Wang X. Phospholipase D alpha 1-derived phosphatidic acid
23 interacts with ABI1 phosphatase 2C and regulates abscisic acid signaling. *Proceedings of the
24 National Academy of Sciences of the United States of America*. 2004;101:9508-13.

25 [363] Diaz M, Sanchez-Barrena MJ, Gonzalez-Rubio JM, Rodriguez L, Fernandez D, Antoni R,
26 et al. Calcium-dependent oligomerization of CAR proteins at cell membrane modulates ABA
27 signaling. *Proceedings of the National Academy of Sciences of the United States of America*.
28 2016;113:E396-405.

29 [364] Nicolas WJ, Grison MS, Trepout S, Gaston A, Fouche M, Cordelieres FP, et al.
30 Architecture and permeability of post-cytokinesis plasmodesmata lacking cytoplasmic
31 sleeves. *Nat Plants*. 2017;3:17082.

32 [365] Lahiri S, Toulmay A, Prinz WA. Membrane contact sites, gateways for lipid
33 homeostasis. *Curr Opin Cell Biol*. 2015;33:82-7.

34 [366] Grison MS, Fernandez-Calvino L, Mongrand S, Bayer EM. Isolation of plasmodesmata
35 from Arabidopsis suspension culture cells. *Methods in molecular biology*. 2015;1217:83-93.

36 [367] Deleu M, Crowet JM, Nasir MN, Lins L. Complementary biophysical tools to investigate
37 lipid specificity in the interaction between bioactive molecules and the plasma membrane: A
38 review. *Biochimica et biophysica acta*. 2014;1838:3171-90.

39 [368] Martinez D, Legrand A, Gronnier J, Decossas M, Gouguet P, Lambert O, et al. Coiled-
40 coil oligomerization controls localization of the plasma membrane REMORINs. *J Struct Biol*.
41 2018.

42 [369] Pandey A, Shin K, Patterson RE, Liu XQ, Rainey JK. Current strategies for protein
43 production and purification enabling membrane protein structural biology. *Biochem Cell
44 Biol*. 2016;94:507-27.

45 [370] Sarver SA, Keithley RB, Essaka DC, Tanaka H, Yoshimura Y, Palcic MM, et al.
46 Preparation and electrophoretic separation of Bodipy-Fl-labeled glycosphingolipids. *J
47 Chromatogr A*. 2012;1229:268-73.

3901
3902
3903
3904
3905
3906
3907
3908
3909
3910
3911
3912
3913
3914
3915
3916
3917
3918
3919
3920
3921
3922
3923
3924
3925
3926
3927
3928
3929
3930
3931
3932
3933
3934
3935
3936
3937
3938
3939
3940
3941
3942
3943
3944
3945
3946
3947
3948
3949
3950
3951
3952
3953
3954
3955
3956
3957
3958
3959
3960

1 [371] Cheng HT, Megha, London E. Preparation and properties of asymmetric vesicles that
2 mimic cell membranes: effect upon lipid raft formation and transmembrane helix
3 orientation. *The Journal of biological chemistry*. 2009;284:6079-92.
4 [372] Pluhackova K, Bockmann RA. Biomembranes in atomistic and coarse-grained
5 simulations. *J Phys Condens Matter*. 2015;27:323103.
6 [373] Lyubartsev AP, Rabinovich AL. Force Field Development for Lipid Membrane
7 Simulations. *Biochimica et biophysica acta*. 2016;1858:2483-97.
8 [374] Wassenaar TA, Ingolfssoon HI, Priess M, Marrink SJ, Schafer LV. Mixing MARTINI:
9 electrostatic coupling in hybrid atomistic-coarse-grained biomolecular simulations. *The*
10 *journal of physical chemistry B*. 2013;117:3516-30.
11 [375] Poger D, Caron B, Mark AE. Validating lipid force fields against experimental data:
12 Progress, challenges and perspectives. *Biochimica et biophysica acta*. 2016;1858:1556-65.
13 [376] Lopez CA, Sovova Z, van Eerden FJ, de Vries AH, Marrink SJ. Martini Force Field
14 Parameters for Glycolipids. *J Chem Theory Comput*. 2013;9:1694-708.
15 [377] Izquierdo E, Delgado A. Click Chemistry in Sphingolipid Research. *Chem Phys Lipids*.
16 2018.
17 [378] Best MD. Click chemistry and bioorthogonal reactions: unprecedented selectivity in the
18 labeling of biological molecules. *Biochemistry*. 2009;48:6571-84.
19 [379] Stanislas T, Platre MP, Liu M, Rambaud-Lavigne LES, Jaillais Y, Hamant O. A
20 phosphoinositide map at the shoot apical meristem in *Arabidopsis thaliana*. *BMC Biol*.
21 2018;16:20.
22 [380] Ma Y, Pandzic E, Nicovich PR, Yamamoto Y, Kwiatek J, Pigeon SV, et al. An
23 intermolecular FRET sensor detects the dynamics of T cell receptor clustering. *Nat Commun*.
24 2017;8:15100.
25 [381] Ma Y, Poole K, Goyette J, Gaus K. Introducing Membrane Charge and Membrane
26 Potential to T Cell Signaling. *Front Immunol*. 2017;8:1513.
27 [382] Oncul S, Klymchenko AS, Kucherak OA, Demchenko AP, Martin S, Dontenwill M, et al.
28 Liquid ordered phase in cell membranes evidenced by a hydration-sensitive probe: effects of
29 cholesterol depletion and apoptosis. *Biochimica et biophysica acta*. 2010;1798:1436-43.
30 [383] Tarazona P, Feussner K, Feussner I. An enhanced plant lipidomics method based on
31 multiplexed liquid chromatography-mass spectrometry reveals additional insights into cold-
32 and drought-induced membrane remodeling. *The Plant journal : for cell and molecular*
33 *biology*. 2015;84:621-33.
34 [384] Ray A, Jatana N, Thukral L. Lipidated proteins: Spotlight on protein-membrane binding
35 interfaces. *Prog Biophys Mol Biol*. 2017;128:74-84.
36 [385] Prakash P, Zhou Y, Liang H, Hancock JF, Gorfe AA. Oncogenic K-Ras Binds to an Anionic
37 Membrane in Two Distinct Orientations: A Molecular Dynamics Analysis. *Biophysical journal*.
38 2016;110:1125-38.
39 [386] Sayyed-Ahmad A, Cho KJ, Hancock JF, Gorfe AA. Computational Equilibrium
40 Thermodynamic and Kinetic Analysis of K-Ras Dimerization through an Effector Binding
41 Surface Suggests Limited Functional Role. *The journal of physical chemistry B*.
42 2016;120:8547-56.
43 [387] Tian T, Harding A, Inder K, Plowman S, Parton RG, Hancock JF. Plasma membrane
44 nanoswitches generate high-fidelity Ras signal transduction. *Nature cell biology*. 2007;9:905-
45 14.
46 [388] Pigeon SV, Tabarin T, Yamamoto Y, Ma Y, Nicovich PR, Bridgeman JS, et al. Functional
47 role of T-cell receptor nanoclusters in signal initiation and antigen discrimination.

3961
3962
3963
3964
3965
3966
3967
3968
3969
3970
3971
3972
3973
3974
3975
3976
3977
3978
3979
3980
3981
3982
3983
3984
3985
3986
3987
3988
3989
3990
3991
3992
3993
3994
3995
3996
3997
3998
3999
4000
4001
4002
4003
4004
4005
4006
4007
4008
4009
4010
4011
4012
4013
4014
4015
4016
4017
4018
4019
4020

1 Proceedings of the National Academy of Sciences of the United States of America.
2 2016;113:E5454-63.

3 [389] Williamson DJ, Owen DM, Rossy J, Magenau A, Wehrmann M, Gooding JJ, et al. Pre-
4 existing clusters of the adaptor Lat do not participate in early T cell signaling events. *Nat*
5 *Immunol.* 2011;12:655-62.

6 [390] Zech T, Ejsing CS, Gaus K, de Wet B, Shevchenko A, Simons K, et al. Accumulation of
7 raft lipids in T-cell plasma membrane domains engaged in TCR signalling. *EMBO J.*
8 2009;28:466-76.

9 [391] Rentero C, Zech T, Quinn CM, Engelhardt K, Williamson D, Grewal T, et al. Functional
10 implications of plasma membrane condensation for T cell activation. *PloS one.*
11 2008;3:e2262.

12 [392] Kinoshita M, Suzuki KG, Matsumori N, Takada M, Ano H, Morigaki K, et al. Raft-based
13 sphingomyelin interactions revealed by new fluorescent sphingomyelin analogs. *J Cell Biol.*
14 2017;216:1183-204.

15 [393] Kusumi A, Fujiwara TK, Chadda R, Xie M, Tsunoyama TA, Kalay Z, et al. Dynamic
16 organizing principles of the plasma membrane that regulate signal transduction:
17 commemorating the fortieth anniversary of Singer and Nicolson's fluid-mosaic model. *Annu*
18 *Rev Cell Dev Biol.* 2012;28:215-50.

19 [394] Kusumi A, Suzuki K. Toward understanding the dynamics of membrane-raft-based
20 molecular interactions. *Biochimica et biophysica acta.* 2005;1746:234-51.

21 [395] Fujimoto M, Suda Y, Vernhettes S, Nakano A, Ueda T. Phosphatidylinositol 3-kinase and
22 4-kinase have distinct roles in intracellular trafficking of cellulose synthase complexes in
23 *Arabidopsis thaliana*. *Plant Cell Physiol.* 2015;56:287-98.

24 [396] Hirano T, Munnik T, Sato MH. Phosphatidylinositol 3-Phosphate 5-Kinase,
25 FAB1/PIKfyve Kinase Mediates Endosome Maturation to Establish Endosome-Cortical
26 Microtubule Interaction in *Arabidopsis*. *Plant physiology.* 2015;169:1961-74.

27 [397] Aubert A, Marion J, Boulogne C, Bourge M, Abreu S, Bellec Y, et al. Sphingolipids
28 involvement in plant endomembrane differentiation: the BY2 case. *The Plant journal : for*
29 *cell and molecular biology.* 2011;65:958-71.

30 [398] Wang E, Norred WP, Bacon CW, Riley RT, Merrill AH, Jr. Inhibition of sphingolipid
31 biosynthesis by fumonisins. Implications for diseases associated with *Fusarium moniliforme*.
32 *The Journal of biological chemistry.* 1991;266:14486-90.

33 [399] Kruger F, Krebs M, Viotti C, Langhans M, Schumacher K, Robinson DG. PDMP induces
34 rapid changes in vacuole morphology in *Arabidopsis* root cells. *Journal of experimental*
35 *botany.* 2013;64:529-40.

36 [400] Baba T, Yamamoto A, Tagaya M, Tani K. A lysophospholipid acyltransferase antagonist,
37 CI-976, creates novel membrane tubules marked by intracellular phospholipase A1
38 KIAA0725p. *Molecular and cellular biochemistry.* 2013;376:151-61.

39 [401] Brown WJ, Plutner H, Drecktrah D, Judson BL, Balch WE. The lysophospholipid
40 acyltransferase antagonist CI-976 inhibits a late step in COPII vesicle budding. *Traffic.*
41 2008;9:786-97.

42 [402] Chambers K, Judson B, Brown WJ. A unique lysophospholipid acyltransferase (LPAT)
43 antagonist, CI-976, affects secretory and endocytic membrane trafficking pathways. *Journal*
44 *of cell science.* 2005;118:3061-71.

45 [403] Wu P, Gao HB, Zhang LL, Xue HW, Lin WH. Phosphatidic acid regulates BZR1 activity
46 and brassinosteroid signal of *Arabidopsis*. *Molecular plant.* 2014;7:445-7.

4021
4022
4023
4024
4025
4026
4027
4028
4029
4030
4031
4032
4033
4034
4035
4036
4037
4038
4039
4040
4041
4042
4043
4044
4045
4046
4047
4048
4049
4050
4051
4052
4053
4054
4055
4056
4057
4058
4059
4060
4061
4062
4063
4064
4065
4066
4067
4068
4069
4070
4071
4072
4073
4074
4075
4076
4077
4078
4079
4080

1 [404] Motes CM, Pechter P, Yoo CM, Wang YS, Chapman KD, Blancaflor EB. Differential
2 effects of two phospholipase D inhibitors, 1-butanol and N-acylethanolamine, on in vivo
3 cytoskeletal organization and Arabidopsis seedling growth. *Protoplasma*. 2005;226:109-23.
4 [405] Li G, Xue HW. Arabidopsis PLDzeta2 regulates vesicle trafficking and is required for
5 auxin response. *The Plant cell*. 2007;19:281-95.
6 [406] Staxen I, Pical C, Montgomery LT, Gray JE, Hetherington AM, McAinsh MR. Abscisic
7 acid induces oscillations in guard-cell cytosolic free calcium that involve phosphoinositide-
8 specific phospholipase C. *Proceedings of the National Academy of Sciences of the United*
9 *States of America*. 1999;96:1779-84.

10

4081
4082
4083
4084
4085
4086
4087
4088
4089
4090
4091
4092
4093
4094
4095
4096
4097
4098
4099
4100
4101
4102
4103
4104
4105
4106
4107
4108
4109
4110
4111
4112
4113
4114
4115
4116
4117
4118
4119
4120
4121
4122
4123
4124
4125
4126
4127
4128
4129
4130
4131
4132
4133
4134
4135
4136
4137
4138
4139
4140

1 **Table 1: Examples of inhibitors used to modify *in vivo* the pools of lipids, and some recent related**
2 **references.**

3 The used concentration of the inhibitors is indicative, and must be tested for each plant species or
4 tissues. To address the modification of the PM lipid pool, a phase partition to purify PM vesicles must
5 be conducted coupled with a dedicated lipidomic approach. PLD, Phospholipase D; PLC,
6 Phospholipase C, DAG, Diacylglycerol; VLCFAs, Very Long Chain Fatty Acids; HMG-CoA reductase, 3-
7 hydroxy-3-methyl-glutaryl-coenzyme A reductase.
8

	Inhibitors of:	Name	References
Phosphoinositides	PI3-Kinase (50-100 μM)	LY-294002	[395]
	PI3P 5-Kinase (1 μM)	YM-201636	[396]
	PI4-Kinase (30-60 μM)	Phenylarsine oxide (PAO)	[114] [395]
	PI3-Kinase (1 μM)	Wortmannin	[280] [31]
	PI3-Kinase + PI4-Kinase (30 μM)	Wortmannin	
Sphingolipids	Ceramide synthase (1 μM)	Fumonisin B1 (1 mg)	[397] [398]
	Glucosylceramide synthase (50 μM)	DL-THREO-PDMP	[399]
	VLCFAs / sphingolipid (50-100 nM)	Metazachlor	[232]
Diacylglycerol/ Phosphatidic Acid	Lyso PA Acyl transferase	CI-976	[400-402]
	PLD-derived PA formation (50 μM)	(R)-(+)-Propranolol hydrochloride	[403]
	PLD-derived PA formation (0.2-0.4%)	1- butanol	[404] [405]
	PLC-derived DAG formation (5 μM)	U73122 (active analog)	[31] [406]
	PLC-derived DAG formation (5 μM)	U73343 (inactive analog)	[406]
	PLC-derived DAG formation (50 μM)	Edelfosine	[280]
	DAG-Kinase (50 μM)	R59022	[280]
Sterols	Cyclopropylsterol isomerase 1, CPI1	Fenpropimorph	[7] [172] [159]
	HMG-CoA reductase	Lovastatin	[7]

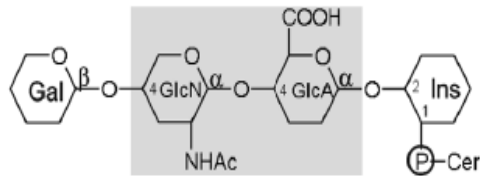
9

A Tobacco leaf GIPC

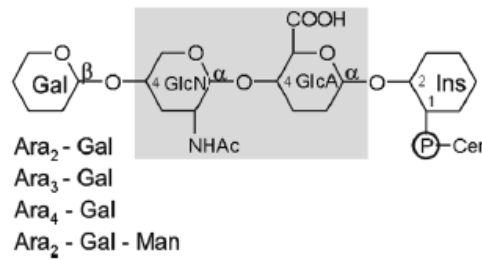
Series A



Series B



Series D-G



B Maize seed GIPC

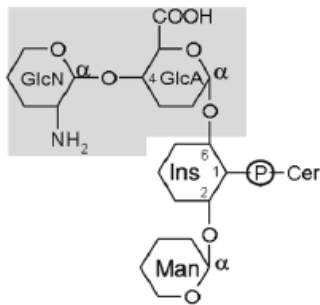
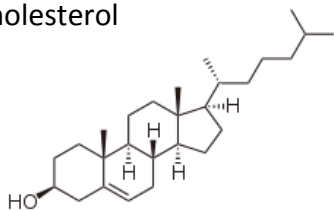


Figure 1: Determined structures of GIPC glycosidic polar head from tobacco and maize.

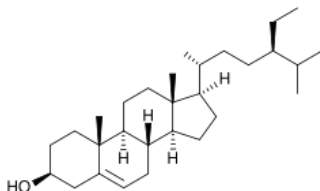
A, tobacco GIPC of series A are major in tobacco leaves (top) with glucuronic acid (GlcA) and either glucosamine (GlcN) or N-acetyl glucosamine (GlcNAc). Other minor polar head of series B and higher glycosylated GIPC with arabinose (Ara), galactose (Gal) and Manose (Man) have been identified, but the precise structure remains to be determined. Grey part is the conserved glycan moiety of glucuronic-Hex. Cer indicates the ceramide moiety, in tobacco, with t18:0 and t18:1 for LCB, and VLCFA mostly alpha 2-hydroxylated ; B, GIPC found in corn seeds with branched polar head

A, Free phytosterols

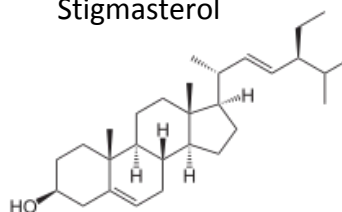
Cholesterol



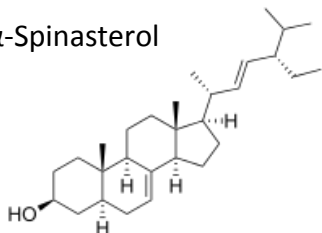
β -Sitosterol



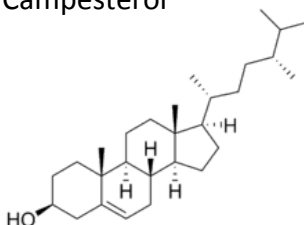
Stigmasterol



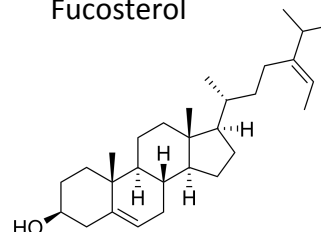
α -Spinasterol



Campesterol

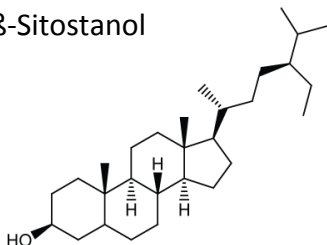


Fucosterol



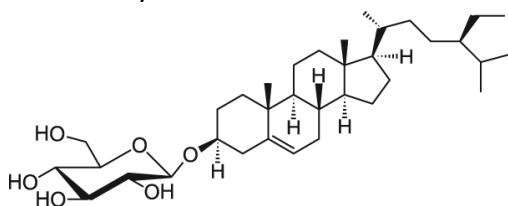
B, Phytostanol

β -Sitostanol

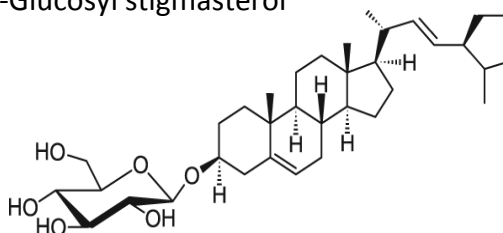


C, Conjugated phytosterols

β -D-Glucosyl sitosterol



β -D-Glucosyl stigmasterol



Palmitate β -D-Glucosyl sitosterol

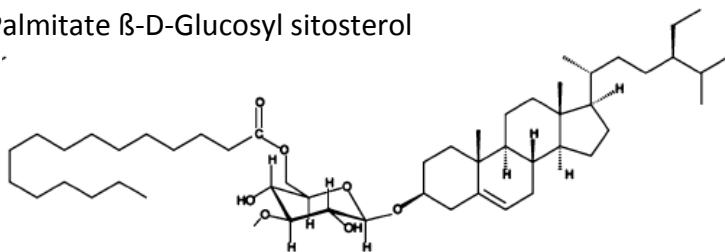


Figure 2: Structures of specific plasma membrane phytosterols compared with animal cholesterol.

A, free phytosterols ; B, phytostanol ; C, conjugated phytosterols.

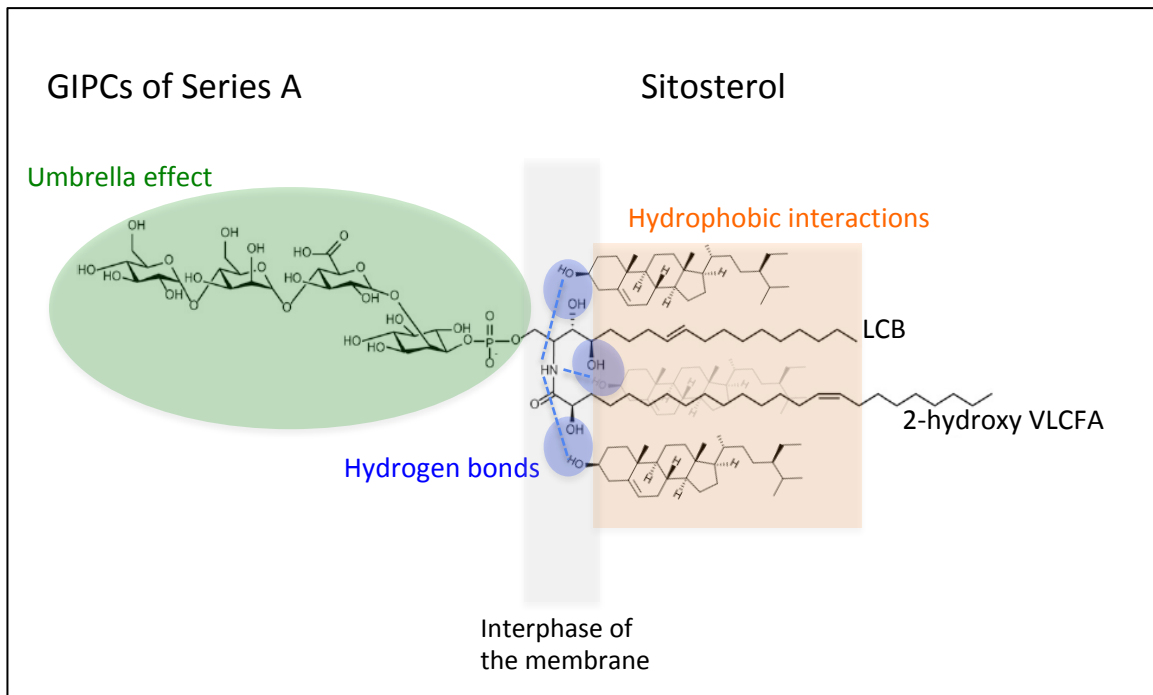


Figure 3: Biophysical features involved between a GIPC of series A and three molecules of sitosterols. These interactions are important for nanodomain formations in the PM. LCB, Long Chain Base; VLCFA, Very Long Chain Fatty Acid.

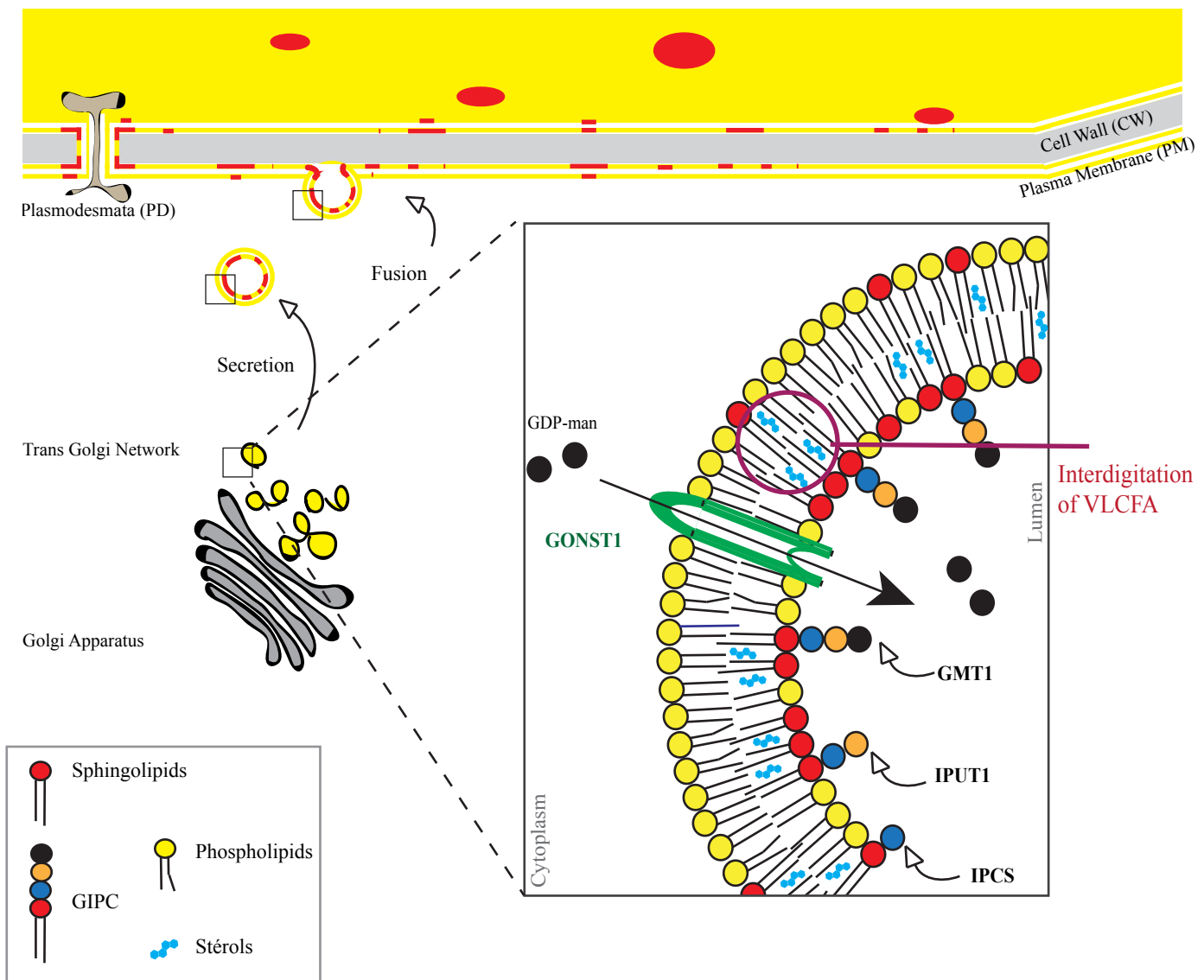


Figure 4: Formation of GIPC- and sterol-enriched domains along the secretory pathway.

GIPCs are synthesized in the lumen of the trans Golgi network (TGN) by grafting on the ceramide sequentially inositol-phosphate (IPCS, inositolphosphorylceramide synthase), glucuronic acid (IPUT1, inositol phosphorylceramide glucuronosyltransferase) and mannose (GMT1, GIPC mannosyl-transferase1). Golgi-localized nucleotide sugar transporter (GONST1) is responsible for the import of GDP-mannose to fuel GIPC synthesis. After vesicular fusion to the PM, GIPC polar heads face the apoplasm. Polyglycosylated GIPCs form nanodomains in the PM (in red).

Table 1: Examples of inhibitors used to modify *in vivo* the pools of lipids, and some recent related references.

The used concentration of the inhibitors is indicative, and must be tested for each plant species or tissues. To address the modification of the PM lipid pool, a phase partition to purify PM vesicles must be conducted coupled with a dedicated lipidomic approach. PLD, Phospholipase D; PLC, Phospholipase C, DAG, Diacylglycerol; VLCFAs, Very Long Chain Fatty Acids; HMG-CoA reductase, 3-hydroxy-3-methyl-glutaryl-coenzyme A reductase.

	Inhibitors of:	Name	References
Phosphoinositides	PI3-Kinase (50-100 μ M)	LY-294002	[1]
	PI3P 5-Kinase (1 μ M)	YM-201636	[2]
	PI4-Kinase (30-60 μ M)	Phenylarsine oxide (PAO)	[3] [1]
	PI3-Kinase (1 μ M)	Wortmannin	[4] [5]
	PI3-Kinase + PI4-Kinase (30 μ M)	Wortmannin	
Sphingolipids	Ceramide synthase (1 μ M)	Fumonisin B1 (1 mg)	[6] [7]
	Glucosylceramide synthase (50 μ M)	DL-THREO-PDMP	[8]
	VLCFAs / sphingolipid (50-100 nM)	Metazachlor	[9]
Diacylglycerol/ Phosphatidic Acid	Lyso PA Acyl transferase	CI-976	[10-12]
	PLD-derived PA formation (50 μ M)	(R)-(+)-Propranolol hydrochloride	[13]
	PLD-derived PA formation (0.2-0.4%)	1- butanol	[14] [15]
	PLC-derived DAG formation (5 μ M)	U73122 (active analog)	[5] [16]
	PLC-derived DAG formation (5 μ M)	U73343 (inactive analog)	[16]
	PLC-derived DAG formation (50 μ M)	Edelfosine	[4]
	DAG-Kinase (50 μ M)	R59022	[4]
Sterols	Cyclopropylsterol isomerase 1, CPI1	Fenpropimorph	[17] [18] [19]
	HMG-CoA reductase	Lovastatin	[17]

[1] Fujimoto M, Suda Y, Vernhettes S, Nakano A, Ueda T. Phosphatidylinositol 3-kinase and 4-kinase have distinct roles in intracellular trafficking of cellulose synthase complexes in *Arabidopsis thaliana*. *Plant Cell Physiol*. 2015;56:287-98.

[2] Hirano T, Munnik T, Sato MH. Phosphatidylinositol 3-Phosphate 5-Kinase, FAB1/PIKfyve Kinase Mediates Endosome Maturation to Establish Endosome-Cortical Microtubule Interaction in *Arabidopsis*. *Plant physiology*. 2015;169:1961-74.

[3] Simon ML, Platre MP, Marques-Bueno MM, Armengot L, Stanislas T, Bayle V, et al. A PtdIns(4)P-driven electrostatic field controls cell membrane identity and signalling in plants. *Nat Plants*. 2016;2:16089.

[4] Cacas JL, Gerbeau-Pissot P, Fromentin J, Cantrel C, Thomas D, Jeannette E, et al. Diacylglycerol kinases activate tobacco NADPH oxidase-dependent oxidative burst in response to cryptogein. *Plant Cell Environ*. 2017;40:585-98.

[5] Furt F, Konig S, Bessoule JJ, Sargueil F, Zallot R, Stanislas T, et al. Polyphosphoinositides are enriched in plant membrane rafts and form microdomains in the plasma membrane. *Plant physiology*. 2010;152:2173-87.

- [6] Aubert A, Marion J, Boulogne C, Bourge M, Abreu S, Bellec Y, et al. Sphingolipids involvement in plant endomembrane differentiation: the BY2 case. *The Plant journal : for cell and molecular biology*. 2011;65:958-71.
- [7] Wang E, Norred WP, Bacon CW, Riley RT, Merrill AH, Jr. Inhibition of sphingolipid biosynthesis by fumonisins. Implications for diseases associated with *Fusarium moniliforme*. *The Journal of biological chemistry*. 1991;266:14486-90.
- [8] Kruger F, Krebs M, Viotti C, Langhans M, Schumacher K, Robinson DG. PDMP induces rapid changes in vacuole morphology in *Arabidopsis* root cells. *Journal of experimental botany*. 2013;64:529-40.
- [9] Wattelet-Boyer V, Brocard L, Jonsson K, Esnay N, Joubes J, Domergue F, et al. Enrichment of hydroxylated C24- and C26-acyl-chain sphingolipids mediates PIN2 apical sorting at trans-Golgi network subdomains. *Nat Commun*. 2016;7:12788.
- [10] Baba T, Yamamoto A, Tagaya M, Tani K. A lysophospholipid acyltransferase antagonist, CI-976, creates novel membrane tubules marked by intracellular phospholipase A1 KIAA0725p. *Molecular and cellular biochemistry*. 2013;376:151-61.
- [11] Brown WJ, Plutner H, Drecktrah D, Judson BL, Balch WE. The lysophospholipid acyltransferase antagonist CI-976 inhibits a late step in COPII vesicle budding. *Traffic*. 2008;9:786-97.
- [12] Chambers K, Judson B, Brown WJ. A unique lysophospholipid acyltransferase (LPAT) antagonist, CI-976, affects secretory and endocytic membrane trafficking pathways. *Journal of cell science*. 2005;118:3061-71.
- [13] Wu P, Gao HB, Zhang LL, Xue HW, Lin WH. Phosphatidic acid regulates BZR1 activity and brassinosteroid signal of *Arabidopsis*. *Molecular plant*. 2014;7:445-7.
- [14] Motes CM, Pechter P, Yoo CM, Wang YS, Chapman KD, Blancaflor EB. Differential effects of two phospholipase D inhibitors, 1-butanol and N-acylethanolamine, on in vivo cytoskeletal organization and *Arabidopsis* seedling growth. *Protoplasma*. 2005;226:109-23.
- [15] Li G, Xue HW. *Arabidopsis* PLDzeta2 regulates vesicle trafficking and is required for auxin response. *The Plant cell*. 2007;19:281-95.
- [16] Staxen I, Pical C, Montgomery LT, Gray JE, Hetherington AM, McAinsh MR. Abscisic acid induces oscillations in guard-cell cytosolic free calcium that involve phosphoinositide-specific phospholipase C. *Proceedings of the National Academy of Sciences of the United States of America*. 1999;96:1779-84.
- [17] Grison MS, Brocard L, Fouillen L, Nicolas W, Wewer V, Dormann P, et al. Specific membrane lipid composition is important for plasmodesmata function in *Arabidopsis*. *The Plant cell*. 2015;27:1228-50.
- [18] Gronnier J, Crowet JM, Habenstein B, Nasir MN, Bayle V, Hosy E, et al. Structural basis for plant plasma membrane protein dynamics and organization into functional nanodomains. *Elife*. 2017;6.
- [19] Laloi M, Perret AM, Chatre L, Melser S, Cantrel C, Vaultier MN, et al. Insights into the role of specific lipids in the formation and delivery of lipid microdomains to the plasma membrane of plant cells. *Plant physiology*. 2007;143:461-72.